Polynuclear Ruthenium And Osmium Complexes, And Related Electron-Dense Staining Reagents.

A Thesis Submitted for the Degree of

Doctor of Philosophy

of the University of London

By

Jonathan Phillip Hall, B.Sc., A.R.C.S.

Department of Chemistry,

Imperial College of Science and Technology,

London,   SW7 2AY.

November, 1979.

ABSTRACT

POLYNUCLEAR RUTHENIUM AND OSMIUM COMPLEXES, AND RELATED ELECTRON-DENSE

STAINING REAGENTS.

Jonathan Phillip Hall.

A large part of the work presented in this thesis concerns oxo or

nitrido bridged trinuclear ruthenium or osmium complexes, some of which

show selectivity as stains for electron microscopy of biological tissues.

Species containing lead, uranium or tungsten also have staining properties,

and are also discussed here.

The intensely-coloured trinuclear compound, ruthenium red, shown

to contain the linear $[(NH_3)_5Ru-O-Ru(NH_3)_4-O-Ru(NH_3)_5]^{6+}$ cation,

readily gives resonance-enhanced Raman spectra; isotopic substitution

by ^2H, ^{15}N and ^{18}O enabled the assignment of the main bands. Similar

data for ruthenium brown, $[Ru_3O_2(NH_3)_{14}]Cl_7$ and two related bis(1,2-

diaminoethane)-substituted species are given. Excitation profiles for

the Raman bands parallel the electronic absorption spectra. The new

nitrido-bridged complexes, $[Os_3N_2(NH_3)_8(H_2O)_6]Cl_6$, $[Os_3N_2(NH_3)_8(H_2O)_6]Cl_7$

and $[Ru_3N_2(NH_3)_8(H_2O)_5(OH)]Cl_5$ are described, and on the basis of the

resonance Raman and infrared spectra of normal, ^2H, and ^{15}N-substituted

forms of the complexes, similar structures to that of ruthenium red

are proposed. Related structures are proposed for $[Os_3N_2(NH_3)_6(OH)_4(H_2O)_2]Cl_2$

and $[Os_3N_2(NH_3)_4(OH)_8(H_2O)_2]$ and the cyano derivatives, $K_4[Os_3N_2(CN)_{10}-$

$(H_2O)_4]$ and $K_4[Os_3N_2(CN)_8(H_2O)_2(OH)_4]$.

The application of some ruthenium and osmium trinuclear species as cell staining agents is discussed. Staining reagents formed in solution on treatment with sulphur dioxide are also mentioned, and to help elucidate the mechanism of staining by these solutions, a range of mononuclear sulphito complexes of the platinum group metals, osmium, ruthenium, iridium, rhodium, platinum, and palladium were prepared. The Raman spectra are recorded, and, aided by infrared data, assigned as suggesting that in most of the complexes, the sulphito group is bonded via sulphur.

Interactions of staining reagent solutions containing lead(II) species, dioxouranium(VI) (uranyl) species, or tungstophosphoric acid ($H_3PW_{12}O_{40}$) with amino acids and nucleotides are investigated.

CONTENTS

PAGE:

LIST OF TABLES AND FIGURES.

PAGE:

ACKNOWLEDGEMENTS

NOMENCLATURE, ABBREVIATIONS AND SYMBOLS.

NOMENCLATURE

For convenience, trivial names of certain trinuclear ruthenium and osmium species have been used throughout this thesis.

Ruthenium red, $[Ru_3O_2(NH_3)_{14}]Cl_6.4H_2O$, is tetradeca-ammino di-μ-oxo tri-ruthenium hexachloride tetrahydrate.

Ruthenium brown, $[Ru_3O_2(NH_3)_{14}]Cl_7.4H_2O$, is tetradeca-ammino di-μ-oxo tri-ruthenium heptachloride tetrahydrate.

Ruthenium violet, $[Ru_3N_2(NH_3)_8(H_2O)_5(OH)]Cl_5$, is octa-ammino penta-aquo hydroxo di-μ-nitrido tri-ruthenium pentachloride.

Osmium violet, $[Os_3N_2(NH_3)_8(H_2O)_6]Cl_6$, is octa-ammino hexa-aquo di-μ-nitrido tri-osmium hexachloride.

Osmium brown, $[Os_3N_2(NH_3)_8(H_2O)_6]Cl_7$, is octa-ammino hexa-aquo di-μ-nitrido tri-osmium heptachloride.

Gautier's compound, $[Os_3N_2(NH_3)_6(OH)_4(H_2O)_2]Cl_2$ is hexa-ammino tetra-hydroxo di-aquo di-μ-nitrido tri-osmium dichloride.

VIBRATIONAL SPECTRA

Frequencies for infrared (IR) and Raman (R) spectra are quoted in wavenumbers, cm^{-1}. Stretching (ν), rocking (ρ) or deformation (δ) modes may be symmetric (s) or asymmetric (as). Intensities of bands are described as s, strong; m, medium ; w, weak ; v, very ; and band shapes as b, broad ; sp, sharp ; and sh, shoulder. Depolarisation ratio (ρ) values may be quoted for solution Raman spectra. In some cases, intensities of Raman bands are given relative to the strongest band = 10.

ABBREVIATIONS.

DNA = Deoxyribonucleic acid

RNA = Ribonucleic acid

AMP = Adenosine monophosphate

dAMP = Deoxyadenosine monophosphate

CMP = Cytidine monophosphate

GMP = Guanosine monophosphate

dGMP = Deoxyguanosine monophosphate

TMP = Thymidine monophosphate

en = 1,2-Diaminoethane, $NH_2CH_2CH_2NH_2$

py = Pyridine, C_5H_5N

M = Metal

χ = Mass susceptibility

μ_{eff} = Effective magnetic moment

Λ^o = Limiting conductance

$\overset{o}{A}$ = Angstrom unit, 10^{-10} m

TO MY PARENTS

AND JEZEBEL

Chapter One

Introduction

Much of the work described in this thesis is concerned with
trinuclear oxo and nitrido bridged ruthenium and osmium complexes,
some of which are used as biological staining agents in electron
microscopy. A general survey of polynuclear oxo and nitrido bridged
species of platinum group metals is therefore given here. A brief
outline of electron microscope studies of the ultrastructure of
cells aided by metal complexes as stains is included here.

Section 1-A.

Polynuclear Oxo and Nitrido Bridged Species of Platinum Group Metals.

The oxo (O^{2-}) and nitrido (N^{3-}) ligands are isoelectronic; and

their chemistries as ligands are similar in many respects. Both can

function as terminal ligands in transition metal complexes where

the metal is normally in a high oxidation state, leaving sufficient

empty d orbitals to accept electrons from the strong electron

donors, O^{2-} and N^{3-}. The commonest nitrido and oxo complexes of

the platinum group metals have d^0 or d^2 configurations; an example of

the latter is the osmium(VI) species, $K_2[OsNCl_5]$. With the Os-N

bond on the z-axis and the equatorial Os-Cl bonds aligned on the x

and y axes, the σ bond between metal and nitrido ligand is formed

from the metal $5d_{z^2}$ + 6s with the nitrogen sp_σ. Two π bonds are

formed from the $5d_{xz}$ and $5d_{yz}$ with the $2p_x$ and $2p_y$ orbitals respectively.
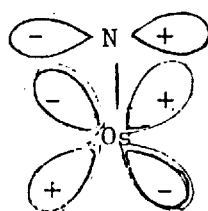
(xz plane)

$5d_{xz}$ and $2p_x$ orbitals

The osmium 6s, 6p and $5d_{x^2-y^2}$ orbitals are used for Os-Cl σ bonds.

The osmium $5d_{xy}$ orbital is non-bonding, and accommodates the two d

electrons of osmium(VI).

In the case of oxo or nitrido bridged polynuclear species, however, lower metal oxidation states are found, as the ligand can now donate electrons to the d orbitals of two or three metal atoms. Both terminal and bridged oxo[1] and nitrido[2] complexes are discussed in recent reviews. The bonding of various bridging ligands, including O^{2-} and N^{3-}, and structures of the complexes found, have been reviewed.[3]

In this discussion, attention will be confined to systems containing two or three metal atoms with oxo or nitrido bridges, emphasis being placed on ruthenium and osmium.

Structure and Bonding.

The binuclear oxo bridged species $K_4[Ru_2OCl_{10}]$ contains a linear bridge with an eclipsed (D_{4h}) structure:[4]

$$\left[Cl\!-\!Ru\!-\!O\!-\!Ru\!-\!Cl \right]^{4-} \qquad (\text{Ru-O } 1.801 \text{ Å})$$
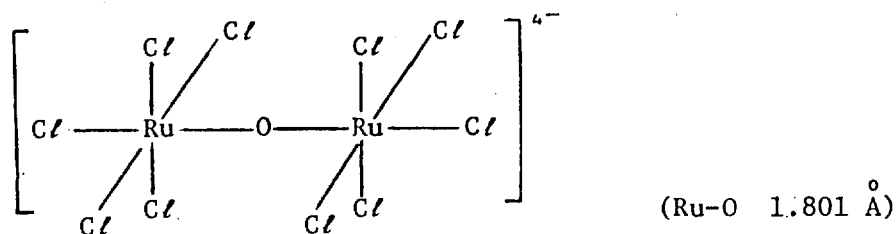
A similar structure is found for the nitrido bridged $K_3[Ru_2NCl_8(H_2O)_2]$:[5]

$$\left[H_2O\!-\!Ru\!-\!N\!-\!Ru\!-\!OH_2 \right]^{3-} \qquad (\text{Ru-N } 1.720 \text{ Å})$$
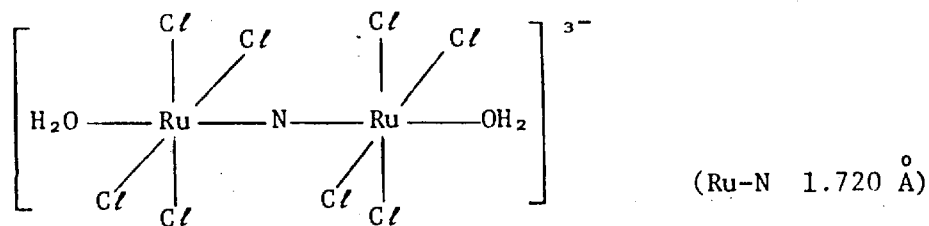
In both cases, the bridge ligand lies symmetrically between the metal atoms.

An account of the bonding for the centrosymmetric D_{4h} structure

of $[Ru_2OCl_{10}]^{4-}$ has been provided by Dunitz and Orgel;[6] this may

be applied to the nitrido bridged species also, as the two complexes

are isoelectronic. The σ system involves the sp_{σ} orbital of the

bridging group overlapping with the metal d_{z^2} orbitals, the metal-

bridge-metal axis is the z axis. The filled $2p_x$ and $2p_y$ orbitals

of the bridging group overlap to form a pair of π bonds with the

d_{xz} and d_{yz} of the Ru^{IV} atoms. The resulting electronic configuration

is $(e_u^b)^4 (b_{2g})^2 (b_{2u})^2 (e_g)^4 (e_u^a)^0$, in agreement with the observed diamagnetism

of the complexes. Similar considerations apply to the Os^{IV} species

$[Os_2OCl_{10}]^{4-}$ and $[Os_2NCl_8(H_2O)_2]^{3-}$ and the ammine species

$[Ru_2N(NH_3)_8Cl_2]Cl_3$ and $[Os_2N(NH_3)_8Cl_2]Cl_3$. Bent oxo or nitrido bridges

are less favourable for π overlap, and so are not commonly encountered

in platinum group complexes.

The $[(NH_3)_5Ru-O-Ru(en)_2-O-Ru(NH_3)_5]^{6+}$ cation has been shown to

possess a linear structure, with the central Ru-N bonds at 45° to those

of the terminal units, which are eclipsed.[7]
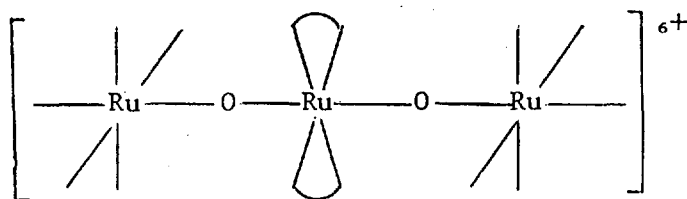
A π-bonding molecular orbital scheme, related to that for

$[Ru_2OCl_{10}]^{4-}$ has been constructed for the parent compound, ruthenium

red $[(NH_3)_5Ru-O-Ru(NH_3)_4-O-Ru(NH_3)_5]^{6+}$.[8] A similar structure has

been postulated for a system containing an Os-N-Os-N-Os backbone.[9]

A linear backbone has very recently been found for the rhenium

complex, $[O = Re(L)-O-Re(L)-O-Re(L) = O]^+$, (L = NN'-ethylenebis-

(acetylacetiminate)).[10]

A rather different trinuclear structure is that containing one

oxo or nitrido group at the centre of an equilateral M_3 triangle.

Examples of this structure are $[M_3O(OOCR)_6]^+$, where M = Cr, Fe, Ru and

$A\ell$, $[Ir_3O(SO_4)_9]^{10-}$ and $[Ir_3N(SO_3)_6(H_2O)_3]^{4-}$ [11]; a molecular orbital

scheme has been derived.[8]

Vibrational Spectra

The centrosymmetric binuclear species of D_{4h} symmetry are

expected to show one Raman active, and one infrared active metal-

bridging ligand stretching modes, of a_{1g} and a_{2u} symmetry. These

are found to be widely separated in frequency, the Raman active

$\nu^s_{M_2O}$ being near 240 cm^{-1} [12] and $\nu^s_{M_2N}$ near 310 cm^{-1}; while the infrared

active asymmetric stretches, mostly motion of the bridging group, are

seen near 860 cm^{-1} ($\nu^{as}_{M_2O}$)[14] and 1080 cm^{-1} ($\nu^{as}_{M_2N}$).[13] A greater degree

of π-bonding for the nitrido than the oxo bridged species is borne

out by the stretching force constants calculated from these frequencies,

e.g., $K_4[Ru_2OC\ell_{10}]$, K_{Ru-O} 3.8 mdyn $\overset{o}{A}^{-1}$, and $K_3[Ru_2NC\ell_8(H_2O)_2]$, K_{Ru-N}

5.5 mdyn $\overset{o}{A}^{-1}$.[15] In bent M-O-M species, ν^{as} is near 750 cm^{-1}, while

ν^s is near 500 cm^{-1}.

Linear trinuclear species are expected to show two Raman active

(a_{1g}) and two infrared active (a_{2u}) (D_{4h} symmetry) metal-bridging ligand

stretches; the Raman bands seen near 800 and 200 cm^{-1} are assigned to

the a_{1g} modes of the Ru_3O_2 system.[16] The triangular iridium complexes,

$K_{10}[Ir_3O(SO_4)_9]$ and $Cs_4[Ir_3N(SO_4)_6(H_2O)_3]$ have Raman bands at 233 cm^{-1} ($\nu^s_{Ir_3O}$)[16]

and 240 cm^{-1} ($\nu^s_{Ir_3N}$).[15]

Section 1-B.

Inorganic Biological Staining Reagents.

The technique of electron microscopy allows study of the ultrastructure of plant and animal cells at much greater resolution than that given by light microscopy. The presence of metal atoms is required to enhance the feeble contrast of the cell sections provided by the component carbon, hydrogen, nitrogen and oxygen atoms, these latter being poor electron scatterers. Heavier atoms are better electron scatterers, and so show up as darker areas on the electron micrograph. The aim of staining therefore is to obtain high local concentrations of metal-containing species bound at certain chemically different sites of biochemical interest in the cells. It is essential that the stain does not produce artificial structures.

The cells require some preparation before examination by electron microscopy. Fixation is always necessary, to preserve the cellular ultrastructure with the minimum change from the living state. Typical fixatives are aldehydes such as glutaraldehyde, which cross-links cell proteins, and osmium tetraoxide, which binds to lipids. The fixative is used in a buffered aqueous solution. Staining may be carried out simultaneously with, or subsequent to fixation. The blocks of tissue must then be dehydrated prior to embedding in a plastic resin, which holds the material together while extremely thin (100-1000 $\overset{o}{A}$) slices or sections are cut. The sections, which are supported on metal grids, may be stained at this stage (described as poststaining or counterstaining) before examination by electron microscopy.

Fixation, except in the case of metal complexes such as osmium tetraoxide and potassium permanganate, does not increase the electron density contrast. Staining, before or after sectioning is normally required.

Some stains may bind electrostatically. An example is ruthenium red, $[Ru_3O_2(NH_3)_{14}]^{6+}$; this cation is believed to bind to anionic parts of biopolymers such as pectin (a reaction long utilised in light microscopy)[17] and DNA.[18] Ruthenium red is often used in conjunction with osmium tetraoxide.[19,20] Lead and uranyl (UO_2^{2+}) solutions are frequently used as counterstains, where penetration into the very thin sections allows uptake of the stain.[21]

Other metals in complexes that have been used as stains include bismuth, gold, indium, iron, lanthanum, mercury, silver, thallium, thorium, vanadium and zirconium.[21]

CHAPTER TWO

POLYNUCLEAR RUTHENIUM AND OSMIUM COMPLEXES.

Abstract

Resonance Raman and infrared spectral data are presented

for the trinuclear μ-oxo ruthenium complexes $[Ru_3O_2(NH_3)_{10}(L)_4]^{6+}$

and $[Ru_3O_2(NH_3)_{10}(L)_4]^{7+}$ (L = NH_3, $\frac{1}{2}$ en) and the structures of these

species in solution are discussed. The preparation and properties

of some new trinuclear μ-nitrido osmium and ruthenium complexes;

$[Os_3N_2(NH_3)_8(H_2O)_6]Cl_6$, $[Os_3N_2(NH_3)_8(H_2O)_6]Cl_7$, $K_4[Os_3N_2(CN)_{10}(H_2O)_4].4H_2O$,

$K_4[Os_3N_2(CN)_8(OH)_4(H_2O)_2]$, $[Ru_3N_2(NH_3)_8(H_2O)_5(OH)]Cl_5$ and related

species are reported. Evidence that these complexes contain a linear

M-N-M-N-M unit are provided by resonance Raman spectra, infrared

spectra and other properties.

The behaviour of these oxo and nitrido bridged ammine complexes

in electron microscopic cell staining studies is discussed.

Section 2-A. Introduction.

2-A-1. Ruthenium.

Ruthenium Red.

An intensely red ruthenium species was obtained by Joly[22] in 1892 by reaction of ruthenium chloride with ammonia solution; the product was formulated as " $Ru_2(OH)_2C\ell_4(NH_3)_7.3H_2O$ " . This material , christened " Ruthenium Red" by the botanist Mangin,[17] who investigated its biological staining properties, is converted reversibly to a brown species in hydrochloric acid, this new product being " $Ru_2(OH)_2C\ell_4(NH_3)_7-HC\ell.3H_2O$ " ,[22] Later work by Morgan and Burstall[23] in 1936 lead to a reformulation as " $[Ru(OH)C\ell(NH_3)_4]C\ell.H_2O$ " for the red material. This formula was soon refuted,[24] however, on the basis that a mononuclear Ru^{III} species would not show the observed strong colour and diamagnetism.

An extensive study of ruthenium red by Fletcher, et al.,[25] in 1961 produced the formula now accepted as correct. The red species undergoes a reversible oxidation to the yellow-brown " Ruthenium Brown" , requiring one electron per three ruthenium atoms. Fourteen ammonia groups and six chloride ions were found to be associated with every three ruthenium atoms. Coupled with the observed average oxidation state of $+ {}^{10}/3$ for the ruthenium, this indicated the presence of oxo bridges holding together a trinuclear cation. The formula $[(NH_3)_5Ru-O-Ru(NH_3)_4-O-Ru(NH_3)_5]-,C\ell_6.4H_2O$ is in accordance with the experimental observations.[25]

The formula $[Ru_3(NH_3)_{12}(H_2O)_3C\ell_8(OH)_3]$ has been claimed for material reported to be ruthenium red, in an X-ray study[26]; the data presented were not, however, consistent with the formula reported. It is possible that a mononuclear impurity in the commercial sample used had been selected for study. Some confusion has thus arisen in

the literature, particularly that pertaining to the use of ruthenium

red as a cytological stain, over the formulation of the species.

Hereinafter, " ruthenium red" will be used for the species

$[Ru_3O_2(NH_3)_{14}]^{6+}$, chloride being the most commonly encountered

counter-ion to the red cation. The systematic name of this complex

is tetradeca-ammine di-μ-oxo tri-ruthenium hexachloride, but the

trivial name will be used for convenience.

The preparation of ruthenium red by reaction of aqueous ruthenium

trichloride with concentrated ammonia solution also generates a

variety of ammine-complex impurities. Commercial ruthenium trichloride

hydrate is known to contain both Ru^{III} and Ru^{IV} species; a Raman

study of aqueous solutions indicated the presence of $[RuCl_6]^{2-}$,

$[Ru_2OCl_{10}]^{4-}$, $[Ru_2O_2Cl_4]$ and $[Ru_2OCl_6]^{2-}$.[27] Admixture of impurities

with ruthenium red may have been responsible for the incorrect

formulations[22,23] made for the complex.

Ruthenium Brown.

The yellow-brown material readily obtained by the reversible one-

electron oxidation of ruthenium red contains the $[Ru_3O_2(NH_3)_{14}]^{7+}$

cation. The systematic nomenclature for the chloride salt is tetradeca-

ammine di-μ-oxo tri-ruthenium heptachloride, the trivial name, ruthenium

brown will be used hereafter for convenience.

1,2-Diaminoethane Analogues.

The four ammine ligands on the central ruthenium atom can be

replaced in aqueous solution by two 1,2-diaminoethane groups, (en)

to give $[Ru_3O_2(NH_3)_{10}(en)_2]Cl_6$; an X-ray diffraction study[7] on a

crystal of the substituted product indicates a linear N-Ru-O-Ru-O-Ru-N

backbone. The central equatorial Ru-N bonds are twisted at $45°$

with respect to the equatorial Ru-N bonds of the end groups, these

latter sets thus being eclipsed. A molecular orbital scheme for

this structure has been devised.[28] Oxidation of this complex produces

the 1,2-diaminoethane analogue of ruthenium brown, $[Ru_3O_2(NH_3)_{10}(en)_2]Cl_7$.[28]

Ruthenium Violet.

One impurity associated with ruthenium red, yielding an intense

blue-violet solution, was noted by Fletcher, et al.,[25] this was

isolated and used successfully as an electron-dense stain by Luft.[19]

Although a preparation of purified ruthenium red, and this blue-

violet material, named " ruthenium violet" , has been described,[19]

no investigation into the nature of the latter species has yet been

carried out.

A compound bearing some similarity to ruthenium violet is of

the empirical formula $Ru_4N_{11}O_{12}H_{33}$, obtained from ruthenium tetraoxide

and gaseous ammonia at $-70°C$.[29]

2-A-2. Osmium.

No directly corresponding osmium analogues of ruthenium red are

known, though a variety of nitrido bridged rather than oxo bridged

species have been described. These ammine complexes have been

formulated as containing three osmium atoms per molecule, and to this

extent are related to ruthenium red.

Long before ruthenium was discovered, Berzelius in 1829[30]

obtained a black material from reaction of osmium tetraoxide with

concentrated ammonia solution. This was later formulated as

$[OsO_2(NH_3)_2H_2O]$ by Claus,[31] and more recently, as $[Os_3N_2(NH_3)_4(OH)_8(H_2O)_2].$[32]

Two broad bands near 1000 cm^{-1} in the infrared spectrum of this

species are assigned to asymmetric stretching vibrations of the metal-

nitrido system, shifting ca. 20 cm^{-1} to lower frequencies on ^{15}N

substitution.[32] The halogen-substituted salt $Cs_3[Os_3N_2X_{11}(NH_3)_3].2H_2O$

is obtained by reaction of $[Os_3N_2(NH_3)_4(OH)_8(H_2O)_2]$ with aqueous

HX (X = Cℓ or Br) in the presence of CsX.[9,32] The infrared bands

assigned to the osmium-nitrido backbone are again evident near 1000 cm^{-1}.

The structure (I) has been suggested.[32]

$$\left[\begin{array}{c} \ce{H3N-Os....N....Os....N....Os-NH3} \end{array} \right]^{3-} \qquad (I)$$
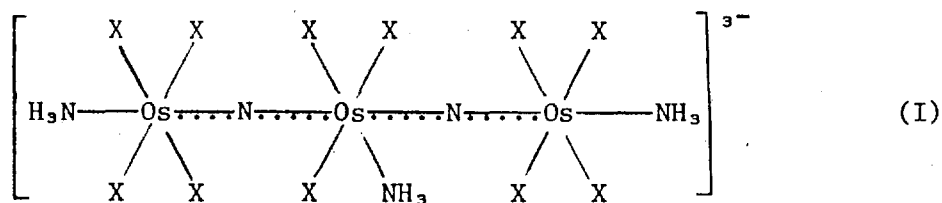
Prolonged reaction of osmium tetraoxide with liquid ammonia produces

a material of empirical formula $Os_3N_7O_9H_{21}$.[33] Based on the infrared

spectra of the compound and deuteriate, the structure $[(NH_3)_2(O)(OH)_2-$

$Os=N-Os(OH)_3(NH_3)-N=Os(NH_3)_2(O)(OH)_2]$ was put forward.[34] Following

a study of ^{15}N-substituted material, an alternative structure (II)

was proposed.[13,15]

$$\ce{HO-Os....N....Os....N....Os-OH} \qquad (II)$$
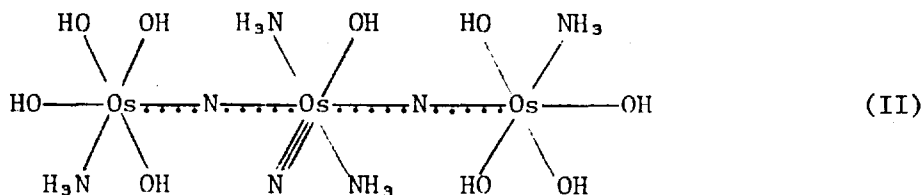
Three bands, sensitive to ^{15}N-substitution, are observed near 1000 cm^{-1} in the infrared and are assigned to Os-N (bridging) and Os-N (terminal) asymmetric stretching vibrations.[15]

Another, closely related osmium ammine complex has been prepared by Gautier, et al.,[35]; following treatment of a solution of the complex with sulphur dioxide, it has been used to visualise aldehydic groups formed by acid hydrolysis of polysaccharides and DNA for electron microscope studies.[35] The preparation of the complex is similar to that of ruthenium red,with osmium tetraoxide in hydrochloric acid being used in place of ruthenium trichloride. A brown-black material is obtained on treatment with ammonia solution and oxygen and heating the mixture, precipitation is induced by addition of ethanol. The ethanol precipitation, however, is probably responsible for bringing down a mixture of species. A simplified preparation, yielding a product with identical electronic and infrared spectra, has been described,[36] merely involving treatment of an aqueous solution of osmium tetraoxide with concentrated aqueous ammonia solution at room temperature. The ammine complex has two infrared bands near 1000 cm^{-1}, assigned to vibrations of a bridging nitrido system.[36]

Binuclear ruthenium and osmium nitrido-bridged species are well known, these include $[Os_2N(NH_3)_8Cl_2]^{3+}$, $[Ru_2N(NH_3)_8Cl_2]^{3+}$, $[Os_2NCl_8(H_2O)_2]^{3-}$ and $[Ru_2NCl_8(H_2O)_2]^{3-}$.[18] The asymmetric stretching vibration $\nu_{M_2N}^{as}$ appears as a strong sharp band in the range 1050-1130 cm^{-1} in the infrared spectra of these complexes and the symmetric $\nu_{M_2N}^{s}$ band in the Raman between 260 and 360 cm^{-1}.[18]

2-A-3 Resonance Raman Spectroscopy.

Alone or in conjunction with infrared spectroscopy, the technique

of Raman spectroscopy affords valuable information concerning the

symmetry and structure of the species under examination. The strong

absorptions in the visible region of the complexes considered in

this Chapter preclude the recording of conventional Raman spectra.

These electronic absorption bands may, however, be put to advantage

since they give rise to resonance Raman spectra,[37] these may be

obtained for dilute samples where photodecomposition may be minimised.[38]

Where the wavelength of the incident light is close to an

electronic absorption band maximum of the species under investigation,

the scattered light is of much greater intensity than that from the

normal Raman effect. The intensity of a resonance-enhanced Raman band

will increase as the wavelength of the incident light approaches the

λ_{max} of the absorption band; the excitation profile so obtained will

be expected to peak close to the position of the resonant electronic

transition.[37] Empirically, those vibrations which determine the vibrational

structure of the absorption band nearest the exciting line appear

with high intensities. Totally symmetric vibrations tend to give the

greatest intensities.[38] Overtone series based on totally symmetric

modes are often observed in resonance enhanced spectra.

A full discussion of the theory underlying the resonance Raman

effect and applications in inorganic chemistry is to be found in

the literature.[39,40]

Section 2-B.   The X-ray Molecular Structure of $[Ru_3O_2(NH_3)_{14}](S_2O_3)_3$-

   $.4H_2O$.[†]

Apart from usefulness in interpreting the infrared and resonance

Raman spectra and in understanding the chemical properties, the

structure of the $[Ru_3O_2(NH_3)_{14}]^{6+}$ cation of ruthenium red is relevant

to the mode and selectivity in binding to biological substrates. An

electron microscopic study of ruthenium red bound to isolated DNA[18]

indicates stacking together of a few molecules of the complex at

specific sites on the DNA strand.

While the chloride salt of ruthenium red yields only microcrystals

unsuitable for X-ray study, the thiosulphate anion readily produces

iridescent green crystals, in a mixture of two forms, both red by

transmitted light. The very thin plates proved more satisfactory

for X-ray scattering, though preliminary results on the long double

needles indicated a similar structure for the cation.

The title compound crystallises in the monoclinic system, space

group $P2_1/c$.[41,42] The unit cell dimensions vary reversibly on

exposure to X-rays; data were collected on a crystal that had stabilised,

with the volume at its highest. Refinement has now reached $R = 0.095$.

High thermal motion and some disorder affects some of the thiosulphate

anions and the water molecules.

The structure of the ruthenium red cation is depicted in Figure 2.1.

As suggested by Fletcher, et al.,[25] it does indeed contain an essentially

linear N-Ru-O-Ru-O-Ru-N backbone, with ammine groups completing the

coordination octahedra of the ruthenium atoms. A similar structure has

---

[†] The structure determination was carried out by Dr. M.A.A.F. de C.T. Carrondo

and Dr.A.C.Skapski.

Figure 2.1.   Structure of the Ruthenium Red Cation in

$[Ru_3O_2(NH_3)_{14}].(S_2O_3)_3.4H_2O.$
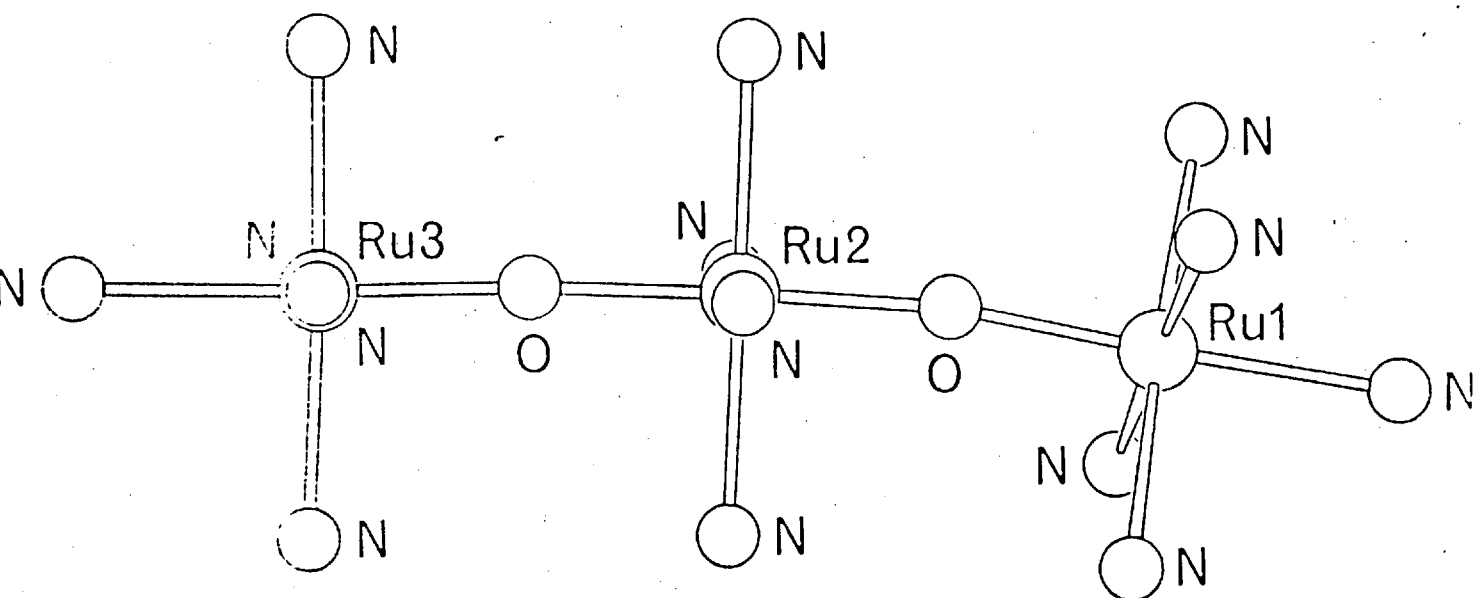
been found for the related 1,2-diaminoethane-substituted ruthenium

red, in which the four ammine ligands on the central ruthenium are

replaced by two bidentate groups.[7] In this second structure, the

N-Ru-N axes through the central ruthenium are twisted at 45° relative

to the Ru-N bonds of the outer groups; the two outer groups being

mutually eclipsed, (as in Figure 2.8b). In the structure of the cation

of non-substituted ruthenium red, the central, Ru(2)-N and one

end, Ru(3)-N bond axes are virtually eclipsed (dihedral angle 4°);

while the Ru(1)-N axes are twisted by 31° with respect to Ru(2)-N,

in the opposite direction (Figure 2.1).

The four Ru-O bond lengths are not significantly different,

falling in the range 1.845-1.857 $\overset{o}{A}$; while the 1,2-diaminoethane-

substituted complex has somewhat longer Ru-O bond lengths (1.850-

1.891 $\overset{o}{A}$).[7] This slight change could be construed as indicating slightly

stronger bonding in the non-substituted species. The backbone of the

thiosulphate salt of the ruthenium red cation shows a slight bend

(8.5° from linearity) in the Ru(1)-O-Ru(2) section, this may be a result

of packing or hydrogen-bonding forces in the crystal. It should be

noted that the 1,2-diaminoethane-substituted cation crystallises without

crystal water, limiting hydrogen bonding to interactions with the

chloride ions only.[7] The fourteen Ru-N bond lengths fall in the

range 2.087-2.172 $\overset{o}{A}$, with a mean of 2.125 $\overset{o}{A}$, and so are unexceptional;

the mean value for the substituted species is similar, at 2.129 $\overset{o}{A}$.

Although a molecular orbital scheme allowing for the observed

linearity of the Ru_3O_2 system and the net diamagnetism of the formally

Ru^{III,III,IV} complex has been constructed for the 45° twisted structure
of the 1,2-diaminoethane complex;[28] the 31° twisted structure of the
non-substituted species does not allow a simple scheme. The stability
of the bonding system is not decreased by the 31° twist, indeed, the
Ru-O bond lengths are slightly shorter in this complex. It is probable
that a totally eclipsed system, or a twisted structure of 45° rather
than 31° is formed in solution. The low symmetry form could be
stabilised by hydrogen bonding or crystal packing forces in the solid
state.

Section 2-C.   Resonance Raman Studies on Ruthenium Red, Ruthenium Brown
               and Related Species.

2-C-1   Introduction.

The intense colour of ruthenium red, arising from the very strong
electronic transition at 537 nm (ε = 67800 M^{-1} cm^{-1}) suggested that
the resonance Raman effect might permit spectra to be obtained from
dilute samples. The system was indeed found to be amenable to study
by this technique, excitation by the 530.9 nm line of a krypton ion
laser yielding good spectra from dilutions of 10^{-5} M (ca. 10 ppm).
Recent studies on the simpler binuclear oxo-bridged systems [Ru$_2$OCℓ_{10}]$^{4-}$,
[Ru$_2$OBr$_{10}$]$^{4-}$, [Os$_2$OCℓ_{10}]$^{4-}$ and [W$_2$OCℓ_{10}]$^{4-}$ [43,44,45] show that resonance
Raman spectroscopy is a good method for studying the oxo bridge. During
the course of our work on the assignment of the resonance Raman bands,
preliminary results of a study of the resonance Raman spectrum of
ruthenium red used as a probe for biological calcium binding sites
appeared.[46]

Figure 2.2. Resonance Raman Spectra of Ruthenium Red, Ruthenium Brown and their 1,2-Diaminoethane Analogues.

(a) $[Ru_3O_2(NH_3)_{14}]^{6+}$
(b) $[Ru_3O_2(NH_3)_{14}]^{7+}$
(c) $[Ru_3O_2(NH_3)_{10}(en)_2]^{6+}$
(d) $[Ru_3O_2(NH_3)_{10}(en)_2]^{7+}$

Aqueous solution (5×10^{-5} M)
Exciting radiation 530.9 nm
(a), (c) and 476.2 nm,(b) and (d)

Raman shift/cm^{-1}
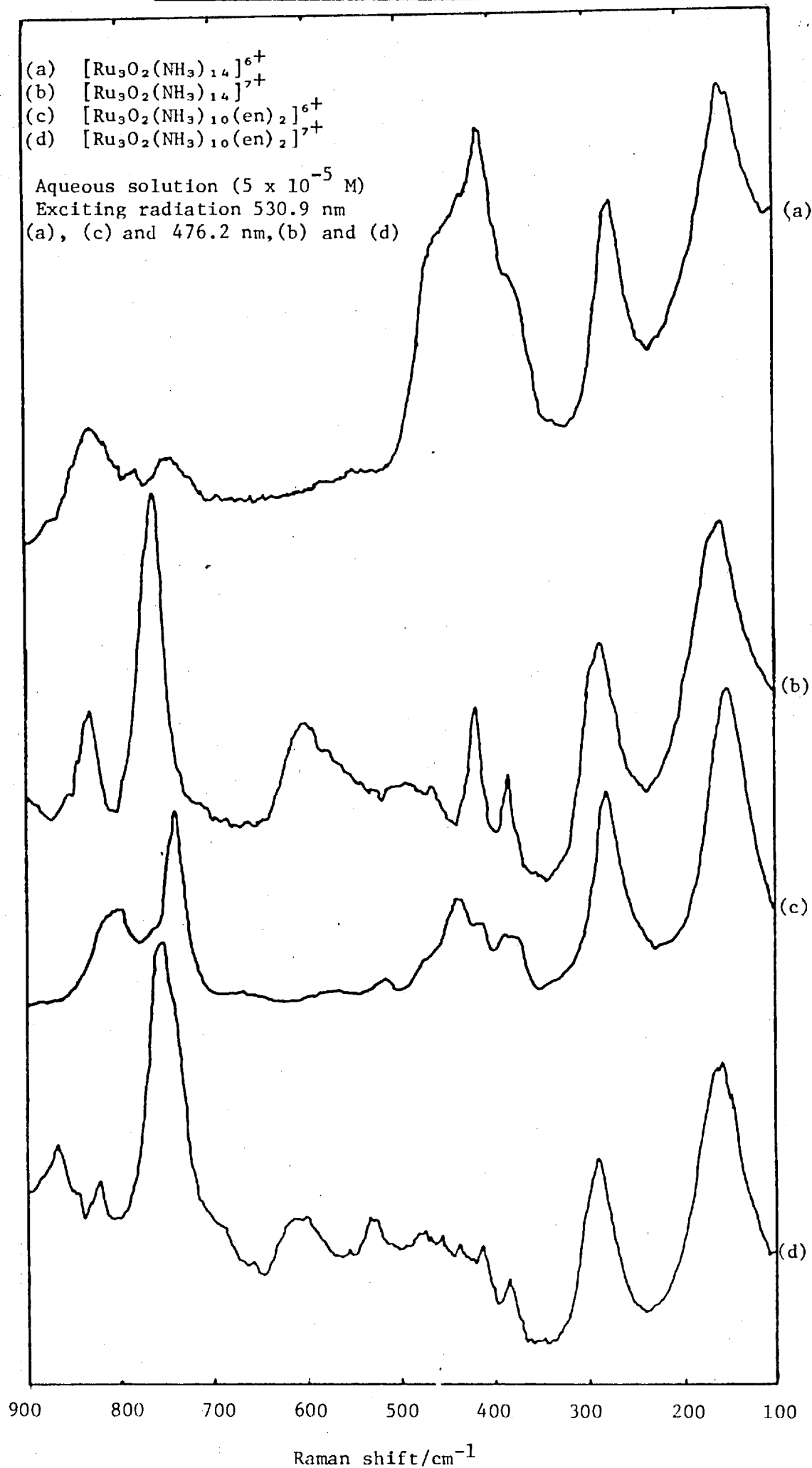
Ruthenium brown, with a strong electronic transition at 459 nm and the 1,2-diaminoethane derivatives of ruthenium red and brown also readily give resonance Raman spectra. The Raman spectra at resonance for ruthenium red, ruthenium brown and their 1,2-diaminoethane derivatives are superimposed in Figure 2.2.

2-C-2 Ruthenium Red.

The Raman spectrum of ruthenium red has been obtained over the range 60-1200 cm^{-1} using excitation at various wavelengths from 450-650 nm, using aqueous solutions 5×10^{-5} M in concentration. Typically, the intensity enhancement from 647.1 nm, which is well clear of the 537 nm electronic absorption band, to 530.9 nm is fifty-fold. Taking into account the different concentrations, the Raman bands of ruthenium red are of the order of 10^4 times more intense than the symmetric stretch ν_1 of the sulphate ion used as a standard, indicating that a strong resonance effect is involved. The spectra recorded for ruthenium red and isotopically substituted species in solution, 530.9 nm excitation, are reproduced in Figure 2.3, wavenumber values and assignments are given in Table 2.1.

Excitation profiles, showing the variation in intensity of eight Raman bands relative to the intensity of the 981 cm^{-1} band of the sulphate ion, with changing excitation wavelength, are shown in Figure 2.4. These results were obtained using seven lines from a krypton ion laser. Better profiles have been obtained on the same sample, (J.R. Campbell, published in reference 47), using a dye laser

Figure 2.3. Resonance Raman Spectra of Normal and Isotopically
Substituted Ruthenium Red.

Raman shift/cm^{-1}
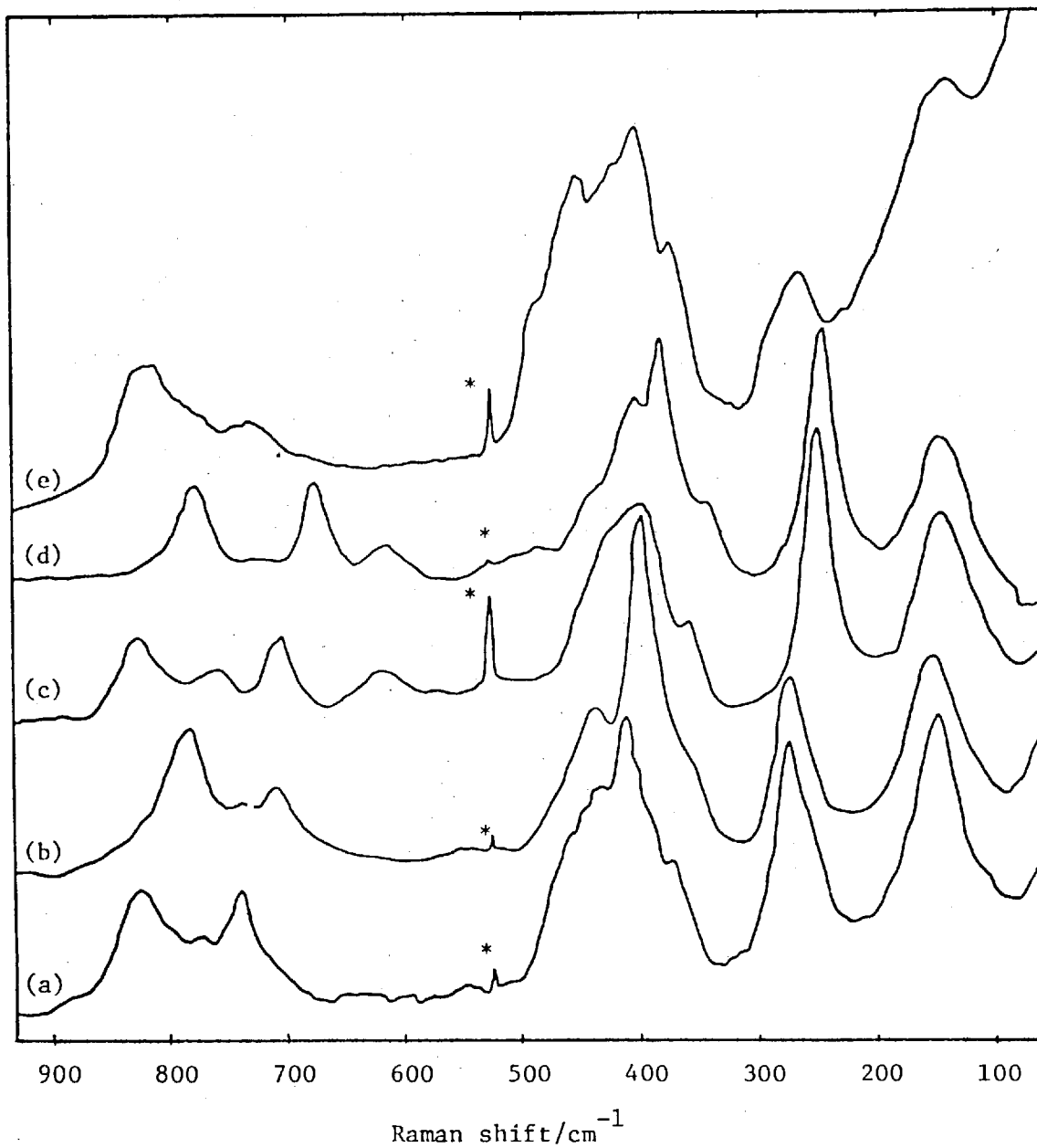
530.9 nm excitation

* Hg line

(a) $^{1}H^{14}N^{16}O$

(b) $^{1}H^{14}N^{18}O$

(c) $^{2}H^{14}N^{16}O$

(d) $^{2}H^{14}N^{18}O$

(e) $^{1}H^{15}N^{16}O$

Table 2.1. Raman Band Wavenumbers for Normal and Isotopically Substituted Ruthenium Red.

	$\nu(RuO)$		$\rho(N_{eq}H_3)$			$\nu(RuN_{eq})$	$\nu(Ru'N')$	$\nu(Ru\cdot N_{ax})$		$\delta(ORuN_{eq})$	$\nu(RuO)$
$[Ru_3O_2(NH_3)_{14}]Cl_6 \cdot 4H_2O$*	816(3)		744(4)	744(4)		477(3)	446(5)	408(10)	375(6)	281(8)	168(9
$[Ru_3O_2(NH_3)_{14}]^{6+}$	827(4)	778(2)	742(4)	742(4)	545($\frac{1}{2}$)	474(2)	443(5)	413(10)	370(2)	274(8)	150(8
ρ	0.30		0.24	0.24			0.32	0.28	0.30	0.27	0.26
$[Ru_3O_2(N^2H_3)_{14}]^{6+}$	825(3)	759(2)	705(3)	615(1)	534(-)	450(2)	428(5)	400(9)	354(2)	250(10)	144(6
$[Ru_3O_2(^{15}NH_3)_{14}]^{6+}$	826(3)	783(1)	731(2)	731(2)		457(2)	430(7)	406(10)	370(2)	270(4)	150(5
$[Ru_3{}^{18}O_2(NH_3)_{14}]^{6+}$	786(4)	739(1)	710(2)	710(2)	546($\frac{1}{2}$)	475(1)	442(4)	397(10)	362(2)	274(5)	151(5
$[Ru_3{}^{18}O_2(N^2H_3)_{14}]^{6+}$	780(4)	718(1)	676(4)	615(2)	523($\frac{1}{2}$)	443(2)	409(5)	384(10)	338(2)	246(10)	144(6
Assignment	$\nu(RuO)$ ν_1		$\rho(N_{eq}H_3)$			$\nu(RuN_{eq})$ ν_2	$\nu(Ru'N')$ ν_3	$\nu(Ru\cdot N_{ax})$ ν_4		$\delta(ORuN_{eq})$ ν_5	$\nu(RuO)$ ν_6

* Solid state spectra. All other data relate to aqueous solutions. Wavenumbers in cm^{-1}; relative intensities in parenthesis. ρ = depolarisation ratio at resonance.

34

Figure 2.4

Excitation Profiles for Raman Bands of Ruthenium Red.

1.2

Electronic
Absorption
Spectrum

0

Absorbance

18

Relative
intensity

12

22

○   150 cm^{-1}

●   274 cm^{-1}

8

8

□ $\left\{\begin{array}{l} 370 \text{ cm}^{-1} \\ 413 \text{ cm}^{-1} \end{array}\right\}$

▨ $\left\{\begin{array}{l} 443 \text{ cm}^{-1} \\ 474 \text{ cm}^{-1} \end{array}\right\}$

10

△   742 cm^{-1}

▲   827 cm^{-1}

420   500   580   660

wavelength/nm
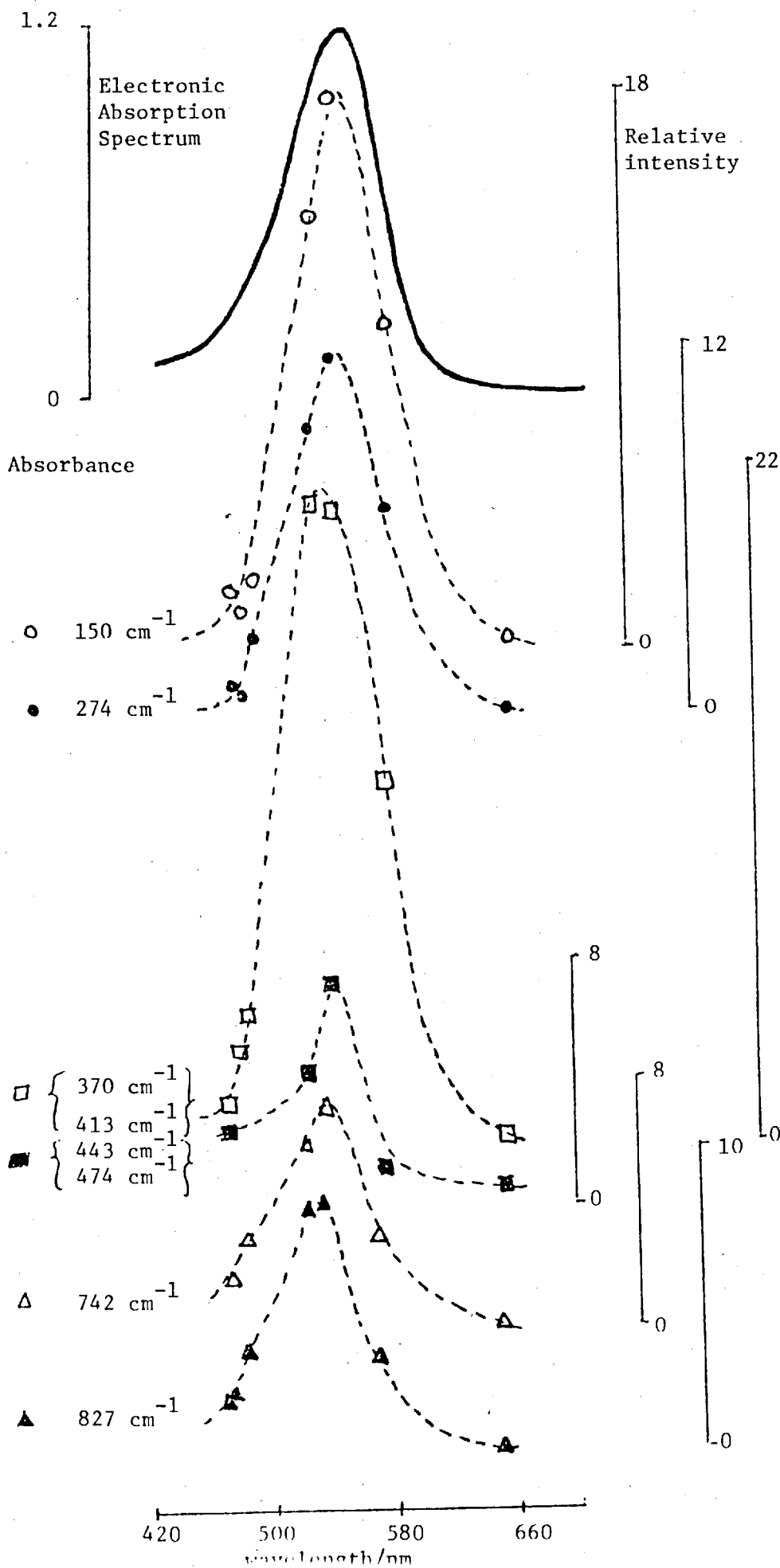
tuneable over the range of interest, providing a better disposition
of points. The peaks of the excitation profiles are in the range
520-540 nm, close to the position of the electronic absorption band
maximum at 537 nm. All the observed resonance Raman bands of ruthenium
red have a depolarisation ratio near 0.3, suggesting axial symmetry
for these modes.[43]

2-C-3 Ruthenium Brown and 1,2-Diaminoethane Derivatives.

The resonance Raman spectrum of ruthenium brown closely resembles
that of ruthenium.red. The spectra recorded for ruthenium brown and
isotopically substituted species in solution, 476.2 nm excitation, are
reproduced in Figure 2.5 , wavenumber values and assignments are given
in Table 2.2. Excitation profiles for eight Raman bands are
depicted in Figure 2.6. The profiles peak around 440-465 nm, close
to the observed electronic transition at 459 nm. Depolarisation
ratio values clcse to 0.3 are found for the resonance Raman bands
in the solution.

Raman wavenumbers for $[Ru_3O_2(NH_3)_{10}(en)_2]^{6+}$ and $[Ru_3O_2(NH_3)_{10}(en)_2]^{7+}$
are given in Table 2.3, and excitation profiles for $[Ru_3O_2(NH_3)_{10}(en)_2]^{6+}$
in Figure 2.7. For the reduced (6+) form, the profiles peak between
530 and 545 nm; the observed electronic absorption band being found
at 534 nm.

2-C-4 Solid-State Raman and Infrared Spectra.

In dilute solid samples (usually potassium bromide discs), ruthenium
red and its closely related derivatives give resonance enhanced spectra

Figure 2.5. Resonance Raman Spectra of Normal and Isotopically Substituted Ruthenium Brown.
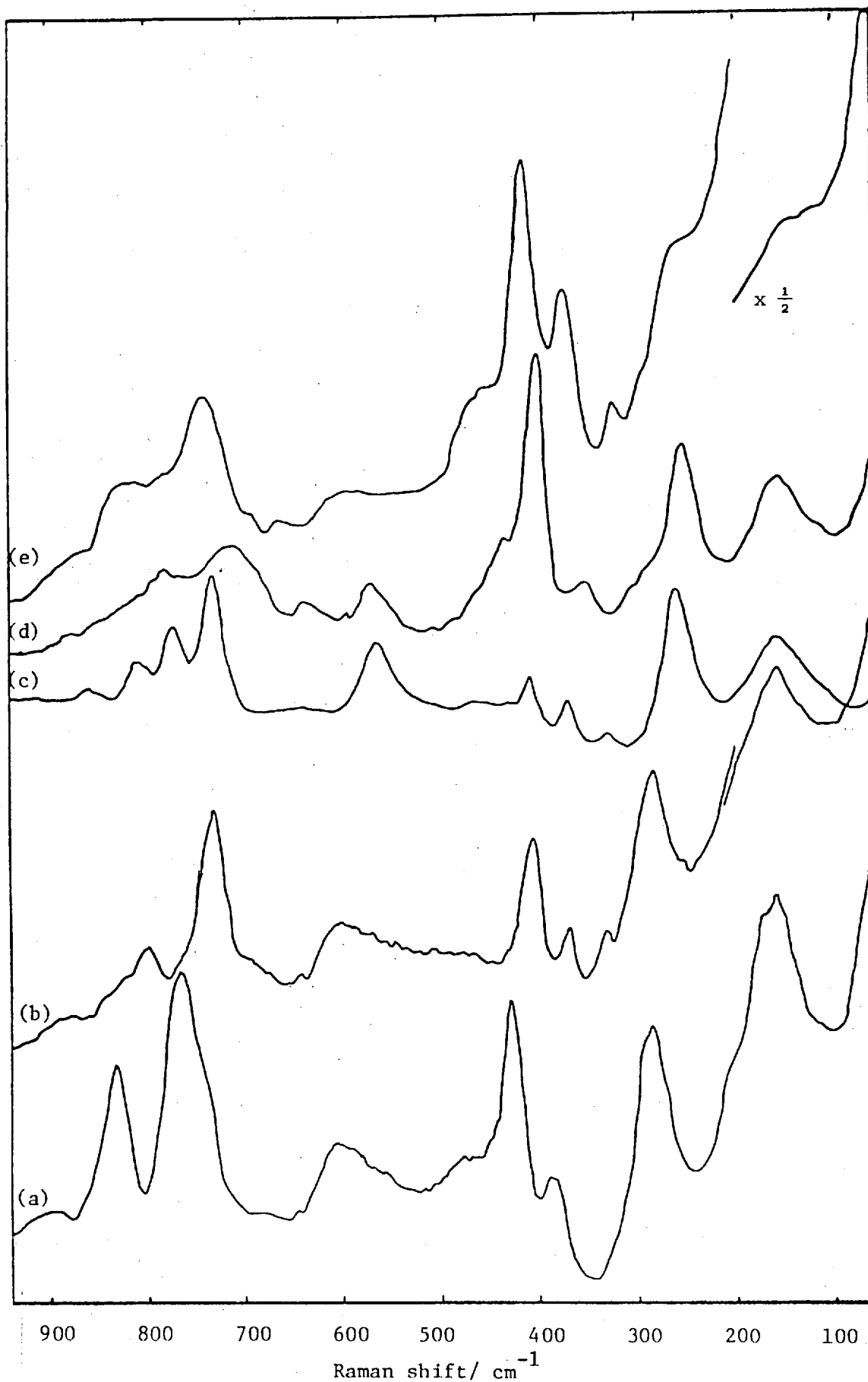
(a) $^1H^{14}N^{16}O$ (d) $^2H^{14}N^{18}O$

(b) $^1H^{14}N^{18}O$ (e) $^1H^{15}N^{16}O$

(c) $^2H^{14}N^{16}O$ 476.2 nm excitation

Table 2.2. Raman Band Wavenumbers for Normal and Isotopically Substituted Ruthenium Brown.

Compound											
$[Ru_3O_2(NH_3)_{14}]Cl_7\cdot4H_2O$*	895(½)	810(2)	745(4)	745(4)	550(1)	480(1)	450(1)	428(3)	373(2)	275(6)	155(10)
$[Ru_3O_2(NH_3)_{14}]^{7+}$		898(1)	829(6)	761(10)	761(10)	599(3)	469(2)	443(2)	424(9)	385(3)	281(8)	157(9)
ρ			0.26	0.28	0.28	0.31		0.44	0.28	0.58	0.31	0.39
$[Ru_3O_2(N^2H_3)_{14}]^{7+}$		856(1)	803(3)	730(9) 770(5)	562(5)	562(5)	458(2)	428(2)	405(4)	368(3)	258(10)	154(6)
$[Ru_3O_2(^{15}NH_3)_{14}]^{7+}$		887(1)	816(3)	738(5)	738(5)		454(2)	obsc.	413(10)	371(4)	270(2)	155(3)
$[Ru_3{}^{18}O_2(NH_3)_{14}]^{7+}$		880(1)	795(2)	728(7)	728(7)	598(2)	467(½)		403(5)	365(2)	282(6)	156(10)
$[Ru_3{}^{18}O_2(N^2H_3)_{14}]^{7+}$		840(½)	778(2)	710(3)	569(2)	569(2)	460(1)	423(3)	401(10)	349(1)	253(6)	153(4)
Assignment		$\nu(RuO)$ ν_1		$\rho(N_{eq}H_3)$			$\nu(RuN_{eq})$ ν_2	$\nu(Ru'N')$ ν_3	$\nu(RuN_{ax})$ ν_4		$\delta(ORuN_{eq})$ ν_5	$\nu(RuO)$ ν_6

* See footnotes to Table 2.1

Figure 2.6

39

Excitation Profiles for Raman Bands of Ruthenium Brown.

0.7

Electronic
Absorption
Spectrum

Absorption

(Data 340-460 nm obtained by
J.R. Campbell, using a Spex
14018 (R6) instrument)

0

8

0

O   157 cm^{-1}

6

•   281 cm^{-1}

4

⊓   385 cm^{-1}

0

6

0

◪   424 cm^{-1}

2

△ $\begin{cases} 443 \text{ cm}^{-1} \\ 469 \text{ cm}^{-1} \end{cases}$

0

4

14

▲   599 cm^{-1}

0

Relative
intensity

▽   761 cm^{-1}

4

0

▼   829 cm^{-1}

4

0

340   420   500

wavelength/nm

comparable to the solution spectra detailed above. The rather broad

(halfwidth ca. 40 cm^{-1}) solution bands sharpen somewhat in the solid

state. The wavenumbers of the resonance Raman bands of the solids are

listed with the solution data in Tables 2.1, 2.2, and 2.3.

Infrared spectra are less informative than the Raman data,

measurements being possible only on solid samples in this case. Some

data previously appeared in the literature[16,25,28] on the infrared

spectra of ruthenium red and ruthenium brown; the spectra of normal

and deuteriated samples of these salts have been measured and are

listed, together with the corresponding data for the 1,2-diaminoethane

derivatives in Table 2.4.

2-C-5 Structure and Group Theory.

The solid-state structures of $[Ru_3O_2(NH_3)_{14}](S_2O_3)_3.4H_2O$ and

$[Ru_3O_2(NH_3)_{10}(en)_2]C\ell_6$ have been discussed in Section 2-B. It is

probable, however, that a change in the conformation of the coordination

octahedra occurs when the cation is freed from the crystal lattice on

solution. Possible structures for the ruthenium red cation in

solution, omitting protons, are depicted in Figure 2.8. At this stage,

it is simpler to consider the structure of highest symmetry, Figure

2.8c (D_{4h}). The effect of rotation of the coordination octahedron

around one end ruthenium atom would be to lower the symmetry and lead

to splitting of vibrational modes. Chemical,[25] polarographic and

electronic spectral data[28] and the similarity of resonance Raman spectra

suggest that ruthenium brown has a very similar structure to ruthenium red.

Table 2.3. Raman Band Wavenumbers for $[Ru_3O_2(NH_3)_{10}(en)_2]^{6+}$ and $[Ru_3O_2(NH_3)_{10}(en)_2]^{7+}$

$[Ru_3O_2(NH_3)_{10}(en)_2]Cl_6$*		814(1)	790(1) 760(½)	736(2)		570(¼)	530(½) 510(½)	470(½)	427(2)	427(2)	368(4) 312(1)	283(4) 240(1)	156(10)
$[Ru_3O_2(NH_3)_{10}(en)_2]^{6+}$ ρ		810(3) 0.33	770(1)	744(6) 0.26		575(½)	521(1)	474(1) 0.25	437(6) 0.28	410(3) 0.29	374(2) 0.28	279(7) 0.27	152(10) 0.27
$[Ru_3O_2(N^2H_3)_{10}(en\text{-}d_4)_2]^{6+}$		798(2)	750(1) 706(3)	616(½)		556(½)	505(½)	442(1)	400(2)	380(1)	354(1)	253(10)	146(10)
$[Ru_3O_2(NH_3)_{10}(en)_2]Cl_7$*	855(3)	815(3)	760 740 (7)	760 740 (7)	690(1)	590(1)	530(2)	470(1) 450(2)	428(4)	410(1)	375(4)	282(7)	160(10)
$[Ru_3O_2(NH_3)_{10}(en)_2]^{7+}$ ρ	870(3)	820(1) 0.33	754(8) 0.31	754(8) 0.31	690(1) 0.35	603(2) 0.22	527(1)	460(1)	435(1)	412(1)	381(2) 0.26	289(6) 0.27	157(10) 0.36
$[Ru_3O_2(N^2H_3)_{10}(en\text{-}d_4)_2]^{7+}$	848(1)	798(1)	736(10)	562(3)		562(3)	492(2)	440(2)	422(2)	400(2)	365(2)	263(10)	150(8)
Assignment		$\nu(RuO)$ ν_1		$\rho(N_{eq}H_3)$				$\nu(RuN_{eq})$ ν_2	$\nu(Ru'N')$ ν_3	$\nu(RuN_{ax})$ ν_4		$\delta(ORuN_{eq})$ ν_5	$\nu(RuO)$ ν_6

* See footnotes to Table 2.1

41

Figure 2.7

Excitation Profiles for Raman Bands of $[Ru_3O_2(NH_3)_{10}(en)_2]^{6+}$.
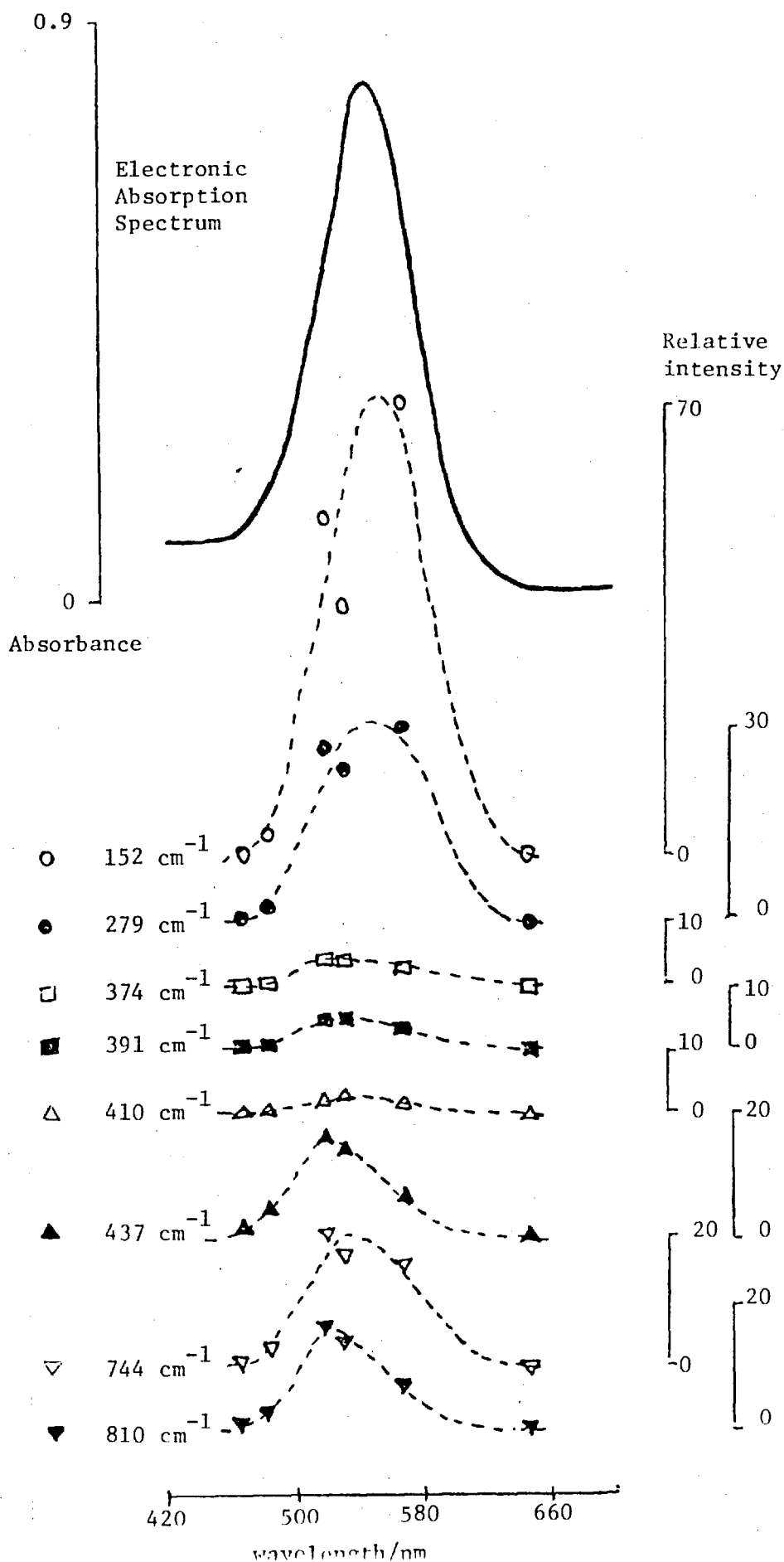
Table 2.4. Infrared Band Maxima/cm^{-1} of Ruthenium Red, Ruthenium Brown and Their 1,2-Diaminoethane Analogues.

	ν(RuO), ρ(NH₃), ρ(NH₂), and ρ(CH₂)	en or H₂O modes	ν(RuN)	ν(RuO), δ(ORuN) and δ(NRuN)
$[Ru_3O_2(NH_3)_{14}]Cl_6.4H_2O$ [a]	845sh, 805s, 753m, 670w	560vw, 520w	470vw, 450m,sp, 425w	318m,sp, 260s, 241, 200
$[Ru_3O_2(N^2H_3)_{14}]Cl_6.4^2H_2O$	780sh, 798s, 650m, 630w	565w, 525w	447sh, 427ms	300s,sp, 260sh, 230s
$[Ru_3O_2(NH_3)_{14}]Cl_7.4H_2O$	845s, 710mw	580w, 535w	478m, 418w	305sh, 280ms
$[Ru_3O_2(N^2H_3)_{14}]Cl_7.4^2H_2O$	820sh, 800ms, 650m	558w	452m, 402w	260sh, 230ms
$[Ru_3O_2(NH_3)_{10}(en)_2]Cl_6$ [b]	825m, 800ms, 785s, 753vw, 700vw	548m	473s, 436ms, 401w	318s,sp, 270s, 230 , 170 , 154
$[Ru_3O_2(N^2H_3)_{10}(en-d_4)_2]Cl_6$	808ms, 778m, 675vw, 641mw, 610mw	573vw, 530vw	448m, 443sh, 415mw, 393w	298s,sp, 250s
$[Ru_3O_2(NH_3)_{10}(en)_2]Cl_7.4H_2O$	840ms, 810ms, 760mw, 690w	590w, 530vw, 508mw	470w, 453vw, 405w	310mw, 283vw, 265m
$[Ru_3O_2(N^2H_3)_{10}(en-d_4)_2]Cl_7.4^2H_2O$	820sh, 797s, 705vw, 660vw, 640w	570vw, 490w	460mw, 395mw,b	320vw, 240m
Assignment	ν(RuO), ρ(NH₃), ρ(NH₂), and ρ(CH₂)	en or H₂O modes	ν(RuN)	ν(RuO), δ(ORuN) and δ(NRuN)

[a] Additional far-infrared bands at 117, 93 and 58 cm^{-1}

[b] Additional far-infrared bands at 123, 95 and 60 cm^{-1}

For the eclipsed D_{4h} structure (Figure 2.8c), group theory gives the distribution of the 51 vibrational modes from the 19 skeletal atoms as:

$$\Gamma_{3N-6} = 6a_{1g} + a_{2g} + 3b_{1g} + 2b_{2g} + 6e_g + a_{1u} + 6a_{2u} + b_{1u} + 3b_{2u} + 8e_u.$$

Of these, seventeen (a_{1g}, b_{1g}, b_{2g}, e_g) will be Raman active, and fourteen (a_{2u}, e_u) infrared active. The a_{1g} symmetry coordinates are given in Figure 2.9.

2-C-6 Assignment of Raman Bands.

The observed depolarisation ratios for the Raman bands of ca. 0.3 is in accordance with axial symmetry for the vibrational modes.[43]

Of the Raman-active modes, only the six a_{1g} polarised modes, in D_{4h} symmetry, are expected. Assignment of these six modes for ruthenium red will be the first step.

The bands for ruthenium red at 827 and 150 cm^{-1} are assigned to ν_1 and ν_6, as predominantly metal-oxygen stretches. The ν_1 mode is mainly a movement of the oxygen atoms between the metal atoms along the z-axis (i.e., the N-Ru-O-Ru-O-Ru-N axis) and will thus be much affected by ^{18}O substitution, as observed, but relatively little by ^2H or ^{15}N substitution. The lower frequency ν_6 mode involves movement of the outer RuN_5 units of the backbone rather than of the oxygen atoms, ^2H or ^{15}N substitution will increase the effective masses of the terminal $Ru(NH_3)_5$ groups and so the band should be sensitive to such isotopic substitution but relatively unaffected by ^{18}O substitution, as observed. These frequencies for ruthenium red, in which the average metal-oxygen distance is 1.851 Å,[42] may be compared with 887 and 256 cm^{-1}

Figure 2.8.   Possible Structures of the Ruthenium Red Cation in Solution.

C_{4v} a

D_{4h} b

D_{4h} c
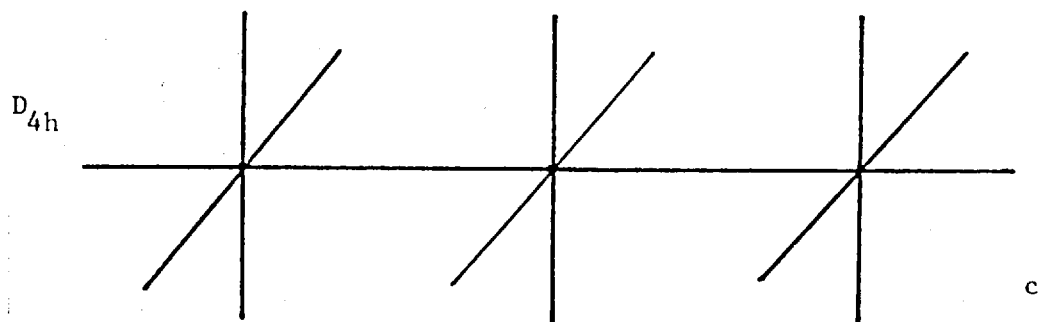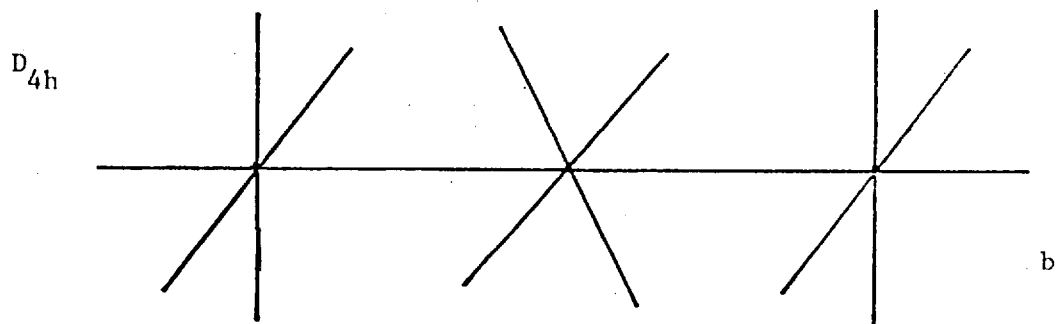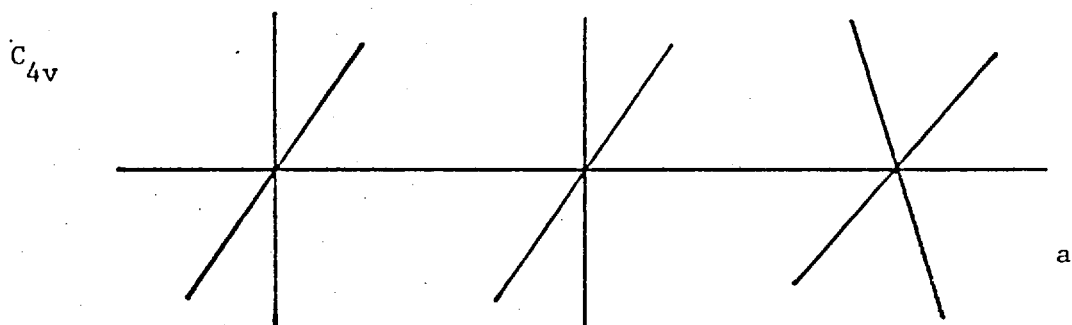
Figure 2.9

a_{1g} Symmetry Coordinates, D_{4h} Eclipsed Structure.

$\nu_s(ORu'O)$ ν_1

$\nu_s(RuN_{eq})$ ν_2

$\nu_s(Ru'N')$ ν_3

$\nu_s(RuN_{ax})$ ν_4

$\delta_s(ORuN_{eq})$ ν_5

$\nu_s(RuO)$ ν_6
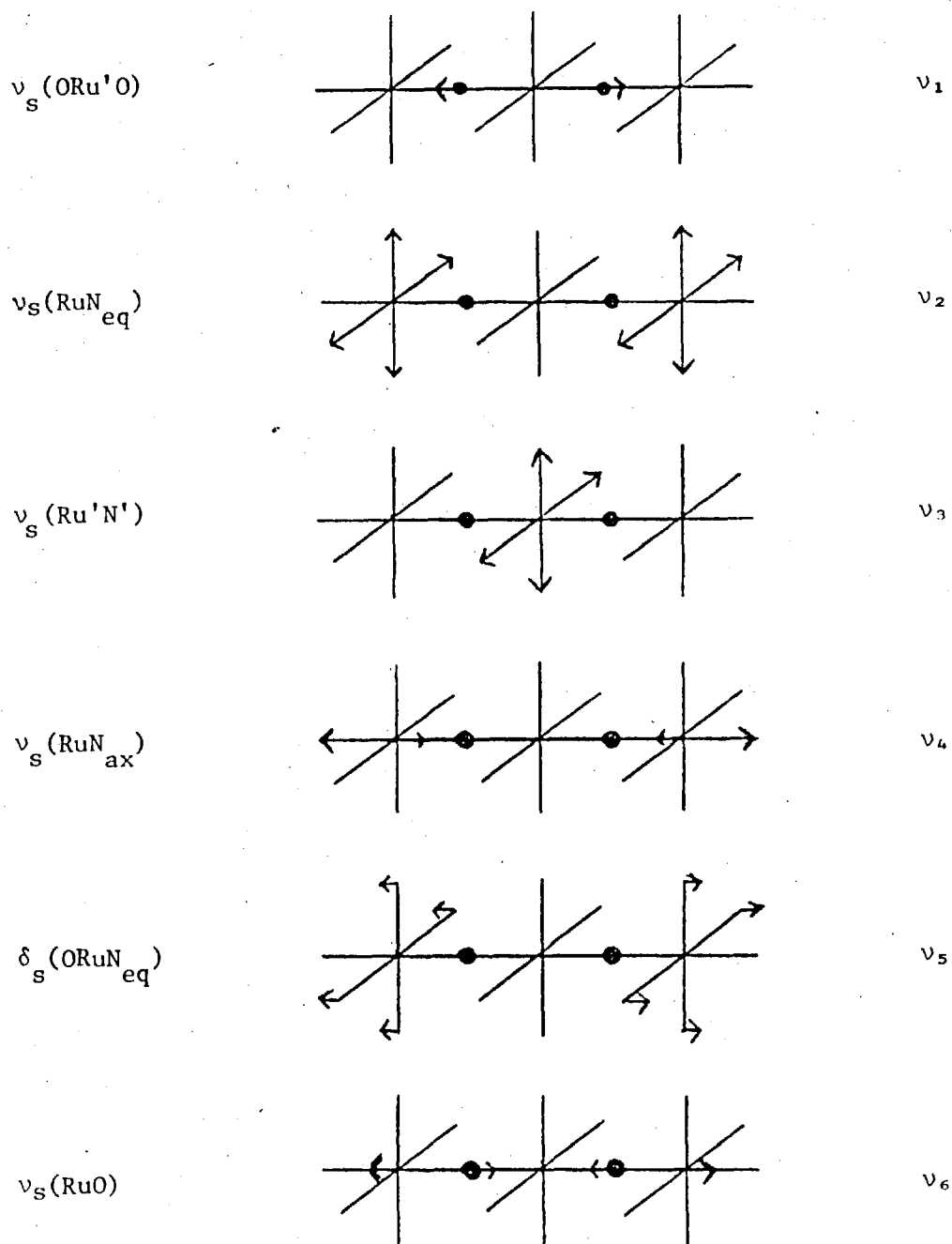
for the asymmetric (infrared active) and symmetric (Raman active)

Ru_2O stretches in $K_4[Ru_2OCl_{10}]$,[43] which has Ru-O bond lengths of

1.801 $\overset{o}{A}$,[4] a slightly shorter and therefore stronger bond.

The other four a_{1g} modes principally concern the metal-ammine

stretches ν_2 (equatorial Ru'-N' stretch of the central RuN_4 unit),

ν_3 (equatorial stretch of the terminal RuN_4 units), ν_4 (Ru-N axial

stretch) and the deformation $\delta(ORuN_{eq})$, ν_5. In the normal Raman spectra

of comparable complexes, $\nu(Ru-N)$ frequencies are found between 500-

463 cm^{-1} and $\delta NRuN$ near 270 cm^{-1} in $[Ru(NH_3)_6]Cl_3$,[48] at 520-428 cm^{-1}

and 230 cm^{-1} in $[Ru_2(N_2)(NH_3)_{10}]Cl_4$;[49] and at 488-454 and 256-240 cm^{-1}

in $[Ru(NH_3)_5Cl]Cl_2$.[50] The 413 cm^{-1} band of ruthenium red, which

is much affected by ^2H, ^{15}N or ^{18}O substitution, is now assigned as

ν_4; the somewhat low frequency may be due to coupling of this axial

mode with the Ru-O stretching modes, as these ammine groups are _trans_

to the oxo ligand; hence the shift on ^{18}O substitution. The 474 and

443 cm^{-1} bands are then good candidates for ν_2 and ν_3; they are unlikely

to be coupled with axial Ru-O stretches and are little affected by

^{18}O substitution, but do change with ^2H or ^{15}N substitution. The lower

frequency for ν_3 is consistent with the known lability of the central

ammine groups in ruthenium red (e.g., ease of replacement by 1,2-diamino-

ethane) relative to the end groups. Finally, the band at 274 cm^{-1} in

ruthenium red, being little affected by ^{18}O substitution but very

sensitive to ^2H or ^{15}N substitution is likely to be the deformation ν_5.

Assignment of the remaining bands in the spectra in this simplified

scheme now requires allowance to be made for the protonic modes or

the possible lower symmetry for the cations. Thus, the band in the spectrum

of ruthenium red at 742 cm^{-1} may well arise from the symmetric $\rho_s(NH_3)$

rocking mode , where the protons of the equatorial ammine groups

on the terminal ruthenium atoms are moving parallel to the RuORuORu axis. In [Ru(NH$_3$)$_6$]Cℓ_3[48] the ρ(NH$_3$) rocking mode appears at 788 cm^{-1}. On deuteriation, the 742 cm^{-1} band of ruthenium red drops to 615 cm^{-1}, comparable with the drop on deuteriation of the analogous mode in [Ru(NH$_3$)$_6$]Cℓ_3.[48] A second band, behaving differently on isotopic substitution, also appears at 742 cm^{-1} in the spectrum of normal ruthenium red, ' and as for the band at 778 cm^{-1}, no positive assignment can be offered. The 370 cm^{-1} band, which is sensitive both to ^{2}H and ^{18}O substitution, and a weak band at 545 cm^{-1} are also difficult to assign. Assignment as bands due to coordinated water following aquation of an ammine ligand can be ruled out, as the bands persist in strongly ammoniacal solution, or in the solid state.

The same general guidelines are used to assign the ν_1-ν_6 and ρ_s(NH$_3$) modes for ruthenium brown and the 1,2-diaminoethane analogues. Assignments are given in Tables 2.2 and 2.3. The 1,2-diaminoethane species exhibit slightly more bands than the parent compounds; though no bands are seen that may be assigned to stretches or deformations of the N-CH$_2$-CH$_2$-N system. The increase in the number of bands may then be due to the decrease in symmetry, e.g., D$_{4h}$ to D$_{2h}$, caused by the presence of the bidentate ligands.

2-C-7 Absence of Overtones; Presence of Sulphate Ions.

No overtones of the Raman bands of ruthenium red are observed; and in this respect the system differs from K$_4$[Ru$_2$OCℓ_{10}] where well-defined progressions on ν_1 and other modes are seen both in the solid state and in solution.[43] An absence of overtones has also been noted in the resonance Raman spectra of [Pd$_3$(CNCH$_3$)$_8$](PF$_6$)$_2$,[51]

$[Pd_3(CNCH_3)_8(P(C_6H_5)_3)_2](PF_6)_2$,[51] and $[C\ell Re(PMe_2Ph)_4-N=N-MoC\ell_4-N=N-Re(PMe_2Ph)_4C\ell]$. [52]

It was found that the presence of the sulphate ion, used as a reference for excitation profile measurement, at concentrations near 0.1 M, lead to a net increase in intensity of all the Raman bands compared to the band intensities for the complex in water alone. Most affected by this were, for ruthenium red, the 742 and 413 cm^{-1} bands, the latter also moving to 397 cm^{-1} in 0.1 M Na_2SO_4 solution. The reported sensitivity of this band to the environment in biological systems,[46] interacting with anionic sites, is another manifestation of the same effect. Ruthenium red displays a metachromic effect, the electronic absorption maximum moving to longer wavelengths, with an increase in the extinction coefficient, in the presence of anionic species such as polygalacturonic acid (which binds Ca^{2+} and ruthenium red) and chloride ion.[53] Interactions between ruthenium red cations, at high concentrations, or when in close proximity on binding to biopolymers in an ordered arrangement,[18] or in the presence of high concentrations of other ionic species, would lead to changes in the electron distribution and polarisability and so affect the electronic and resonance Raman spectra.

Force constant calculations have been performed on the resonance Raman data presented in this section, by Campbell (details in reference 47). The assignments of the 827, 413, 274 and 150 cm^{-1} bands of ruthenium red were confirmed and the Ru-O bond force constant was calculated to be 3.67 mdyn $\overset{o}{A}^{-1}$ for ruthenium red, and 3.83, 3.62 and 3.78 mdyn $\overset{o}{A}^{-1}$ for ruthenium brown and the two 1,2-diaminoethane derivatives.[47]

Section 2-D. Trinuclear Ruthenium Ammine Complexes.

2-D-1 Ruthenium Red.

Preparation of Normal and Isotopically Substituted Forms.

Methods of preparing ruthenium red have been well described

in the literature,[22,25,28] supplemented by a scheme for its purification.[19]

Reaction of the mononuclear species [Ru(NH₃)₅Cl]Cl₂ with aqueous

ammonia in the presence of oxygen also generates ruthenium red; this

method was used to prepare the ^{18}O substituted complex, which was

required for aiding the assignment of the Raman bands. Exclusion of

oxygen was found to inhibit the formation of the complex, suggesting

that the oxidation from $3Ru^{III}$ to Ru^{III}, Ru^{IV}, Ru^{III} is by oxygen.

A mechanism for the formation of ruthenium red could thus be seen

to involve the generation of species such as $[Ru(NH_3)_5(H_2O)]^{3+}$ and

$[Ru(NH_3)_4(H_2O)_2]^{3+}$; conversion to $[Ru(NH_3)_5(OH)]^{2+}$ would then lead

to hydroxo-bridged complexes, followed by deprotonation to yield oxo-

bridged species. On monitoring the resonance Raman spectrum of a

dilute solution of $[Ru_3{}^{16}O_2(N^2H_3)_{14}]Cl_6$ in $^2H_2{}^{18}O$, it was established

that no exchange of the bridging ^{16}O had taken place over four weeks.

Polarography and Cyclic Voltammetry of Ruthenium Red.

In addition to the potential corresponding to the polarographic

oxidation of ruthenium red to ruthenium brown at +0.49 V, a

reduction wave for ruthenium red near -0.6 V has been observed,

although no experimental details are given.[28] A closer investigation

of the polarographic properties of ruthenium red has now been carried

out, using a deoxygenated, chloride-free 10^{-4} M solution of ruthenium

red nitrate in 0.1 M sodium perchlorate solution, in the presence of

a maximum suppressant (Triton X100) at the dropping mercury electrode.

The reduction wave is observed at -0.59 ± 0.02 V vs. the SCE. The shape of a cyclic voltammagram obtained at a hanging drop mercury electrode suggested that this reduction is non-reversible. Electrolysis at the controlled potential of -0.8 V of a deoxygenated 10^{-4} M solution of ruthenium red in 0.1 M sodium chloride caused the loss of the 537 nm maximum in the electronic spectrum due to $[Ru_3O_2(NH_3)_{14}]^{6+}$, and hence the red colour; a band near 295 nm appeared, which is probably due to a mononuclear species such as $[Ru(NH_3)_5Cl]Cl_2$ (335 nm) or $[Ru(NH_3)_6]Cl_3$ (290 nm). Ruthenium red was not reformed on addition of an oxidising agent such as hydrogen peroxide. Reduction of ruthenium red thus appears to proceed, after the gain of one electron, to the 5+ charged cation, which if not oxidised back very rapidly, will decompose to mononuclear species;

$$[Ru_3O_2(NH_3)_{14}]^{6+} \; \underset{-e}{\overset{e}{\rightleftharpoons}} \; [Ru_3O_2(NH_3)_{14}]^{5+} \longrightarrow \text{mononuclear Ru}^{III} \text{ complexes}$$
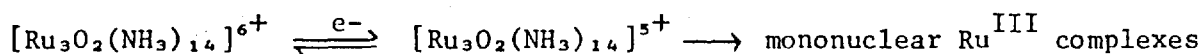
Chemical Reactions.

Reaction of ruthenium red with SO_2 or HSO_3^- and SO_2 in warm aqueous solution again leads to the reduction and breakdown of the trinuclear system, the product being mainly $[Ru(NH_3)_4(HSO_3)_2]$; see Chapter 3 (sulphito complexes). The major product obtained on treatment of ruthenium red with hot aqueous potassium cyanide is $K_4[Ru(CN)_6]$; some unreacted ruthenium red is precipitated as the insoluble brown salt $[Ru_3O_2(NH_3)_{14}]_2^{6+}[Ru(CN)_6]_3^{4-}.12H_2O$. This behaviour with cyanide may be contrasted with that of the binuclear species $K_3[Ru_2NCl_8(H_2O)_2]$, which forms $K_5[Ru_2N(CN)_{10}]3H_2O$ [9]; and the related trinuclear nitrido-bridged osmium species (Section 2-E) which form stable cyano-substituted trinuclear complexes.

Ruthenium Brown.

Oxidation of ruthenium red by dilute hydrogen peroxide in the presence of acid gives ruthenium brown. Another convenient method in aqueous solution is the use of Ce^{IV}, which, as $(NH_4)_2[Ce(NO_3)_6]$, was used to convert isotopically (e.g., ^{18}O, ^{15}N) substituted ruthenium red to ruthenium brown without loss of the label.

The reduction of the nitrate salt of ruthenium brown by sodium sulphite has been monitored using a magnetic titration balance by Dr. N.B. Pouzder,[54] μ_{eff} decreasing by 1.10 B.M. per molecule.

Molecular Orbital Scheme for Ruthenium Red.

Earley and Fealey[28] present a molecular orbital scheme for the 1,2-diaminoethane derivative of ruthenium red, with the central RuN_4 unit rotated by 45° relative to the eclipsed terminal RuN_4 units, as found in the solid state.[7] The energy spacings of the orbitals were arranged to suit the observed electronic spectra,[28] although a band they assign to ruthenium red at 13200 cm^{-1} (758 nm) coincides with the main absorption band of ruthenium violet (Section 2-D-3), an impurity often found with ruthenium red. A revised ordering of the orbitals in this D_{4h} scheme, on the basis that the lowest energy transition corresponds to the 537 nm electronic absorption band of ruthenium red, $(e_g^* \leftarrow e_u)$ is :

Figure 2.10. Molecular Orbital Scheme for Ruthenium Red.
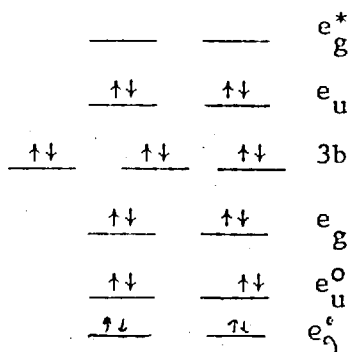
(modified from ref. 28)

This scheme closely resembles that of Campbell[47] for a totally eclipsed structure, the e_u orbital is now described as antibonding rather than non-bonding.

2-D-2 Pyridine-Substituted Complex.

Attempts to prepare other substituted forms of ruthenium red in a manner analogous to that for the 1,2-diaminoethane complex[7] using other amines such as pyridine, ethylamine or triethylene tetramine were unsuccessful. When, however, pyridine was introduced into the preparation of ruthenium red from ruthenium trichloride prior to the addition of ammonia solution a green material was formed, together with a yellow solid, identified as $[Ru(py)_4C\ell_2]$. This green solid is soluble in ethanol and in water, giving a blue solution. The main absorption maximum is at 610 nm ($\epsilon = 11300$ M^{-1} cm^{-1}) ; on undergoing a reversible oxidation, a non-isolable red species results (515 nm,ϵ 6640 M^{-1} cm^{-1}). The infrared spectrum of the blue complex does not greatly differ from that of ruthenium red, with few extra bands being evident. Frequencies are listed in Table 2.5.

The intense colour of the solution suggested that resonance Raman spectra could be obtained with 568.2 nm or 647.1 nm excitation. The spectra obtained closely resemble those of ruthenium red, implying a similarity of structure; wavenumber values are listed in Table 2.5. The Raman bands (100-1000 cm^{-1}) have depolarisation ratios close to 0.3, indicating axial symmetry. The pyridine-containing complex has strong resonance Raman bands at 812 and 130 cm^{-1}, corresponding to the 827 (ν_1) and 150 (ν_6) cm^{-1} ruthenium red bands. Other bands in the spectrum of the pyridine complex have close counterparts; (ruthenium red bands in brackets) 765 (778, $\rho(NH_3)$), 465 (474, ν_2), 408 (413, ν_4)

Table 2.5

Raman Band Wavenumbers for the Pyridine Complex, $[Ru_3O_2(NH_3)_{10}(py)_4]Cl_8 \cdot 2H_2O$.

Solid State (568.2 nm excitation)	806(3)	754(3)	645(2)	461(4)	412(8)	382(10)	327(2)	293(5)	–	145(8)
Solution (647.1 nm excitation)	812(3)	765(3)	645(1)	465(4)	408(4)	388(9)	335(2)	305(10)	200(2)	130(9)
ρ	0.31	0.32	0.29	0.29	0.32	0.33	–	0.35	–	0.34
Assignment	ν(Ru–O)	ρ(NH$_3$)	py. def.	ν(Ru–N$_{eq}$)	ν(Ru–N$_{ax}$)	–	–	δ(ORuN$_{eq}$)	ν(Ru–py)	ν(Ru–O)

Frequencies in cm^{-1}, relative intensities in parentheses, ρ = depolarisation ratio.

Infrared spectrum, potassium bromide disc : 3340sh, 3000s,b, 1580m, 1470vw, 1430sh, 1385ms, 1275ms, 1215sh, 1130w,b, 1000w,b, 790sh, 750ms, 687ms, 530w, 450w.

and 305 (274, ν_5). The Ru-N$_{py}$ stretch is best assigned to the

200 cm^{-1} band, observed at 208 cm^{-1} (e$_g$) and 229 cm^{-1} (a$_{1g}$) for

[Pt(py)$_4$]Cℓ_2.2H$_2$O.[55] Assuming identical force constant values,

the mass difference ($\sqrt{17/79}$) predicts a drop to 216 cm^{-1} for the

metal-pyridine stretching frequency from the 465 cm^{-1} observed

for the NH$_3$ ligands. The 645 cm^{-1} Raman band in [Ru$_3$O$_2$(NH$_3$)$_{10}$(py)$_4$]Cℓ_8

corresponds to an in-plane pyridine ring deformation, seen at 650 cm^{-1}

in the infrared spectrum of trans-[RhCℓ_3(py)$_3$].[56]

It is reasonable on the basis of the Raman spectrum to postulate

a Ru-O-Ru-O-Ru backbone for this species. Analytical data indicate

a formulation as [Ru$_3$O$_2$(NH$_3$)$_{10}$(py)$_4$]Cℓ_8.2H$_2$O, in which the four

pyridine moieties are likely to be coordinated to the central

ruthenium atom. This formula implies a higher oxidation state

for the ruthenium, an average of +4, compared to ruthenium red,

average $+3\frac{1}{3}$. The effective magnetic moment of μ_{eff} = 1.33 B.M. for the

Ru$_3$O$_2$ trimeric molecule, compared to μ_{eff} = 0.68 B.M. for the ruthenium

red and 2.07 B.M. for ruthenium brown (Section 2-H-1), is higher than

expected for a ruthenium IV, IV, IV species, although not sufficiently

paramagnetic for a IV, III, IV state, as is formally found for ruthenium

brown.

2-D-3 Ruthenium Violet.

Fletcher, et al.,[25] noticed a band in the electronic spectrum at

725 nm, assigned to an impurity, in their samples of ruthenium red.

This material was later separated out by Luft who named it " Ruthenium

Violet" , the main electronic band being at 734 nm.[19] In view of

its usefulness as a stain,[19] behaving in a similar fashion to ruthenium

red, identification of the compound is desirable. Since extraction

from ruthenium red preparations yields small quantities only of ruthenium violet, an alternative route was sought. A modification of the literature preparation of ruthenium red,[25] carrying out the reaction for a longer period at a lower temperature, produces a greater amount of the blue-black solid; the main, broad electronic absorption band is at 750 nm (ε = 19900 M^{-1} cm^{-1}).

This complex gives resonance-enhanced Raman spectra, closely resembling those of the trinuclear nitrido-bridged osmium complex, osmium violet, discussed in Section 2-E-1. In particular, the 1060 and 315 cm^{-1} Raman bands correspond to the 1100 and 222 cm^{-1} bands of osmium violet, assigned as stretching modes of the M_3N_2 backbone. Material prepared using $^{15}NH_3$ gave a poor Raman spectrum. The infrared and Raman spectra of ruthenium violet are included in Table 2.7. Ruthenium violet often gives a poor infrared spectrum, depending on the degree of hydration (no spectrum could be obtained for a deuteriated sample); where spectra were obtained, the characteristic ammine bands were present, but bands near 300 cm^{-1} due to coordinated chloride were absent. A broad band near 1040 cm^{-1} suggests the presence of a nitrido group; the binuclear complex $[Ru_2N(NH_3)_8C\ell_2]C\ell_3$ has the asymmetric stretch $\nu_{Ru_2N}^{as}$ at 1050 cm^{-1} in the infrared.[13]

The formula best in agreement with the properties and analytical data for ruthenium violet is $[Ru_3N_2(NH_3)_8(H_2O)_5(OH)]C\ell_5$, which requires for the ruthenium an average oxidation state of +4, a value indicated by its X-ray photoelectron spectrum, Section 2-F-1. In an attempted determination of the oxidation state of the ruthenium, by the use of cerium(IV), it was found that the ceric ion was consumed in a side reaction, besides oxidising the ruthenium to Ru^{VIII},

in a similar fashion to that observed for ruthenium red.[25] The observed low effective magnetic moment for ruthenium violet (μ_{eff} = 0.80 B.M.) indicates an even total oxidation state, for no unpaired electrons. Conductivity measurements indicate that the complex is a 5:1 electrolyte in aqueous solution. The above formula is very similar to that of osmium violet, $[Os_3N_2(NH_3)_8(H_2O)_6]Cl_6$. Deprotonation of an aquo ligand to give a coordinated hydroxo group, under some conditions, appears to take place also for the osmium complex.

Reaction of ruthenium violet with hot aqueous potassium cyanide gave $K_4[Ru(CN)_6]$ as the main product. The corresponding osmium nitrido complexes yield nitrido-bridged trinuclear cyano complexes under similar conditions indicating the Ru_3N_2 system is less stable than the Os_3N_2 system.

Ruthenium tetraoxide in carbon tetrachloride solution reacts with aqueous ammonia to produce a black compound. This resembles the reported $Ru_4N_{11}O_{12}H_{33}$, obtained from RuO_4 and gaseous ammonia at -70 °C.[29] The new compound has a single rather broad band at 1030-1040 cm^{-1} in the infrared spectrum, assigned to a nitrido group. A band observed near 1830 cm^{-1} is characteristic of a coordinated nitrosyl group ($[Ru(NO)(NH_3)_5]Cl_3$ has ν_{NO} at 1903 cm^{-1}),[15] which results from the oxidation of ammonia by ruthenium tetraoxide. A possible formulation based on the analytical data is $[Ru_3^{IV}N_2(NH_3)_4(NO)(OH)_7(H_2O)_2]$.

Section 2-E.   Polynuclear Osmium Complexes.

2-E-1   Osmium Violet.

The osmium-based analogue of ruthenium red, " $[Os_3O_2(NH_3)_{14}]^{6+}$"

might well have many desirable properties for the staining of tissue

samples, the increased electron density arising from osmium, perhaps

diminishing the need for counterstaining.   Having found that ruthenium

red, on treatment with sulphur dioxide acted as a Schiff-type

reagent for acid-hydrolysed DNA,[57] Gautier, et al., set out to make

an osmium-containing version of ruthenium red.   The product, derived

from osmium tetraoxide,[35] appears to be a nitrido-bridged hydroxo-

ammine complex.[36]   Reaction of a range of osmium starting materials

has been carried out with the aim of preparing the osmium analogue of

ruthenium red.   The main ammine product obtained, however, closely

resembles ruthenium violet (Section 2-D-3) rather than ruthenium red;

this new osmium complex, which gives deep blue-violet aqueous solutions

has thus been named " Osmium Violet" .

A convenient method of preparing osmium violet is by reacting

$[OsCl_6]^{2-}$ with ammonia solution near 100 °C in a pressure bottle to stop

the loss of ammonia.   The same compound may be obtained from osmium

tetraoxide or the pentammine $[Os(NH_3)_5Cl]Cl_2$ as the starting material.

Other products from these reactions are the brown-black species

" Osmium Brown" , discussed in Section 2-E-2 and binuclear complexes

such as $[Os_2N(NH_3)_8Cl_2]Cl_3$.   The properties of osmium violet as a stain

are discussed in Section 2-G.   A related species is obtained by reaction

of $[OsBr_6]^{2-}$ with ammonia solution, (vibrational spectra in Table 2.7).

Spectra, Structure and Properties.

The frequencies for the infrared and Raman spectra of osmium

violet and isotopically substituted species are listed in Table 2.6.

The characteristic infrared bands at 1078, 1040 and 1020 cm^{-1}

suggest the presence of bridging nitrido groups in osmium violet;

the binuclear species $[Os_2N(NH_3)_8C\ell_2]C\ell_3$ shows a strong absorption

in this region, at 1104 cm^{-1},[13] assigned to the metal-nitrido

stretching vibration $\nu^{as}_{Os_2N}$. These osmium violet bands are barely

affected by deuteriation, but are shifted by ca. 20 cm^{-1} to lower

wavenumbers on ^{15}N substitution. Bands in regions typical for an

ammine complex are observed, but no bands due to coordinated halogen

are seen. Coordinated water is also evident.

The chemical properties of this complex are in accordance with

two nitrido bridges linking three osmium atoms, a structure which

has been postulated for other osmium nitrido species.[9,13,36]

Hot concentrated sodium hydroxide liberates eight out of ten

nitrogen atoms as ammonia, which suggests that two nitrogen atoms

remain bound to three osmium atoms. Analytical data also indicate

six chlorine atoms for three osmium atoms; the chlorine is readily

replaced, in aqueous solution, by other anions, such as pyrophosphate

or thiosulphate and the resulting sparingly soluble salts contain

no chlorine. No infrared bands characteristic of coordinated $-NH_2$

(near 540 cm^{-1})[14] or $-NH$ (near 660 cm^{-1})[14] are observed. Thus, the

empirical ratio $3Os : 2N^{3-} : 8NH_3 : 6C\ell^-$ is obtained. If higher

polymers are ruled out as likely to have a very low solubility, then

the argument is in favour of a trinuclear complex. Oxidation state

determinations (Section 2-F-2) indicate an average of +4 for the

osmium atoms; the same value is also suggested by X-ray photoelectron

spectroscopy results (Section 2-F-1). This oxidation state, the same

as for the $[OsCl_6]^{2-}$ starting material, is in agreement with the

observed near diamagnetism (μ_{eff} = 0.64 B.M.) of the product. To

fit this oxidation state requirement, the remaining ligands to fill

the osmium coordination octahedra must be neutral, e.g., water.

The complex may thus be formulated as $[Os_3N_2(NH_3)_8(H_2O)_6]Cl_6$. At

this stage it is not possible to determine the arrangement of NH_3

and H_2O ligands around the osmium atoms, the general structure is:

$$\left[\begin{array}{ccccc} L\quad L & & L\quad L & & L\quad L \\ |\,/ & & |\,/ & & |\,/ \\ L{-}{-}Os{\cdots}N{\cdots}Os{\cdots}N{\cdots}Os{-}{-}L \\ /| & & /| & & /| \\ L\quad L & & L\quad L & & L\quad L \end{array} \right]^{6+} \qquad 6Cl^-$$
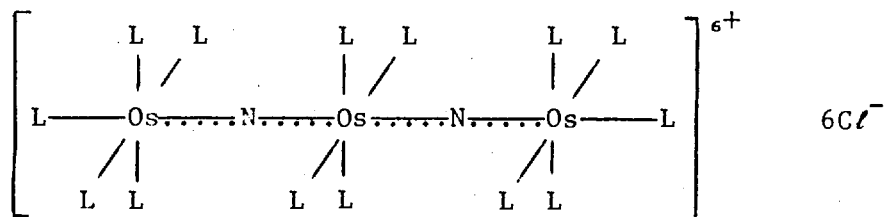
where L = $8NH_3$ + $6H_2O$.

The choice of sites for the two sets of ligands may be responsible

for the amorphous nature of the bulk solid, which gives virtually no

X-ray powder diffraction lines. Variation of the reaction conditions

does not seem to allow the coordination of more than eight ammine ligands.

The preparation, from $[OsCl_6]^{2-}$ for example, involves the complete

replacement of chloro ligands by NH_3 and H_2O groups. The nitrido

groups must be formed by deprotonation of bridging amido ligands from

coordinated ammonia. In some samples, the amount of chloride found is

less than that required for 6Cl:3Os. This appears to be dependent on

Table 2.6

Raman and Infrared Band Wavenumbers for Osmium Violet and Isotopically Substituted Species.

Raman

$[Os_3N_2(NH_3)_8(H_2O)_6]^{6+}$*	1100(1)	835sh	792(10)	585($\frac{1}{4}$)	511($\frac{1}{2}$)	460(1)	380($\frac{1}{4}$)	334(1)	287(4)	222(4)
ρ	0.25	-	0.33	0.45	0.31	0.26	-	0.36	0.32	0.35
$[Os_3N_2(NH_3)_8(H_2O)_6]Cl_6$	1075(1)	900(2)	780(10)	580($\frac{1}{2}$)	500(1)	466(2)	385(1)	323(1)	267(8)	212(10)
$[Os_3N_2(N^2H_3)_8(^2H_2O)_6]Cl_6$	1095($\frac{1}{2}$) 1015($\frac{1}{2}$)	900(1)	785(4)	580($\frac{1}{2}$)	-	462(1)	380(1)	340(2)	254(6)	212(10)
$[Os_3{}^{15}N_2(^{15}NH_3)_8(H_2O)_6]Cl_6$	1048($\frac{1}{2}$)	900(1)	761(6)	560($\frac{1}{4}$)	-	468(1)	385(1)	330(1)	262(6)	212(10)
Assignment	$\nu(Os\text{-}N_{br})$					$\nu(Os\text{-}N_{eq})$	$\nu(Os\text{-}O_{ax})$		$\delta(N_{br}OsN_{eq})$	$\nu(Os\text{-}N_{br})$

*Solution spectrum, other data on solid state. 568.2 nm excitation, frequencies in cm^{-1}, relative intensities in parentheses, ρ = depolarisation ratio.

Infrared

$[Os_3N_2(NH_3)_8(H_2O)_6]Cl_6$	1078ms, 1040m, 1020m	865m, 740s	555ms, 510w	475mw	270m
$[Os_3N_2(N^2H_3)_8(^2H_2O)_6]Cl_6$	1065ms	700ms	520ms	460sh	-
$[Os_3{}^{15}N_2(^{15}NH_3)_8(H_2O)_6]Cl_6$	1055ms, 1025sh	850m, 770ms	558ms	470mw	obsc
Assignment	$\nu^{as}(OsN_{br})$	-	coord. H_2O rock	$\nu(Os\text{-}N)$	$\delta(NOsN)$

Figure 2.11

Excitation Profiles for Raman Bands of Osmium Violet.

225 cm^{-1} ○

290 cm^{-1} ◉

345 cm^{-1} ◻

385 cm^{-1} ▦

460 cm^{-1} △

520 cm^{-1} ▲

800 cm^{-1} ▽

1095 cm^{-1} ▼
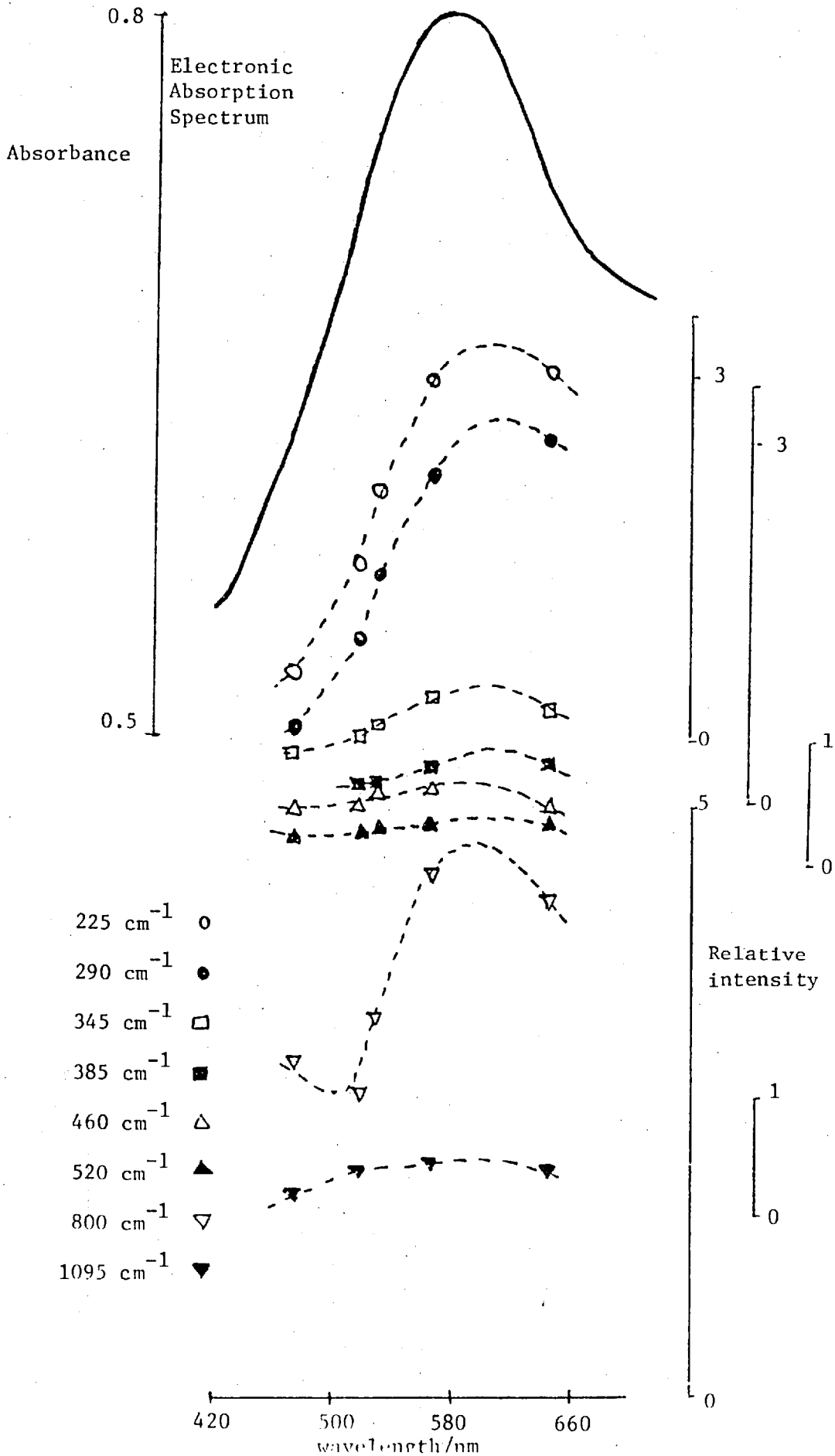
conditions in the solution at the point of precipitation; deprotonation
of a coordinated water molecule to give a hydroxo group would lower
the charge on the cation, and so require one less anion.

Electronic and Raman Spectra.

The electronic absorption bands are broad, maxima are observed
near 590 nm (ε = 13950 M^{-1} cm^{-1}) and 710 nm (ε = 12500 M^{-1} cm^{-1}).
The position and strength of these absorptions suggested that resonance
Raman spectra might be obtained, using 568.2 and 647.1 nm excitation.
Spectra were obtained for dilute solutions, and solids diluted in
potassium bromide discs. Since Raman bands of comparable intensity
were obtained for 10^{-4} M osmium violet solution (568.2 nm excitation)
as for 1 M sodium acetate used as a reference, it is clear that considerable
(of the order of 10^4-fold) resonance enhancement is occurring.
Excitation profiles for eight bands of osmium violet are given in
Figure 2.11. The maxima of the profiles fall near 600 nm, the
electronic absorption band is close, peaking at 590 nm. The solution
Raman bands (60-1200 cm^{-1}) are polarised; the depolarisation ratio
values ρ near 0.33 indicating axial symmetry. The most prominant bands
are those at 792, 287 and 222 cm^{-1}, these appearing at 780, 267 and
212 cm^{-1} in the solid state.

In view of the uncertainty in the arrangement of the ligands,
precise assignment of the Raman bands is not possible. Since osmium
violet appears to possess a similar symmetry to that of ruthenium red,
similar rules should apply. Axially orientated a_{1g}-type vibrational
modes are expected to be amongst the stronger bands. Two Raman-active

metal-nitrido bridge stretching modes are expected for the osmium trimer. By analogy with ruthenium red, the 1100 and 222 cm^{-1} bands of osmium violet may be compared to the 827 (ν_1) and 150 (ν_6) cm^{-1} ruthenium-oxygen stretches; the 1100 cm^{-1} band is shifted by ca. 30 cm^{-1} to lower wavenumbers by ^{15}N substitution, but is not affected by ^{2}H substitution; while the 222 cm^{-1} band is not noticeably affected by either isotope. This is in accordance with the assignment of the 1100 cm^{-1} band as reflecting primarily nitrogen motion, and the 222 cm^{-1} band a breathing mode of the outer osmium atoms, with their coordinated water and ammonia groups. These values may be compared with those of $[Os_2N(NH_3)_8Cl_2]Cl_3$,[13] where $\nu^s_{M_2N}$ is at 299 cm^{-1} in the Raman, and $\nu^{as}_{M_2N}$ at 1104 cm^{-1} in the infrared spectrum.

The prominent band at 792 cm^{-1} (780 cm^{-1} in the solid state) behaves in a similar fashion to the weaker 1100 cm^{-1} band on isotopic substitution, being unaffected by deuteriation, but moving some 20 cm^{-1} to lower wavenumbers on ^{15}N substitution. This band is, however, rather low in frequency to be satisfactorily assigned as the symmetric Os-N$_{br}$ stretch. Assignment as the $\rho^s(NH_3)$ is ruled out on the deuteriation evidence, where a large drop would be expected.

The 287 cm^{-1} band of osmium violet, affected by both ^{2}H and ^{15}N isotopic substitution, compares well with the ruthenium red a_{1g} deformation $\delta(ORuN_{eq})$, (274 cm^{-1}, ν_5); and so is assigned as $\delta(N_{br}OsL_{eq})$, where N_{br} is the bridging nitrido, and L_{eq} is the equatorial aquo or ammine ligand on the terminal osmium atom.
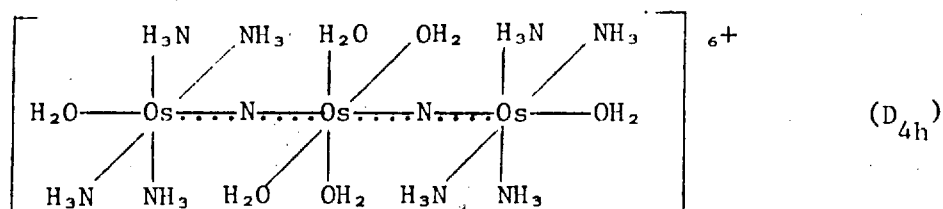
Assignment of the weaker bands may now be considered. For ruthenium red, ν_4 is the axial stretching vibration of the ligand trans to the bridging group, ($\nu(Ru-N_{ax})$) and is assigned to the band at 413 cm^{-1}.

The problem arises with osmium violet that it is uncertain which of water or ammonia groups occupy this axial position. The stretching mode of the $Os-NH_3$ bond would be expected to show as a band in the $450-480$ cm^{-1} region of the Raman spectrum, whereas $Os-OH_2$ is found nearer 400 cm^{-1}. For a group _trans_ to the nitrido bridge, some coupling to the $\nu(M-N_{br})$ mode would be expected, with a resultant lowering of the observed wavenumber; in the case of ruthenium red, $\nu(Ru-N_{ax})$ is found to be $30-60$ cm^{-1} lower than the $\nu(Ru-N_{eq})$ modes. If a similar shift is applied for osmium violet, $\nu(Os-N_{ax})$ would be expected near 420 cm^{-1}, while $\nu(Os-O_{ax})$ would be near 370 cm^{-1}.

The only band observed in the Raman spectrum in this region is a weak band at 380 cm^{-1} (385 cm^{-1} in the solid state), unaffected by ^{15}N substitution, but dropping by 5 cm^{-1} on deuteriation. Assignment of this to an axial aquo ligand may thus be made, with a predicted drop in frequency to 365 cm^{-1} for ^2H_2O (change from NH_3 to N^2H_3 requires a greater drop, to 355 cm^{-1}). The 460 cm^{-1} band is patently a metal-ammonia stretching mode, corresponding to $\nu_2(M-N_{eq})$ or $\nu_3(M'-N')$ in the labelling scheme used for ruthenium red (Section 2-C).

The other weak bands at 835, 585, 511 and 334 cm^{-1} in the solution resonance Raman spectrum of osmium violet are less readily assigned. The resonance Raman data supports the linear Os_3N_2 structure, one arrangement of ligands in agreement with the data is:

$$\left[\begin{array}{c} \overset{H_3N}{\underset{H_3N}{\diagdown}} \overset{NH_3}{\underset{}{\diagup}} \quad \overset{H_2O}{\underset{H_3N}{\diagdown}} \overset{OH_2}{\underset{}{\diagup}} \quad \overset{H_3N}{\underset{H_3N}{\diagdown}} \overset{NH_3}{\underset{}{\diagup}} \\ H_2O \text{---} Os \cdots N \cdots Os \cdots N \cdots Os \text{---} OH_2 \\ \underset{H_3N \quad NH_3}{\diagup} \quad \underset{H_2O \quad OH_2}{\diagup} \quad \underset{H_3N \quad NH_3}{\diagup} \end{array} \right]^{6+} \qquad (D_{4h})$$

Aquo ligands are found <u>trans</u> to the nitrido bridge in the

dimer $K_3[Os_2NCl_8(H_2O)_2]$.[5]

The nitrido N^{3-} and oxo O^{2-} ligands are isoelectronic. For

osmium in the +4 oxidation state, a d^4 electronic configuration is

found. Taking the nitrogen p_x and p_y orbitals and the osmium d orbitals

for an eclipsed D_{4h} structure, a similar molecular orbital scheme to

that for ruthenium red, Figure 2.10, may be considered. The ground

state configuration of $Os^{IV}(d^4)N(p^4)Os^{IV}(d^4)N(p^4)Os^{IV}(d^4)$ for osmium

violet would require the loss of two electrons from the antibonding

$e_u(\pi^*)$ orbital.

2-E-2 Cyanide Derivative of Osmium Violet.

Hot concentrated cyanide will displace all the ammine ligands of

osmium violet. The black product, assuming no change from Os^{IV} has

occurred, analyses as $K_4[Os_3N_2(CN)_{10}(H_2O)_4].4H_2O$. The infrared spectrum

(Table 2.8) still shows strong bands at 1120 and 1040 cm^{-1} assigned to

$\nu_{OsN_{br}}^{as}$. Bands due to coordinated ammonia are missing, while bands

typical of cyano complexes are now seen. The broad band near 3440 cm^{-1}

is assigned to coordinated and crystal water.

The electronic spectrum of the brown-purple solution exhibits

maxima at 370, 460, 510 and 640 nm, (ε values between 4000-6000 M^{-1} cm^{-1}).

Since strong Raman spectra are obtained from dilute solutions or solids

diluted in potassium bromide discs, a degree of resonance enhancement

is implied. Band wavenumbers are given in Table 2.8. In the solution

spectrum, two bands assigned to $\nu(Os-N_{br})$ are seen at 1035 and 234 cm^{-1},

corresponding to the 1100 and 222 cm^{-1} bands of osmium violet.

Three bands are observed in the cyanide carbon-nitrogen stretching

region in the Raman spectra, between 2100 and 2160 cm^{-1}; two of these

are polarised (depolarisation ratio $\rho = 0.4$) and the third band

appears to be depolarised ($\rho \sim 0.75$). These bands are comparatively

weak and so are probably not greatly resonance enhanced. Five

ν_{CN}^{as} bands are found in the infrared spectrum of the solid, between

2030 and 2130 cm^{-1}. The complex is not sufficiently soluble to allow

solution infrared spectra to be obtained. Although two infrared and

Raman bands appear to coincide, this may be accidental. The stronger

Raman bands fall at higher wavenumbers than the stronger infrared

bands and a centrosymmetric structure therefore seems likely.

Several structures may be drawn up to accommodate ten cyano

and four aquo groups. The discussion will here be confined to

consideration of two forms of high symmetry:

(I)

(II)
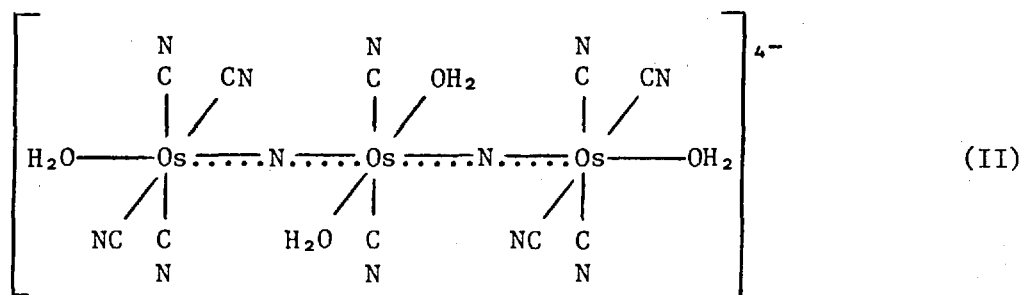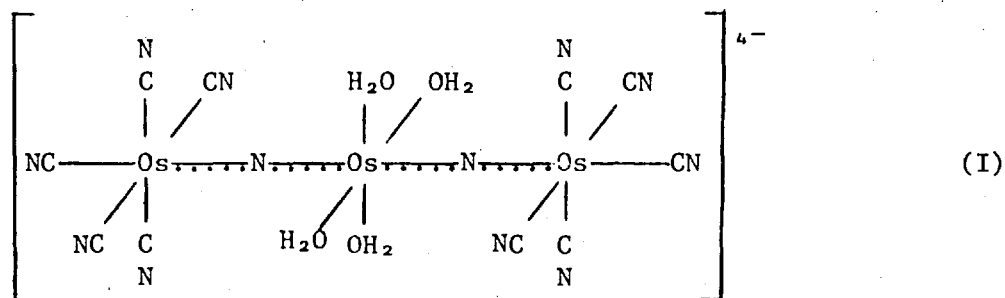
Structure (I) has D_{4h} symmetry;

$$\Gamma_{CN} = 2a_{1g} + b_{1g} + e_g + 2a_{2u} + b_{2u} + e_u$$

Thus, for this structure, four Raman bands (a_{1g}, b_{1g}, e_g), of which the a_{1g} modes are polarised, and three infrared bands (a_{2u}, e_u) are predicted.

Stucture (II) has D_{2h} symmetry;

$$\Gamma_{CN} = 3a_g + b_{2g} + b_{3g} + 2b_{1u} + b_{2u} + 2b_{3u}.$$

Five Raman modes (a_g, b_{2g}, b_{3g}), of which the a_g modes are polarised, and five infrared bands (b_{1u}, b_{2u}, b_{3u}) are expected for this structure. A greater number of bands would be anticipated for a structure of lower symmetry.

If solid-state splitting is responsible for the generation of five infrared bands from the three predicted; and one of the depolarised Raman bands is obscured, then structure (I) is plausible. In the case of structure (II), the observed and predicted number of infrared active C-N stretching modes are in agreement. Of the three polarised a_g modes, two are of the x-axis- and y-axis- orientated cyano groups on the terminal osmium atoms which differ only in symmetry; these groups are expected to have identical bond strengths, and hence appear with the same vibrational frequency. If one of the depolarised Raman modes is obscured, then structure (II) may not be ruled out.

The difference between (I) and (II) concerns the identity of the ligand _trans_ to the nitrido bridge. While aquo ligands occupy this position in $K_3[Ru_2NCl_8(H_2O)_2]$,[5] the π-bonding CO ligand is believed to be _trans_ in $Cs_3[Ru_2NCl_8(CO)_2]$.[9] The cyanide ligand may preferentially occupy the axial position and accept electron density from the nitrido group _via_ the osmium atom.

Table 2.7

Vibrational Spectra of Nitrido-Bridged Ruthenium and Osmium Aquo-Ammine   Complexes.

Complex		$\nu^{s}(M_3N_2)$	$\nu^{as}(M_3N_2)$	$\nu(M-NH_3)$	$\nu(M-OH_2)$	$\delta(NMN)$	Other Bands
Ruthenium Violet,							
$[Ru_3N_2(NH_3)_8(H_2O)_5(OH)]Cl_5$	R	1060(1), 315(4)		470(1), 410(6)	351(10)	265(3)	795(4), 665(3)
	R*	1060(1), 315(3)		480(4), 415(10)	390(10), 350(5)		760(6), 690(1)
	ρ	0.40		0.23 0.24	0.25 0.46		0.38 0.35
	ir		1040mw	475mw		250m	3380ms(νOH) 3240s, 3140s(νNH), 1620ms, 1310s, 810mw, 540m
$[Ru_3N_2(N^2H_3)_8(^2H_2O)_5(O^2H)]Cl_5$							
	R*	1050(1), 335(5) 290(4)		470(4), 410(7)	373(10)		750(7), 635(1)
$[Os_3N_2(NH_3)_8(H_2O)_5(OH)]Br_5$	R	1090(1)		450(1)			780(10), 580($\frac{1}{2}$)
	ir		1070ms, 1025ms	475mw		260mw	840m, 725vs, 570m
Osmium Brown,							
$[Os_3N_2(NH_3)_8(H_2O)_6]Cl_7$	R	1091(4), 1018(2)		475(1), 440($\frac{1}{2}$)	335($\frac{1}{2}$)	272(4)	793(10)
	R*	1105(3), 1025(1) 222(3)		478(2), 444(1)	330(3)	282(6)	802(10), 600(2), 510(2)
	ir		1090ms, 1020m, 965m	470mw		273ms	3400s(νOH),3240vs, 3170vs(νNH), 1615s, 1345s, 1310sh, 833ms 550m

Table 2.7 (cont).

Complex		$\nu^s(M_3N_2)$	$\nu^{as}(M_3N_2)$	$\nu(M-NH_3)$	$\nu(M-OH_2)$	$\delta(NMN)$	Other Bands
$[Os_3N_2(N^2H_3)_8(^2H_2O)_6]Cl_7$	R	1095(2), 1020(1), 212(6)		460(3)	328(2)	256(6)	790(10)
	ir		1100m, 1063ms, 1020ms	450mw		250mw	2340s, 2260s (νN^2H), 1250m, 863m, 790m, 550m
$[Os_3{}^{15}N_2(^{15}NH_3)_8(H_2O)_6]Cl_7$	R	1064(3), 980(1)		490(1), 445($\frac{1}{2}$)			788(10), 577(1)
	ir		1055ms, 968ms	470w		260w	3390s(νOH), 3210vs, 3140vs(νNH), 1605s, 1330s, 845w, 750obs 525mw
$[Os_3N_2(NH_3)_9(H_2O)_3(OH)_2]Br_5$	R	925(1)		485(1)	320(1)	275(4)	790(10), 585(1)
	ir		1105ms, 1020m	485w		260w	3400s(νOH), 3220s, 3150s(νNH), 1610s, 1310s, 835m, 770w, 560m
Gautier's Ammine Complex, $[Os_2N_2(NH_3)_6(H_2O)_2(OH)_4]Cl_2$	R	1100(7), 1030(10)		510(3)	355(2)	280(2)	740(5), 597(5), 560
	ir		1010ms, 970ms	515m			3360s, 3100vs, 1580 1320vs, 715ms
$Os_3N_7O_9H_{21}$	R	1030(10) broad		505(5)		264(6)	745(4), 583(7)
	ir		1070s, 1000vs, 950vs	500vs			3390ms, 3100vs, 158 1320s
$[Os_3N_2(NH_3)_4(OH)_8(H_2O)_2]$	R	1030					590
	ir		1090sh, 965vs				3380s, 3160vs, 1620 1335m, 530s

* Solution spectra, otherwise solid-state spectra. Frequencies in cm^{-1}, ρ = depolarisation ratio.

Table 2.8

Vibrational Spectra of Nitrido-Bridged Osmium Cyano Complexes.

Complex		$\nu^s(Os_3N_2)$	$\nu^{as}(Os_3N_2)$	$\nu(C-N)$	$\nu(Os-CN)$	Other Bands
$K_4[Os_3N_2(CN)_{10}(H_2O)_4].4H_2O$	R	1030(1) 228(7)		2150(1), 2132(1), 2105($\frac{1}{2}$)	520(1), 465(6)	812(10), 750(2), 595(1), 280(1
	R*	1035($\frac{1}{4}$), 234(7)		2157(1)(p), 2149($\frac{1}{2}$)(p), 2135($\frac{1}{4}$)(dp)	524(1), 460(3)	840($\frac{1}{4}$), 800($\frac{1}{4}$), 350($\frac{1}{4}$), 260($\frac{1}{4}$) 120(10)
	ir		1120s 1040vs	2130s, 2105s, 2085ms, 2047vs, 2038sh	550ms, 475m	3440vs,b, 1620s, 905w, 830w, 750ms, 380mw
$K_4[Os_3N_2(CN)_8(OH)_4(H_2O)_2]$	R	1080(8), 993(10)		2140(4), 2110(5), 2078(3) 2065(4), 2040(1), 2020(2)	467(8)	755(4), 608(6), 420(3), 370(2)
	ir		1170s, 1070vs, 960s	2122ms, 2042ms	555w, 465s	3540sh, 3450vs, 3200s, 1625m, 785w, 380w
$K_4[Os_3N_2(CN)_7(OH)_5(H_2O)_2].2H_2O$	ir		1020vs, 930m	2135mw, 2115m, 2045s, 2040vs, 2025s	553s,sp, 460ms	3560m, 3400s, 3170m, 1630m, 1587ms, 1140ms, 765w
$K_5[Os_2N(CN)_8(OH)_2]$	ir		1053s, 965mw	2123m, 2100s, 2065m, 2030s,sp	520mw, 492mw	3540s, 3440vs, 1600s, 808mw, 380w, 255w.

* Solution spectrum, others in solid state. Frequencies in cm^{-1}, p = polarised, dp = depolarised.

2-E-3 Osmium Brown.

A brown-black species is produced as a by-product in the preparation

of osmium violet (Section 2-E-1); and is also noted as a less-soluble

material formed by the reaction of $[OsCl_6]^{2-}$ with ammonia solution

to generate $[Os_2N(NH_3)_8Cl_2]Cl_3$.[15] The spectra and properties of this

material, " Osmium Brown" , giving brown aqueous solutions, are noted

here. The infrared and Raman spectra, listed in Table 2.7, are very

similar to their counterparts for osmium violet. Infrared bands at

1090, 1020 and 965 cm^{-1} are assigned to asymmetric vibrations of bridging

nitrido groups; while the strong solution Raman bands at 1105 and 222 cm^{-1}

are the symmetric vibrations. This spectroscopic evidence supports

an Os_3N_2 backbone for osmium brown. The electronic absorption bands

are at 380 nm ($\varepsilon = 6400$ M^{-1} cm^{-1}) and 320 nm (ε 5300 M^{-1} cm^{-1}). Raman

spectra were obtained using excitation in the blue region near

480 nm, and a degree of resonance enhancement allowed the use of dilute

solids and solutions.

This species seems likely to contain osmium in an average oxidation

state near +4; this value is suggested by X-ray photoelectron

spectroscopy (Section 2-F-1), while the oxidation state determination

using VO_3^- (Section 2-F-2) indicates an average value of +4.33. The

preparation of the complex from an Os^{IV} species, $[OsCl_6]^{2-}$, favours

the formation of a product containing osmium in or near to this

oxidation state. Analytical data (close to 7 Cl per 3 Os) is biased

towards an average oxidation state of $+4\frac{1}{3}$ (IV, V, IV); although the

+4 state (as found for osmium violet, Section 2-E-1) is supported

by the apparent diamagnetism of the complex ($\mu_{eff} = 0.84$ B.M. for

trinuclear molecule). It has not been found to be possible to reduce

osmium brown either chemically, e.g., with Fe^{II} ; or electrolytically,

at a constant potential of -1.0 V. A polarographic investigation of

a solution in 0.1 M sodium acetate showed no oxidation or reduction

waves due to osmium brown. Osmium brown and osmium violet, obtained

from the same reaction, are similar in most respects, apart from

the electronic spectra, but interconversion is not possible. A

differing arrangement of ligands is unlikely to be responsible for

the great difference in electronic spectra; whereas the electronic

spectrum of osmium brown could be interpreted as being due to a

different osmium oxidation state and electronic configuration compared

to osmium violet.

Osmium brown may be best formulated as $[Os_3N_2(NH_3)_6(H_2O)_6]Cl_7$,

although the formula $[Os_3N_2(NH_3)_7(H_2O)_5]Cl_6$ agrees more closely

with the observed diamagnetism of the species.

2-E-4. Gautier's Osmium-Ammine Complex.

In the reported preparation of this species,[35] precipitation is

brought about by addition of ethanol to the aqueous solution, this may

lead to a mixture of species as the product. The resulting brown material

(λ_{max} = 330 nm, ε = 6000 M^{-1} cm^{-1}, in buffer solution) resembles osmium

brown (Section 2-E-3). The infrared and Raman wavenumbers are listed

in Table 2.7. Bands assigned to asymmetric stretching modes of the

nitrido bridges of an Os_3N_2 unit, $\nu^{as}_{Os_3N_2}$ are observed at 1010 and

970 cm^{-1} in the infrared; the Raman bands at 1100 and 1030 cm^{-1} are

symmetric stretching modes of the nitrido bridges, corresponding to

the 1075 cm^{-1} osmium violet band.

Analytical data indicate the presence of two chlorine atoms for

three osmium atoms, no bands that may be assigned to coordinated chlorine

are seen in the spectra. Conductivity results suggest that the substance is a 3:1 electrolyte. Assuming that the final product is in an average oxidation state of +4 for each osmium atom, a formula indicated by the analytical data is $[Os_3N_2(NH_3)_6(H_2O)_2(OH)_4]Cl_2$. The staining reagent obtained from this material on treatment with SO_2 is discussed in Section 2-G-3.

Infrared spectra of a yellow-brown chloro-complex obtained by reaction with hot concentrated hydrochloric acid; and of a brown cyano complex resulting from treatment of Gautier's osmium-ammine complex with hot cyanide solution, are given in Section 2-H. Bands assigned to $\nu^{as}_{Os_3N_2}$ appear at 1015 and 965 cm^{-1} and 1055 and 975 cm^{-1} respectively.

2-E-5 Product from Osmium Tetraoxide with Aqueous Ammonia and Cyano Derivative.

The amorphous black solid produced by prolonged reaction of osmium tetraoxide with aqueous ammonia was reformulated as $[Os_3N_2(NH_3)_4(OH)_8(H_2O)_2]$ by Pawson,[32] the average oxidation state required for this is $+4\frac{2}{3}$. An average oxidation state near +5 is indicated by X-ray photoelectron spectroscopy results (Section 2-F-1); in view of the observed diamagnetism of the compound, the even-totalled average of $\frac{14}{3}$ (i.e., $4\frac{2}{3}$ per osmium) is favoured.

The black solid dissolved in hot concentrated cyanide solution, precipitation by methanol gave a product where the ammine groups have been removed. The dark brown cyano derivative is formulated as $K_4[Os_3N_2(CN)_8(OH)_4(H_2O)_2]$, for osmium in the average of $+\frac{14}{3}$ oxidation state. Vibrational spectra are tabulated in Table 2.8; $\nu^{as}_{Os_3N_2}$ is assigned to bands at 1070 and 960 cm^{-1} in the infrared spectrum; and

$\nu^s_{Os_3N_2}$ to the 1080 and 993 cm^{-1} bands in the Raman. The strong infrared band at 1170 cm^{-1} is the M-O-H bend of the hydroxide ligands. Solution Raman spectra were poor; in the solid state a total of six bands are seen in the cyano C-N stretching region; while only two are evident in the infrared.

2-E-6   Other Nitrido-Bridged Osmium Complexes.

(a)   Product from Osmium Tetraoxide with Liquid Ammonia and

Cyano Derivative.

The black material obtained by reaction of osmium tetraoxide with liquid ammonia, empirical formula $Os_3N_7O_9H_{21}$,[33] has been formulated as $[Os_3^{VI}N_2(NH_3)_4(N)(OH)_9]$,[15] the three infrared bands in the 1100-950 cm^{-1} region being assigned to bridging and terminal nitrido group stretching modes. A broad band at 1030 cm^{-1} in the Raman spectum is also likely to be a nitrido group stretching mode. The black hydroxo-ammine complex is converted to a cyano derivative by treatment with hot concentrated cyanide solution. The brown solid analyses as $K_4[Os_3N_2(CN)_7(OH)_5(H_2O)_2].2H_2O$. Five ν_{C-N} bands are seen in the infrared spectrum (Table 2.8).

(b) $Ba_9Os_3N_{10}$ in Hydrochloric Acid.

The ternary nitride, $Ba_9Os_3N_{10}$ is obtained by heating a mixture of barium nitride and osmium powder under nitrogen.[58] The solid dissolves in cold concentrated hydrochloric acid; the brown chloro complex isolated as the caesium salt is $Cs_4[Os_3N_2(NH_3)_2Cl_{10}(H_2O)_2].4H_2O$. Osmium-nitrido asymmetric stretches are observed at 1010 and 965 cm^{-1} in the infrared; this may be compared with $Cs_3[Os_3N_2Cl_{11}(NH_3)_3].2H_2O$ [9] which has $\nu^{as}_{Os_3N_2}$ at 1025 and 970 cm^{-1}. [32]

(c) Binuclear Nitrido-Bridged Cyano Complex.

The ruthenium complex $K_5[Ru_2N(CN)_{10}]$ [13] has no direct osmium

analogue. Reaction of $Cs_3[Os_2NCl_8(H_2O)_2]$ or " $Os_2N(OH)_5 \cdot nH_2O$" with hot

concentrated potassium cyanide solution yields an orange-brown product

analysing as $K_5[Os_2N(CN)_8(OH)_2]$. Four bands are seen in the infrared

in the C-N stretching region.

Section 2-F. Oxidation State of Ruthenium and Osmium in Their Complexes.

2-F-1 X-Ray Photoelectron Spectra (XPS)[†]

The technique of X-ray photoelectron spectroscopy (of which

ESCA, electron spectroscopy for chemical analysis is an example), may

be used to estimate the oxidation state of metals in their complexes.

Where a compound contains metal atoms in more than one oxidation state

as does, formally, ruthenium in ruthenium red (Ru^{III}, Ru^{III}, Ru^{IV}), then

separate core-level signals are expected for the different oxidation

states.[59] XPS data were obtained for ruthenium and osmium species,

including reference samples of known oxidation state. Since the samples

are insulators, charging relative to the detector may affect the absolute

binding energy values, although relative values are unaffected. Samples

were run as powders on double-sided scotch tape on a gold holder; the

C 1s peak of the tape was used as a reference line.

[†] Spectra were recorded by the Electron Optics Unit, Johnson Matthey Group

Research, using Mg Kα and Al Kα X-ray sources.

(a) Ruthenium

A study of the Ru 3d $\frac{5}{2}$ and Ru 3d $\frac{3}{2}$ peaks has been reported for Ru^{II} and Ru^{III} species in the series $[(NH_3)_5Ru(pyr)Ru(NH_3)_5]^{4+,5+,6+}$, (pyr = pyrazine).[60] Binding energies for 3d $\frac{3}{2}$ are greater than those of 3d $\frac{5}{2}$; with Ru^{III} binding energies lower than those of Ru^{II}. The splitting of the Ru 3d $\frac{5}{2}$ and 3d $\frac{3}{2}$ components is 4.1 $\pm$ 0.1 eV for $[Ru(NH_3)_5C\ell]C\ell_2$;[60] a similar splitting is found for other ruthenium species.

Binding energies for various ruthenium complexes are given in Table 2.9. The most intense peak in the Ru 3d region, 280-290 eV, is often that due to the C 1s reference, which partly obscures the region of interest. Some comparisons may be made with the Ru 3p $\frac{3}{2}$ and 3p $\frac{1}{2}$ peaks, in the 460-490 eV range; the results for ruthenium red, formally $3\frac{1}{3}$, are close to those of the Ru^{III} species, while those of ruthenium brown, formally $3\frac{2}{3}$, indicate a Ru^{IV} oxidation state. The data for ruthenium violet are most consistent with a Ru^{IV} species.

For ruthenium red in a localised III, IV, III oxidation state, as suggested by Mössbauer data,[61] a set of four peaks, near 282.5, 284.0, 286.5 and 288.0 eV would be predicted, by examination of the Ru^{III} and Ru^{IV} 3d $\frac{3}{2}$ and 3d $\frac{5}{2}$ data obtained for the reference complexes. A II, VI, II state would require a greater separation, perhaps to 281, 285, 286 and 290 eV. Two peaks, at 280.5 and 282.0 eV are observed; the separation is too low for these to be a 3d $\frac{5}{2}$ and 3d $\frac{3}{2}$ pair, and the difference (1.5 eV) is similar to that expected for Ru^{III} 3d $\frac{5}{2}$ and Ru^{IV} 3d $\frac{5}{2}$. The 3d $\frac{3}{2}$ counterparts are hidden by the C 1s peak. The localised III, IV, III oxidation state is thus supported by the XPS data.

Table 2.9

X-Ray Photoelectron Spectroscopy Results for Ruthenium Complexes.

Complex	Ru $3d\frac{5}{2}$	Ru $3d\frac{3}{2}$	Ru $3p\frac{3}{2}$	Ru $3p\frac{1}{2}$	O 1s
$[Ru_3O_2(NH_3)_{14}]Cl_6$	280.5 282.0	obsc	463.2	485.5	532.1
$[Ru_3O_2(NH_3)_{14}]Cl_7$	282.6	288.9	464.3	486.6	532.3
$[Ru_3N_2(NH_3)_8(H_2O)_5(OH)]Cl_5$ *	283.4	287.3	465.0	487.3	532.3
$[Ru^{III}(NH_3)_6]Cl_3$	282.6	286.4	463.8	486.1	532.2
$[Ru^{III}(NH_3)_5Cl]Cl_2$	282.6	286.6	463.6	486.0	532.3
$K_3[Ru_2^{IV}NCl_8(H_2O)_2]$	284.0	288(obsc)	464.2	486.4	532.3
$[Ru_2^{IV}N(NH_3)_8Cl_2]Cl_3$	282.4	286.4	463.6	485.9	532.4

Binding energies in eV, relative to C 1s of scotch tape = 285 eV

* Set O 1s = 532.3 eV (C 1s then 287.3 eV), otherwise unusually
low values obtained.

Two peaks, one corresponding to a Ru^{III} 3d $\frac{5}{2}$ (282.6 eV) and the other, Ru^{IV} 3d $\frac{3}{2}$ (288.9 eV) are seen for ruthenium brown. The separation is too great for assignment as a 3d $\frac{5}{2}$ and 3d $\frac{3}{2}$ pair; the other two peaks required are obscured by the C 1s peak. These results suggest a localised IV, III, IV state for ruthenium brown. On the basis of the XPS data, ruthenium violet appears to contain all the ruthenium in the +4 oxidation state; the Ru 3d results (283.4, 287.3 eV) being close to those of $K_3[Ru_2^{IV}NC\ell_8(H_2O)_2]$, 284.0 and 288 eV.

(b) <u>Osmium</u>

The region of interest for osmium species is that of the 4f binding energies; a study based on the Os 4f $\frac{7}{2}$ X-ray photoelectron spectra has identified the oxidation states of osmium compounds formed by reaction of OsO_4 with cell constituents.[62] The splitting of the Os 4f $\frac{7}{2}$ and 4f $\frac{5}{2}$ peaks is found to be near 2.7 eV.[63]

<u>Table 2.10</u>

<u>X-Ray Photoelectron Spectroscopy Results for Osmium Complexes.</u>

Complex	Os 4f $\frac{7}{2}$	Os 4f $\frac{5}{2}$ [†]
Osmium Violet, $[Os_3N_2(NH_3)_8(H_2O)_6]C\ell_6$	53.0	55.4
Osmium Brown, $[Os_3N_2(NH_3)_8(H_2O)_6]C\ell_7$	53.2	55.6
$[Os_3N_2(NH_3)_4(OH)_8(H_2O)_2]$	54.4	56.2
$[Os_2^{IV}N(NH_3)_8C\ell_2]C\ell_3$	53.1	55.4
$Na_2[Os^{VI}O_2(OH)_4]$	56.0	58.1

[†] Binding energies in eV, relative to C 1s of scotch tape = 285.0 eV.

The Os 4f energies indicate that osmium violet and osmium brown are in similar oxidation states, near Os^{IV}, by comparison with the data for $[Os_2N(NH_3)_8C\ell_2]C\ell_3$. The amorphous black product of prolonged reaction of osmium tetraoxide and aqueous ammonia (Section 2-E-5), formulated as $[Os_3N_2(NH_3)_4(OH)_8(H_2O)_2]$[9] is shown by XPS data to contain osmium in an oxidation state intermediate between Os^{IV} and Os^{VI}, i.e., near Os^V. The XPS peaks are rather broad, and may indeed be composed of $4f\frac{7}{2}$ and $4f\frac{5}{2}$ peaks due to the presence of more than one oxidation state of the osmium atoms. In agreement with the observed diamagnetism, an average of $+4\frac{2}{3}$ may be considered; the localised (V, IV, V) states would be in accordance with the observed spectrum.

2-F-2. Determination of the Oxidation State of Osmium Violet.

Osmium violet does not oxidise iodide to iodine in the presence of dilute sulphuric acid; this method has been used for Os^{VI} species.[64] Osmium in lower oxidation states such as Os^{III} will reduce silver ions to the metal.[65] In the case of osmium violet, however, although some reduction to Ag^0 appears to take place, $AgC\ell$ is formed from the chloride ions of the osmium violet salt, and precipitation of osmium violet commences. No quantitative results could be obtained for the oxidation state or the amount of ionic chloride by this method.

Permanganate will oxidise Os^{IV} species, in the presence of dilute sulphuric acid, to Os^{VIII}.[66] Addition of dilute sulphuric acid to solutions of osmium violet gave an immediate precipitate of the sparingly soluble sulphate salt, which did not redissolve on addition of permanganate. On adding an osmium violet solution to neutral

permanganate (0.02 M) the osmium is oxidised to the Os^{VIII} species OsO_4 and $[OsO_3N]^-$, (the latter identified by the infrared spectrum after taking the solution to dryness) with precipitation of hydrated MnO_2. By stepwise addition of the osmium complex and centrifugation to remove the MnO_2, the endpoint could be estimated. The oxidation state found was 3.6, 3.3, 3.2, average +3.4. Ceric ion in sulphuric acid will also oxidise Os^{IV} to Os^{VIII}.[67] Using this procedure for osmium violet led to much Ce^{IV} being consumed in a side reaction, giving an apparent value of the oxidation state of the osmium close to zero.

Metavanadate ion will quantitatively oxidise Os^{II} species[68] and Os^{IV} species [69] to Os^{VI}. A slight modification of the literature procedure[68,69] was used to avoid precipitation of osmium violet sulphate; a solution of osmium violet in 0.1 M sodium acetate was added to an excess of ammonium vanadate (0.01 M NH_4VO_3) in 3 M sulphuric acid. The remaining VO_3^- was back-titrated, after stirring overnight, against ferrous ion with N-phenylanthranilic acid indicator. The oxidation state found was 4.3, 4.1, 4.5, 3.8 and 4.4 ; the average +4.2 $\pm$ 0.3. These data are consistent with an average oxidation state of the osmium atoms in osmium violet of +4.

The oxidation state found for the osmium atoms of osmium brown by the vanadate method was +4.4 and 4.5.

Section 2-G. Staining Activity of Oxo and Nitrido-Bridged Ruthenium and
Osmium Complexes.

2-G-1. Introduction.

The intense colour of ruthenium red attracted the attention of Mangin, a botanist, who found the complex acted as a semi-specific

stain for pectin and related molecules in plant cell walls,[17] in light microscopy. With the advent of electron microscopy, the specificity of ruthenium red ensured a continuing use, with the rather feeble electron density enhancement of the stained material further amplified by counterstaining with lead and uranyl salts. Luft[19] developed a widely used method of selectively labelling mucopolysaccharides of the animal cell coat using osmium tetraoxide in solution with the ruthenium red, thus affording good electron density contrast. Possible mechanisms for this interaction are discussed by Blanquet.[20] Spot-test reactions[19] showed that ruthenium red will precipitate with a wide range of polyanions of biological interest, and that the binding to pectin is a typical example. Pectinic substances, however, being associated with the exterior of the cell, are stained first. An electron microscopic study of the binding of ruthenium red on isolated DNA molecules[18] shows that the inorganic cation binds to selected points on the helix of the nucleic acid. The ruthenium red cation is a cylinder approximately 12 Å in length, and this corresponds closely to the spacing between pairs of anionic phosphate groups on the helix.

The basis for staining by ruthenium red is probably electrostatic, the inorganic cation effectively precipitating as an insoluble salt with anionic moieties of biopolymers. Related to this is the mimicry of the hydrated calcium ion; ruthenium red at low concentrations preferentially attaches to calcium binding sites of mitochondria,[70,71] thus inhibiting uptake of that metal.[72] Phospholipids have been identified[46] as being present at these sites.

2-G-2. Comparison of the Staining Activity of Ruthenium and Osmium Species.[†]

(a) Ruthenium Red.

Prolonged exposure of tissue blocks to buffered ruthenium red solution leads to penetration into plant cells; although animal cells are not, or are only slightly penetrated. Counterstaining was necessary in most cases, the main exception being the granules of opaline silica in barley leaves,[73] which were well contrasted by ruthenium red alone. Ruthenium red is observed, in the test-tube, to precipitate sodium silicate from solution. Nucleic acids in mitochondria, chloroplasts and nuclei bound ruthenium red (Figure 2.12e), though no distinction could be made between DNA and RNA. Ruthenium brown, even in the presence of a mild oxidising agent, was rapidly reduced to the red form on contact with cell tissues.

Old solutions of ruthenium red behaved rather differently, due, presumably, to degradation of the complex. Penetration into cells was greatly reduced, though extracellular mucopolysaccharides were contrasted well without counterstaining,[74] (Figure 2.13a). These results are similar to those obtained from ruthenium red in conjunction with osmium tetraoxide.[20] The staining species present in aged ruthenium red, in view of the observed properties, may be material of a higher molecular weight, possibly colloidal aggregates of hydrated ruthenium dioxide.

(b) Osmium Violet.

This 6+ cationic species behaves in a very similar manner to ruthenium red, imparting colour and electron density to cell contents. Membranes, chromatin, nucleoli and ribosomes gained intensity relative

---

[†] The staining of barley leaf and root cells was investigated by Dr. C. Sargent, at that time of the Botany Department, Imperial College.

to other cell contents. Fair contrast is obtained without counter-staining (Figure 2.13b), and this is ascribed to the increased electron density of osmium compared to ruthenium (the two complexes ruthenium red and osmium violet are likely to be of similar size and shape).

(c) Ruthenium Violet.

An impurity of some ruthenium red preparations, this nitrido bridged cation (Section 2-D-3) resembling osmium violet, was found to act as a stain like ruthenium red, with osmium tetraoxide.[19] In buffered aqueous solution without OsO_4, this species will penetrate into cells and stain selectively similar features as observed for ruthenium red or osmium violet; counterstaining was required,[74] (Figure 2.14a).

(d) Mononuclear and Binuclear Species.

The mononuclear species $[Ru(NH_3)_5Cl]Cl_2$, $[Ru(NH_3)_6]Cl_3$ and $[Os(NH_3)_5Cl]Cl_2$, and the binuclear complexes $[Ru_2N(NH_3)_8Cl_2]Cl_3$, $[Ru_2N(NH_3)_8 (NO_3)_2](NO_3)_3$ (effectively $[Ru_2N(NH_3)_8(H_2O)_2]^{5+}$ in solution) and $[Os_2N(NH_3)_8Cl_2]Cl_3$ in buffered aqueous solution were found to penetrate tissue blocks rather faster than the trinuclear complexes. Uptake of the mononuclear and binuclear complexes was hard to assess, owing to the pale colour of the species. After counterstaining by lead and uranyl salts, a similar specificity of staining as that found for ruthenium red was observed. No quantitative comparison of the contrast obtained was possible.

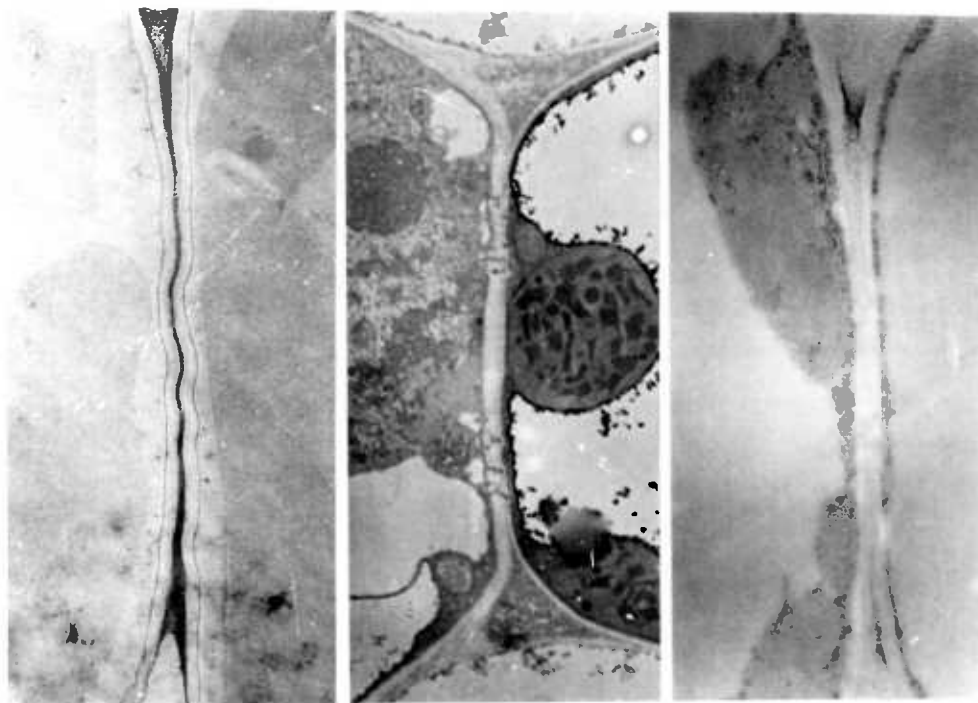Figure 2.12. __Staining of Biological Tissues for Electron Microscopy__

__By Ruthenium Red and Osmium Complexes.__ __(i).__
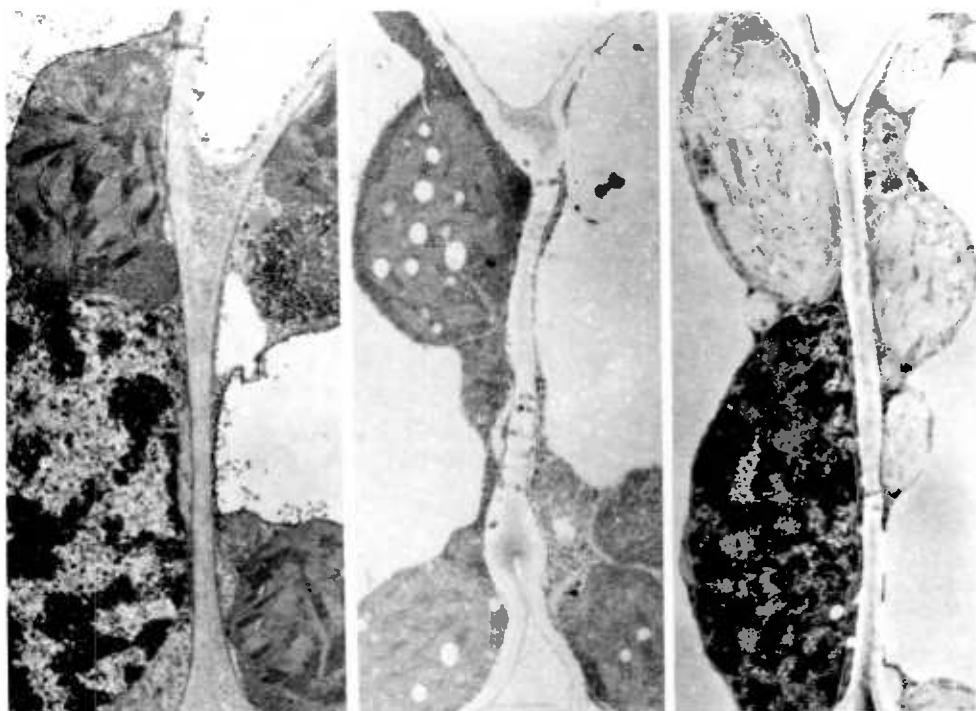
Barley Leaf and Root Tissues.

a. Fixed and stained by osmium tetraoxide, counterstained by lead and uranyl solutions, x 13700.

b. Glutaraldehyde fixed, ruthenium red stained, no counterstain, x 14200.

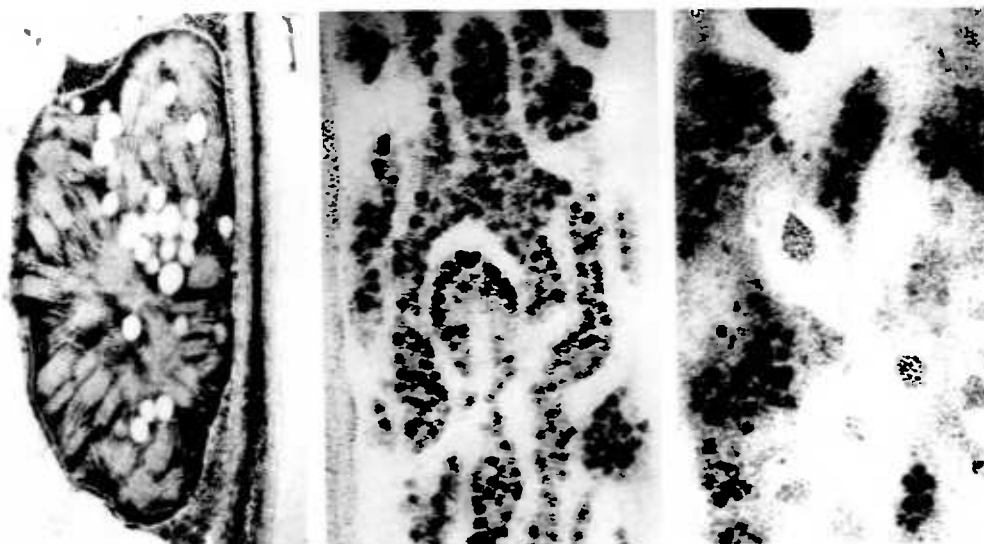c. Glutaraldehyde fixed, ruthenium red stained, lead and uranyl solutions counterstained, x 11800.

Figure 2.13.   Staining of Biological Tissues for Electron Microscopy by
Ruthenium and Osmium Complexes.   (ii).

Barley Leaf and Root Tissues.

a.   Glutaraldehyde fixed, stained by stored (decomposed) solution of
ruthenium red, no counterstain, x 16500

b.   Glutaraldehyde fixed, stained by osmium violet, no counterstain,
x 10700.

c.   Glutaraldehyde fixed, no stain, x 18300.

Figure 2.14.   Staining of Biological Tissues for Electron Microscopy by Ruthenium and Osmium complexes.   (iii).

Barley Leaf and Root Tissues.

a.   Glutaraldehyde fixed, stained by ruthenium violet, counterstained by lead and uranyl solutions, x 27000.

b.   Glutaraldehyde fixed, stained by ruthenium red, counterstained by lead and uranyl solutions, x 96500.

c.   Glutaraldehyde fixed, stained by ruthenium red, counterstained by lead and uranyl solutions, x 82000.

2-G-3. Feulgen-Type Staining.[†]

Specific staining of hydrochloric-acid treated DNA in cell nuclei in a Feulgen-type reaction has been noted for an osmium ammine complex reacted with sulphur dioxide.[35] Acid hydrolysis (5 M hydrochloric acid) generates aldehydic groups from DNA, which are then able to react with a Schiff-type reagent.

Studies using the osmium-ammine complex prepared according to the literature method[35] and ruthenium red, osmium violet, osmium brown and $[Os_2N(NH_3)_8Cl_2](NO_3)_3$ were performed to locate DNA within a single cell organism. After passing sulphur dioxide into the buffered aqueous solutions of each staining agent, any solid formed was centrifuged off. The resulting solutions were lighter in colour, due in part to precipitation of material. Some of the very thin sections of the cells showed physical damage due to the strong acid hydrolysis, but nucleic acid material was visualised by this technique. Contrast was better for the osmium than ruthenium species. The osmium-ammine complex of Gautier, et al., and osmium violet both gave reasonably good contrast of the DNA in the nucleus. Control samples without sulphur dioxide treatment imparted some electron density to other parts of the cell.

On removal of the sulphur dioxide, the staining activity is lost, and the active staining species has not been isolated from solution intact for identification; though sulphito or bisulphito complexes are likely candidates. The mechanism for the interaction of the staining

---

[†] Staining of a single-cell organism, Cryptomonades, was carried out by Dr. S. Morrall, of the Botany Department, Imperial College.

species with aldehydic groups is not clear. One possibility is the

formation of an addition complex,

$$R\text{---}Os\text{---}SO_3\text{---}\overset{\displaystyle H}{\underset{\displaystyle OH}{C}}\text{---}R' \qquad ,$$
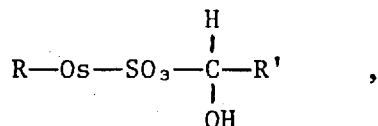
though species of this type could not be isolated.

Section 2-H. E X P E R I M E N T A L.

2-H-1. Oxo-Bridged Trinuclear Ruthenium Species.

Ruthenium Red, Tetradeca-ammine di-μ-oxo Tri-Ruthenium Hexachloride

Tetrahydrate, $[Ru_3O_2(NH_3)_{14}]Cl_6.4H_2O$.

Ruthenium red was prepared as the chloride salt by a simplification

of the literature method.[25] Commercial ruthenium trichloride,

$RuCl_3.xH_2O$ (5 g, 21 mmol) was refluxed with hydrochloric acid (0.25 M,

25 cm^3) and ethanol (5 cm^3) for two hours, then allowed to evaporate

down in a beaker for an hour. Excess concentrated ammonia solution

s.g.0.880, 20 cm^3) was added cautiously; the mixture was stirred in the

presence of air for four hours at 80 ^{o}C. More ammonia solution was

added at intervals to replace the losses due to evaporation. On cooling,

a brown precipitate of ruthenium red formed, this was collected by

filtration. Further batches of solid were obtained from the solution

as the volume decreased by evaporation. The salt was purified from

impurities such as ruthenium violet by recrystallisation from 0.5 M

ammonia solution at 60 ^{o}C, and further purified by addition of a small

amount of saturated sodium chloride to a saturated solution of the

complex. Yield of coppery brown solid, 10%.

Found: Cl, 25.7 ; H, 5.1 ; N, 22.7%. $Cl_6H_{50}N_{14}O_6Ru_3$ requires Cl, 24.8;

H, 5.9 ; N, 22.9%.

Physical Measurements.

Measurements on aqueous solutions over the range $10^{-3} - 10^{-5}$ M

gave the limiting conductance $\Lambda^{\circ} = 1030 \; \Omega^{-1} \; cm^2 \; mol^{-1}$, at 25 $^{\circ}C$.

Mass susceptibility $\chi = -4.2 \times 10^{-9} \; m^3 \; kg^{-1}$ at 294 K, effective magnetic

moment $\mu_{eff} = 0.68$ B.M. per molecule.

The electronic absorption spectrum in aqueous solution has bands

at $\lambda_{max} = 537$ nm ($\varepsilon = 67800 \; M^{-1} \; cm^{-1}$) and 385 nm ($\varepsilon = 7500 \; M^{-1} \; cm^{-1}$).

The thiosulphate tetrahydrate was prepared by addition of

sodium thiosulphate solution to a solution of the chloride, in 3:1

molar proportions. It forms iridescent green crystals, red by

transmitted light.

Found: H, 4.7 ; N, 20.0 ; S, 19.8%. $H_{50}N_{14}O_{15}Ru_3S_6$ requires

H, 5.1 ; N, 20.0 ; S, 19.6%.

Isotopically Enriched forms of Ruthenium Red.

$[Ru_3O_2(N^2H_3)_{14}]Cl_6.4^2H_2O.$ Repeated evaporation to dryness of a

solution of ruthenium red in heavy water (99.8% ^2H) with a little

N^2H_3 gave the deuteriated product. The Raman spectrum was measured

in ^2H_2O solution.

$[Ru_3{}^{18}O_2(NH_3)_{14}]^{6+}.$ To a solution of ammonia in $H_2{}^{18}O$ (99.5%

isotopically enriched) was added $[Ru(NH_3)_5Cl]Cl_2$ (prepared as in

reference 75) and this was held at 75 $^{\circ}C$ under a 10% $^{18}O_2$ (99% isotopic

enrichment) - 90% N_2 atmosphere for six hours before evaporating to

dryness in vacuo. The resonance Raman spectra of solutions of this

material in H_2O and in $H_2{}^{18}O$ were identical, suggesting that no

exchange of bridging oxo ligands with $H_2{}^{16}O$ occurred.

$[Ru_3{}^{18}O_2(N^2H_3)_{14}]^{6+}$. This was made in the same manner as the preceding preparation, N^2H_3, $^2H_2{}^{18}O$ and $[Ru(N^2H_3)_5Cl]Cl_2$ being used.

$[Ru_3O_2(^{15}NH_3)_{14}]^{6+}$. A small scale version of the literature preparation[25] of ruthenium red was used, $^{15}NH_3$ solution being used in place of $^{14}NH_3$ aq. Such a solution was made by addition of aqueous sodium hydroxide to $^{15}NH_4Cl$ (98.6% ^{15}N), collection of the $^{15}NH_3$ in a cold trap, and dissolution in water.

Ruthenium Brown, Tetradeca-ammine di-μ-oxo Triruthenium Heptachloride Tetrahydrate, $[Ru_3O_2(NH_3)_{14}]Cl_7.4H_2O$.

Ruthenium red (0.7 g, 0.82 mmol, in 100 cm^3 water) was oxidised by hydrogen peroxide (25 cm^3 of 30%) in the presence of hydrochloric acid (2 M, 5 cm^3). After warming to 60 $^\circ$c for one hour, the brown powder was collected by filtration from the cooled solution; 70% yield.

Found: Cl, 27.8 ; H, 5.6 ; N, 21.9%. $Cl_7H_{50}N_{14}O_6Ru_3$ requires Cl, 27.6 ; H, 5.5 ; N, 21.6%.

Physical Measurements.

Measurements on aqueous solutions over the range $10^{-4} - 8 \times 10^{-6}$ M gave the limiting conductance $\Lambda^\circ = 1140 \ \Omega^{-1} \ cm^2 \ mol^{-1}$, at 25 $^\circ$C. Mass susceptibility $\chi = 2.75 \times 10^{-9} \ m^3 \ kg^{-1}$ at 294 K, effective magnetic moment $\mu_{eff} = 2.07$ B.M. per molecule, suggests one unpaired electron overall.

The electronic absorption spectrum in aqueous solution has bands at $\lambda_{max} = 459$ nm ($\varepsilon = 42400 \ M^{-1} \ cm^{-1}$) and 360 nm ($\varepsilon = 12600 \ M^{-1} \ cm^{-1}$).

The <u>nitrate</u> salt of ruthenium brown was prepared by the literature method.[25] The reduction of this salt, $[Ru_3O_2(NH_3)_{14}]$-$(NO_3)_7$, $(2.54 \times 10^{-4}$ M solution) by sodium sulphite (0.1 M) has been studied[54] using a magnetic titration balance: from ruthenium brown to ruthenium red, a decrease in μ_{eff} by 1.10 B.M. per molecule was observed.

Isotopically Enriched forms of Ruthenium Brown.

$[Ru_3O_2(N^2H_3)_{14}]^{7+}$, $[Ru_3{}^{18}O_2(NH_3)_{14}]^{7+}$, $[Ru_3{}^{18}O_2(N^2H_3)_{14}]^{7+}$ and $[Ru_3O_2({}^{15}NH_3)_{14}]^{7+}$ were made by the <u>in situ</u> oxidation of the corresponding ruthenium red species by addition of ceric ammonium nitrate or, in the case of the deuteriate, a little 2 M hydrochloric acid and 30% hydrogen peroxide.

Di-μ-oxo-<u>bis</u>(pentammine ruthenium)(<u>bis</u>(1,2-diaminoethane)ruthenium)-hexachloride, $[Ru_3O_2(NH_3)_{10}(en)_2]C\ell_6$.

Green needles of the complex were obtained from an aqueous solution of ruthenium red and 1,2-diaminoethane, following the literature procedure;[7] yield 70%.

Found: C, 5.0 ; Cℓ, 25.4 ; H, 5.7 ; N, 23.3%. $C_4C\ell_6H_{46}N_{14}O_2Ru_3$ requires C, 5.7 ; Cℓ, 25.4 ; H, 5.5 ; N, 23.4%.

The electronic absorption spectrum in aqueous solution has bands at λ_{max} = 543 nm (ε = 79200 M^{-1} cm^{-1}) and 390 nm (ε = 7400 M^{-1} cm^{-1}).

The deuteriated form, $[Ru_3O_2(N^2H_3)_{10}(en-d^4)_2]C\ell_6$ was prepared in the same fashion as deuteriated ruthenium red.

Di-μ-oxo-bis(pentammine ruthenium)[bis(1,2-diaminoethane)ruthenium]

heptachloride tetrahydrate, $[Ru_3O_2(NH_3)_{10}(en)_2]Cl_7.4H_2O$.

The normal and deuteriated forms of this were prepared from

$[Ru_3O_2(NH_3)_{10}(en)_2]Cl_6$ by a procedure analogous to that used to

obtain ruthenium brown derivatives from ruthenium red.

Found: C, 5.1 ; Cl, 24.9 ; H, 5.0 ; N, 20.0%. $C_4Cl_7H_{54}N_{14}O_6Ru_3$

requires C, 5.1 ; Cl, 26.2 ; H, 5.8 ; N, 20.7%.

The electronic absorption spectrum in aqueous solution has bands

at λ_{max} = 474 nm (ε = 44700 M^{-1} cm^{-1}) and 368 nm (ε = 15500 M^{-1} cm^{-1}).

Deca-ammine Tetrapyridine Di-μ-Oxo Triruthenium Octachloride

Dihydrate, $[Ru_3O_2(NH_3)_{10}(py)_4]Cl_8.2H_2O$.

Hydrated ruthenium chloride, $RuCl_3.xH_2O$ (1 g, 4 mmol) was refluxed

with hydrochloric acid (0.25 M, 8 cm^3) and ethanol (2 cm^3) for two

hours. Pyridine (5 cm^3) was added and the mixture, on warming in

air, rapidly turned green. After 15 minutes, concentrated ammonia

solution was added, and the mixture warmed and stirred in air for

three hours at 60 °C. The green solid from the cooled solution was

collected by filtration and washed well with ether to remove the

yellow $[Ru(py)_4Cl_2]$. Yield of water- and ethanol-soluble blue-

green product is 10%.

Found: C, 21.2 ; Cl, 26.2 ; H, 4.9 ; N, 17.1%. $C_{20}Cl_8H_{54}N_{14}O_4Ru_3$

requires C, 21.0 ; Cl, 24.9 ; H, 4.8 ; N, 17.2%.

Physical Measurements.

Mass susceptibility $\chi = 1.24 \times 10^{-9}$ m^3 kg^{-1} at 294 K,

effective magnetic moment = 1.33 B.M. per trinuclear molecule.

Electronic spectra in aqueous solution: λ_{max} 610 nm ($\varepsilon = 11300$

M^{-1} cm^{-1}), 365 nm ($\varepsilon = 9200$ M^{-1} cm^{-1}), on addition of oxidising

agent, VO_3^-, λ_{max} 515 nm ($\varepsilon = 6650$ M^{-1} cm^{-1}), 335 nm ($\varepsilon = 6700$ M^{-1}

cm^{-1}).

2-H-2 Nitrido-Bridged Ruthenium Species.

Ruthenium Violet, Octa-ammine Penta-aquo Hydroxo Di-μ-Nitrido

Triruthenium Pentachloride, $[Ru_3N_2(NH_3)_8(H_2O)_5(OH)]Cl_5$.

Ruthenium chloride hydrate, $RuCl_3.xH_2O$ (2 g, 8 mmol) was

refluxed with hydrochloric acid (0.25 M, 40 cm³) and ethanol (10 cm³)

for two hours, then left to cool. The solution was transferred

to a beaker, and an excess of concentrated ammonia solution (0.880,

100 cm³) added. The mixture was stirred in air at room temperature

for 24 hours. Addition of more ammonia solution and allowing the

mixture to stand overnight led to the deposition of a black precipitate

of ruthenium violet. More solid is obtained as the solution decreases

in volume, total yield 20%.

Found: Cl, 25.5 ; H, 4.4 ; N, 18.2 ; O, 12.3%. $Cl_5H_{35}N_{10}O_6Ru_3$

requires Cl, 23.6 ; H, 4.7 ; N, 18.6 ; O, 12.8%. Material extracted

from ruthenium red preparation; Found: Cl, 25.0 ; H, 4.4 ; N, 18.4%.

Physical Measurements.

Mass susceptibility $\chi = -2.02 \times 10^{-9}$ m^3 kg^{-1} at 294 K,

effective magnetic moment μ_{eff} = 0.80 per trinuclear molecule.

Electronic spectrum in aqueous solution λ_{max} = 750 nm, (ε = 19900 M^{-1} cm^{-1}), 620 nm (ε = 12900 M^{-1} cm^{-1}), 495 nm (ε = 9100 M^{-1} cm^{-1}), 385 nm (ε = 7000 M^{-1} cm^{-1}).

Measurements on aqueous solutions over the range 4×10^{-5} - 6×10^{-6} M gave the limiting conductance Λ° = 780 Ω^{-1} cm^2 mol^{-1}, at 25 $^{\circ}C$.

By comparison with limiting conductance values measured under similar conditions (10^{-4} - 10^{-5} M aqueous solutions) for related species, $[Ru_2N(NH_3)_8(H_2O)_2]^{5+}.5NO_3^-$, ($\Lambda^{\circ}$ = 801 Ω^{-1} cm^2 mol^{-1}) ; $[Ru_2N(NH_3)_8(H_2O)_2]^{5+}.5C\ell^-$, ($\Lambda^{\circ}$ = 782 Ω^{-1} cm^2 mol^{-1}); $[Os_2N(NH_3)_8C\ell_2]^{3+}.3C\ell^-$, ($\Lambda^{\circ}$ = 528 Ω^{-1} cm^2 mol^{-1}) and $[Ru_3O_2(NH_3)_{14}]^{6+}.6C\ell^-$, ($\Lambda^{\circ}$ = 1030 Ω^{-1} cm^2 mol^{-1}); the observed value for ruthenium violet suggests the presence of a 5+ cation in solution.

Isotopically Enriched forms of Ruthenium Violet.

The deuteriated complex was obtained by evaporating to dryness in vacuo a solution in ^2H_2O. The ^{15}N substituted material was prepared by reaction of ruthenium trichloride with $^{15}NH_3$ solution, using the given method. The solution of $^{15}NH_3$ was made by addition of aqueous sodium hydroxide to $^{15}NH_4C\ell$ (98.6%, ^{15}N), collection of the $^{15}NH_3$ in a cold trap, and dissolution in water.

Reaction of Ruthenium Tetraoxide with Ammonia Solution.

Ruthenium tetraoxide (ca. 0.1 g) in carbon tetrachloride (30 cm³) was stirred with ammonia solution (s.g. 0.880, 10 cm³) for 30 minutes. The aqueous layer was then separated, and allowed to evaporate down, leaving a black solid.

Found: H, 3.7 ; N, 15.9%. $H_{23}N_7O_{10}Ru_3$ requires H, 4.0 ;

N, 16.8%.

Infrared spectrum: 3360sh, 3200s, 3080sh, 1830ms, 1610ms,

1310s, 1040m, 810mw, 505 ms (cm^{-1}).

2-H-3. Nitrido-Bridged Osmium Species.

Osmium Violet, Octa-ammine Hexa-aquo Di-µ-Nitrido Tri-Osmium

Hexachloride, $[Os_3N_2(NH_3)_8(H_2O)_6]Cl_6$.

This complex.may be prepared by four methods, all involving

reaction of osmium complexes with ammonia solution.

1. A saturated solution of $Na_2[OsCl_6].xH_2O$ (2 g, 3.6 mmol)

was added to combined solutions of ammonium chloride (6.6 g,

0.12 mol) and sodium hydroxide (4 g, 0.1 mol) dissolved separately

in the minimum volume of water (40 cm^3); and heated in a closed

pressure bottle on a steam bath for six hours. The black solid

was filtered from the cooled solution, washed with a little water,

ethanol and ether, and dried in vacuo; yield 45%.

2. $Na_2[OsCl_6].xH_2O$ (5 g, 9 mmol) was refluxed with hydro-

chloric acid (0.25 M, 75 cm^3) and ethanol (15 cm^3) for three hours.

The brown solution was treated with excess concentrated ammonia

solution (0.880, 100 cm^3) and stirred and heated at 75 °C in air

for four hours, more ammonia solution being added to maintain the

volume. Yield of osmium violet, 15%.

3. $[Os(NH_3)_5Cl]Cl_2$ was prepared from $(NH_4)_2[OsCl_6]$ via

$[Os(NH_3)_5(N_2)]Cl_2$[76] and $[Os(NH_3)_5I]I_2$[77] using the literature methods.

The chloropentammine complex (1 g, 3.2 mmol) was stirred in air with ammonia solution (0.880, 50 cm^3), warmed to 75 $^\circ$C for three hours, more ammonia solution being added to maintain the volume. A total yield of 35% was collected from the cooled solution.

4. Osmium tetraoxide (5 g, 20 mmol) was warmed on a steam bath under reflux with concentrated hydrochloric acid (15 cm^3), water (25 cm^3) and ethanol (10 cm^3) for 40 hours. The resulting dark green solution was reduced in volume by evaporation. An excess of concentrated ammonia solution $\overset{s.g.}{(0.880}$, 100 cm^3) was added, and the mixture stirred in air at 60 $^\circ$C for five hours with further additions of ammonia solution to replace losses. A 25% yield was obtained.

Found: Cℓ, 18.9 ; H, 3.2 ; N, 14.0 ; O, 9.7 ; Os, 54.1%. Cℓ_6H$_{36}$N$_{10}$O$_6$Os$_3$ requires Cℓ, 20.2 ; H, 3.4 ; N, 13.3 ; O, 9.1 ; Os, 54.1%.

A sample was boiled with 45% sodium hydroxide, the ammonia liberated was collected in saturated boric acid solution[33,78] and titrated with hydrochloric acid, using bromocresol green indicator.

Found: 82.1, 85.4% of nitrogen in sample liberated as NH$_3$, required, 80%.

Physical Measurements.

Mass susceptibility χ = -2.9 x 10^{-9} m^3 kg^{-1} at 294 K, effective magnetic moment μ_{eff} = 0.64 per trinuclear molecule. Electronic spectrum in 0.1 M sodium acetate solution shows broad absorption bands at λ_{max} = 710 nm (ϵ = 12500 M^{-1} cm^{-1}), 590 nm (ϵ = 13950 M^{-1} cm^{-1}), 330 nm (ϵ = 6900 M^{-1} cm^{-1}).

The sparingly soluble <u>pyrophosphate</u> salt, $[Os_3N_2(NH_3)_8(H_2O)_5(OH)]^{5+}$-$(P_2O_7)_{1.25}.H_2O$, was obtained immediately on addition of a saturated solution of sodium pyrophosphate to a solution of osmium violet chloride in 0.1 M sodium acetate.

Found: H, 3.3 ; N, 12.3 ; P, 6.7%. $H_{37}N_{10}O_{15.75}Os_3P_{2.5}$ requires H, 3.5 ; N, 13.0 ; P, 7.2%.

The sparingly soluble <u>thiosulphate</u> salt, $[Os_3N_2(NH_3)_8(H_2O)_4(OH)_2]^{4+}$-$(S_2O_3)_2$, was obtained immediately on addition of a saturated solution of sodium thiosulphate to a solution of osmium violet in 0.1 M sodium acetate.

Found: H, 3.0 ; N, 11.8 ; S, 12.3%. $H_{34}N_{10}O_{12}Os_3S_4$ requires H, 3.2 ; N, 13.2 ; S, 12.0%.

The <u>bromide</u> salt of osmium violet, $[Os_3N_2(NH_3)_8(H_2O)_5(OH)]Br_5$, was obtained from $(NH_4)_2[OsBr_6]$ (3 g, 4.3 mmol) with ammonium bromide (12.5 g, 0.13 mol) and sodium hydroxide (4.2 g, 0.1 mol) by method 1 above. Yield was 40%.

Found: Br, 28.4 ; H, 2.7 ; N, 11.3 ; Os, 46.9%. $Br_5H_{35}N_{10}O_6Os_3$ requires Br, 32.2 ; H, 2.8 ; N, 11.3 ; Os, 46.0%.

The product from the preparation of the <u>iodide</u> salt of osmium violet, from $(NH_4)_2[OsI_6]$ (4.7 g, 4.8 mmol) with ammonium iodide (20.9 g, 0.14 mol) and sodium hydroxide (4.7 g, 0.12 mol) using method 1, above, yield 32%, is best formulated as $[Os_3N_2(NH_3)_4(OH)_4$-$(H_2O)_4]I_2$.

Found: H, 2.0 ; I, 23.5 ; N, 7.1 ; Os, 50.5%. $H_{24}I_2N_6O_8Os_3$ requires H, 2.3 ; I, 23.9 ; N, 7.9 ; Os, 53.8%.

Isotopically Enriched forms of Osmium Violet.

$[Os_3N_2(N^2H_3)_8(^2H_2O)_6]C\ell_6$. The deuteriated species was prepared by reaction of solutions of $K_2[OsC\ell_6]$, $N^2H_4C\ell$ (prepared by evaporation in vacuo of $NH_4C\ell$ in ^2H_2O) and NaO^2H (Na dissolved in ^2H_2O) in ^2H_2O using method 1 for osmium violet.

$[Os_3{}^{15}N_2({}^{15}NH_3)_8(H_2O)_6]C\ell_6$. Use of ${}^{15}NH_4C\ell$ (98.6% ${}^{15}N$) in the osmium violet preparation method 1 afforded the ${}^{15}N$-substituted complex.

Tetrapotassium Decacyano Tetra-aquo Di-μ-nitrido Tri-Osmium Tetra-hydrate, $K_4[Os_3N_2(CN)_{10}(H_2O)_4].4H_2O$.

Osmium violet chloride (0.35 g, 0.33 mmol) dissolved in potassium cyanide solution (2 g in 5 cm^3 water) was stirred and boiled under reflux for seven hours. The cooled brown solution was poured into methanol (20 cm^3), the brown precipitate filtered off, and washed with boiling methanol followed by ether. The product was recrystallised by dissolution in water (20 cm^3), addition of methanol until turbid (ca. 10 cm^3) and storage in the refrigerator. The black precipitate was collected, yield 20%.

Found: C, 9.7 ; H, 1.4 ; K, 12.7 ; N, 14.6 ; O, 11.2 ; Os, 45.4%. $C_{10}H_{16}K_4N_{12}O_8Os_3$ requires C, 10.4 ; H, 1.4 ; K, 13.5 ; N, 14.5 ; O, 11.0 ; Os, 49.2%.

The electronic absorption spectrum in aqueous solution has bands at λ_{max} = 640 nm (ε = 4100 M^{-1} cm^{-1}), 510 nm (ε = 6000 M^{-1} cm^{-1}), 460 nm (ε = 5700 M^{-1} cm^{-1}) and 370 nm (ε = 4300 M^{-1} cm^{-1}).

Osmium Brown, Octa-ammine Hexa-aquo Di-μ-nitrido Tri-osmium

Heptachloride, $[Os_3N_2(NH_3)_8(H_2O)_6]Cl_7$.

Osmium brown may be extracted following the evaporation to
low volume of the solutions remaining after precipitation of osmium
violet made by the methods described above. The preparation of
osmium violet from $Na_2[OsCl_6].xH_2O$ (method 2) produces up to 1.5 g
of osmium brown from 5 g of hexachloroösmate. Osmium brown was
also produced in the preparation of $[Os_2N(NH_3)_8Cl_2]Cl_3$ without
the formation of osmium violet. In this method, $Na_2[OsCl_6].xH_2O$,
(1.5 g, 2.7 mmol) was warmed with ammonia solution (0.880, 25 cm^3)
in a sealed pressure bottle on a steam bath for six hours. The
brown-black solid was filtered off, washed with ammonia solution
and dried in vacuo. Yield, 10%.

Found: Cl, 21.7 ; H, 2.9 ; N, 12.6 ; O, 9.4 ; Os, 52.1%.
$Cl_7H_{36}N_{10}O_6Os_3$ requires Cl, 22.8 ; H, 3.2 ; N, 12.9 ; O, 8.8 ;
Os, 52.3%.

On boiling with 45% sodium hydroxide, 73.3 and 85.7% of the
total nitrogen was collected as ammonia, using the same method as
that described for osmium violet. $[Os_3N_2(NH_3)_8(H_2O)_6]Cl_7$ requires
80% N as NH_3.

Physical Measurements

Mass susceptibility $\chi = -2.0 \times 10^{-9}$ m^3 kg^{-1} at 294 K,
effective magnetic moment μ_{eff} = 0.84 B.M. per trinuclear molecule.
Electronic spectrum in 0.1 M sodium acetate solution shows absorption
bands at λ_{max} = 380 nm (ϵ = 6400 M^{-1} cm^{-1}) and 320 nm (ϵ = 5300 M^{-1} cm^{-1}).

The <u>bromide</u> salt of osmium brown, $[Os_3N_2(NH_3)_9(H_2O)_3(OH)_2]Br_3$

was isolated from the solution remaining after the precipitation of

osmium violet bromide from the reaction mixture.

Found: Br, 32.0 ; H, 2.8 ; N, 12.2%. $Br_3H_{35}N_{11}O_5Os_3$ requires

Br, 32.3 ; H, 2.9 ; N, 12.4%.

Isotopically Enriched forms of Osmium Brown.

The deuteriated species was prepared from $K_2[OsCl_6]$ and a

solution of NH_3 in ^2H_2O. Reaction of $Na_2[OsCl_6].xH_2O$ with $^{15}NH_3$

solution (prepared as previously described) gave the ^{15}N-substituted

osmium brown.

Gautier's Osmium -Ammine Complex, Hexa-ammine Di-aquo Tetra-Hydroxo Di-μ-Nitrido Tri-Osmium Dichloride, $[Os_3N_2(NH_3)_6(H_2O)_2(OH)_4]Cl_2$.

The complex was prepared from osmium tetraoxide (5 g, 20 mmol)

according to the literature method.[35] The yield of brown-black

solid, soluble in buffer (0.1 M sodium acetate or 0.1 M sodium

cacodylate solution) was 2.7 g.

Found: Cl, 6.3 ; H, 2.9 ; N, 12.6%. $Cl_2H_{26}N_8O_6Os_3$ requires

Cl, 8.1 ; H, 3.0 ; N, 12.8%.

On boiling with 45% sodium hydroxide solution, 69.5% of the total

nitrogen was collected as ammonia, $[Os_3N_2(NH_3)_6(H_2O)_2(OH)_4]Cl_2$

requires 75%.

Physical Measurements.

Measurements on aqueous solutions over the range 3×10^{-5} -

5×10^{-6} M gave the limiting conductance $\Lambda^° = 480 \ \Omega^{-1} \ cm^2 \ mol^{-1}$ at 25 °C.

The binuclear complex $[Os_2N(NH_3)_8Cl_2]^+.3Cl^-$ under similar conditions has

a limiting conductance $\Lambda^° = 528 \ \Omega^{-1} \ cm^2 \ mol^{-1}$. The result for Gautier's

osmium ammine complex suggests a 3:1 electrolyte.

Mass susceptibility $\chi = -3.5 \times 10^{-9} \ m^3 \ kg^{-1}$ at 294 K,

effective magnetic moment μ_{eff} = 0.38 B.M. per trinuclear molecule.

Reaction of Gautier's compound with hot concentrated hydrochloric

acid formed a yellow-brown chloro complex, with infrared bands

at: 3440m, 3200s, 1600m, 1555m, 1340s, 1015s, 965m, 305m, 280m (cm^{-1}).

Treatment of Gautier's complex with hot cyanide solution yielded

a brown cyano complex, infrared bands at: 3440s, 3200s, 2100s, 2020s,

1615m, 1340 (obsc), 1055m, 975s, 545ms,sp, 475ms, 380m (cm^{-1}).

Osmium Tetraoxide.with Ammonia Solution, Tetra-Ammino Di-aquo Octa-Hydroxo Di-µ-Nitrido Tri-Osmium, $[Os_3N_2(NH_3)_4(OH)_8(H_2O)_2]$.

Concentrated ammonia solution (0.880, 150 cm^3) was added to an

aqueous solution of osmium tetraoxide (3.6 g, 14 mmol in 100 cm^3

water)and the mixture warmed under reflux for 48 hours, yield 90%

of black insoluble solid.

Found: H, 2.4 ; N, 10.6%. $H_{24}N_6O_{10}Os_3$ requires H, 2.9 ;

N, 10.0%.

The cyano derivative, tetra-potassium octa-cyano di-aquo tetra-hydroxo

di-µ-nitrido tri-osmium, $K_4[Os_3N_2(CN)_8(OH)_4(H_2O)_2]$, was obtained

by reaction of the black solid (1 g, 1.2 mmol) in boiling potassium

cyanide solution (2.5 g, in 75 cm^3 water). After seven hours

refluxing, the cooled brown solution was poured into stirred

methanol (150 cm^3), the precipitate filtered off, and washed with

methanol, followed by ether. The product was recrystallised from

water-methanol, after drying in vacuo the yield of rather

hygroscopic dark brown solid was 60%.

Found: C, 8.9 ; H, 1.0 ; K, 13.9 ; N, 13.7%. $C_8H_8K_4N_{10}O_6Os_3$

requires C, 9.0 ; H, 0.8 ; K, 14.7 ; N, 13.1%.

Osmium Tetraoxide with Liquid Ammonia, $Os_3N_7O_9H_{21}$.

The black material, $Os_3N_7O_9H_{21}$ was formed when a solution of

osmium tetraoxide, (1 g, 4 mmol) in liquid ammonia (10 cm^3) was

allowed to warm up and lose the solvent. Yield 87%.

Found: H, 2.1 ; N, 12.1%. $H_{21}N_7O_9Os_3$ requires H, 2.5 ; N, 11.8%.

The cyano complex, tetra-potassium hepta-cyano di-aquo penta-

hydroxo di-μ-nitrido tri-osmium dihydrate, $K_4[Os_3N_2(CN)_7(OH)_5(H_2O)_2].2H_2O$,

was obtained by refluxing the black solid (0.5 g, 0.6 mmol) with

potassium cyanide solution (1 g in 15 cm^3 H_2O) for seven hours;

and collecting the precipitate formed on pouring the cooled solution

into methanol (50 cm^3). After recrystallisation from water/methanol,

the yield of yellow-brown solid was 30%.

Found: C, 7.4 ; H, 0.9 ; K, 13.4 ; N, 11.3%. $C_7H_{13}K_4N_9O_9Os_3$

requires C, 7.7 ; H, 1.2 ; K, 14.3 ; N, 11.5%.

A chloro complex was obtained by refluxing the black solid with

concentrated hydrochloric acid and precipitation as the caesium

salt. Infrared bands at 3460m, 3230ms, 3160s, 1605m, 1555mw, 1018ms,

963s, 318s (cm^{-1}).

Miscellaneous

(i) The ternary nitride $Ba_9Os_3N_{10}$, (prepared as in reference 58) was

slowly added to ice-cold concentrated hydrochloric acid (2.5 g

solid into 10 cm^3 acid). The insoluble barium salts were centrifuged

off, and caesium chloride added to precipitate the brown osmium

chloro complex, analysing as $Cs_4[Os_3N_2(NH_3)_2Cl_{10}(H_2O)_2].4H_2O$.

Found: $C\ell$, 21.3 ; Cs, 41.7 ; H, 0.7 ; N, 3.1%. $C\ell_{10}Cs_4H_{18}N_4O_6Os_3$ requires $C\ell$, 22.3 ; Cs, 33.5 ; H, 0.8 ; N, 3.5%. Infrared bands at: 3500sh, 3300ms,b, 3130s, 1605ms, 1340mw, 1010s, 965s, 535w, 460w, 305s (cm^{-1}).

(ii) The binuclear osmium cyano complex $K_5[Os_2N(CN)_8(OH)_2]$ was produced by dissolving $Cs_3[Os_2NC\ell_8(H_2O)_2]$ (1 g, 0.9 mmol) in potassium cyanide solution (1.5 g in 15 cm^3 water), refluxing for seven hours, and precipitating by pouring into methanol. Yield of the light yellow-brown cyano complex, after recrystallisation from water-methanol was 50%. (A similar product was obtained from " $Os_2N(OH)_5.nH_2O$ ", prepared from $Cs_3[Os_2NC\ell_8(H_2O)_2]$ with sodium hydroxide solution, with aqueous potassium cyanide).

Found: C, 12.5 ; H, 0.1 ; K, 25.8 ; N, 14.4%. $C_8H_2K_5N_9O_2Os_2$ requires C, 11.5 ; H, 0.2 ; K, 23.5 ; N, 15.2%.

(iii) The benzotriazole complex $OsC\ell_3(C_6H_4NHN_2)_3$[79] was heated for four hours at 430 °C to generate $OsC\ell_3$.[80] The product formed did not dissolve in aqueous ammonia.

(iv) The binuclear complexes $[Ru_2N(NH_3)_8(NO_3)_2](NO_3)_3$, $[Ru_2N(NH_3)_8C\ell_2]C\ell_3$, $[Os_2N(NH_3)_8C\ell_2]C\ell_3$ and $Cs_3[Os_2NC\ell_8(H_2O)_2]$ were prepared by the literature methods.[13]

Chapter Three

## Sulphito Complexes of the Platinum Group Metals

ABSTRACT

Raman and infrared spectra are reported, and assigned for a range of mononuclear sulphito complexes of the platinum group metals, Ir, Os, Pd, Pt, Rh and Ru. The spectra are interpreted, using the idealised overall symmetry of the complexes, to suggest likely structures. Coordination via sulphur is found in most cases, with the metal-sulphur stretching mode appearing near 250 cm^{-1} in the Raman spectra. The new species, $[Os(NH_3)_4(SO_3)C\ell]$, $K_4[Os(SO_3)_3(H_2O)_3]$ and $[Os_2N(NH_3)_8(SO_3)(H_2O)]C\ell_3$ are described. The role of osmium and ruthenium sulphito complexes in heavy metal staining for electron microscopy is very briefly discussed.

Section 3-A. Introduction.

Complexes of the sulphite ion, SO_3^{2-}, are known for many metals. A range of complexes containing the sulphito group, coordinated via sulphur or oxygen are known for all the platinum group metals, osmium, ruthenium, iridium, rhodium, platinum and palladium. In most cases, other ligands such as ammino, chloro or aquo groups are also present. A compilation of the known sulphito complexes, some with very odd formulations, of osmium, ruthenium, iridium and rhodium, has been made.[81] A study of osmium and ruthenium sulphito complexes was prompted by the previously noted (Section 2-G) potential involvement of such species in electron microscopy staining reagents.

Structures.

Few structures of sulphito complexes of the group VIII metals have been solved by X-ray crystallographic techniques; coordination via sulphur has been found in most cases. The palladium complex Pd(SO₃)(NH₃)₃ is square-planar.[82]
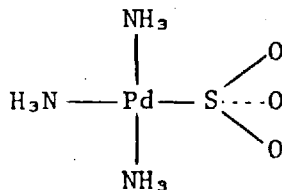
The iridium species $(NH_4)_5[Ir(SO_3)_2C\ell_4]$ has been shown to

contain <u>trans</u> sulphito-groups, with coordination from the sulphur.[83]

The partially solved structure of $(NH_4)_4[Ir(SO_3)_2C\ell_3]$ suggests

that the bidentate SO_3^{2-} group may be bound by oxygen and sulphur.[83]

The sulphur dioxide complex, $[Ru(NH_3)_4C\ell(SO_2)]C\ell$ is sulphur-

bonded.[84]
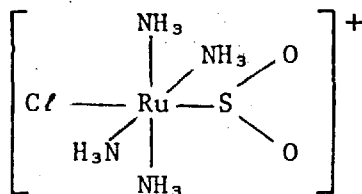
Apart from the platinum group metals, two cobalt species have

been shown to contain monodentate sulphur coordination, <u>cis</u>-

$(NH_4)[Co(NH_3)_4(SO_3)_2]$[85] and $[Co(SO_3)(H_2O)(en)_2]C\ell O_4 \cdot H_2O$.[86]
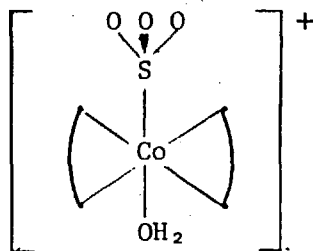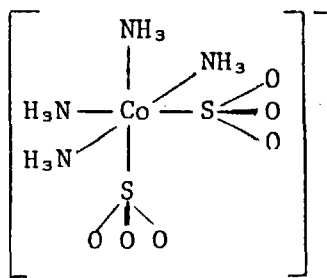
An example of the more rarely encountered monodentate oxygen

coordination is $(NH_4)_9[Fe(OSO_2)_6]$.[87]
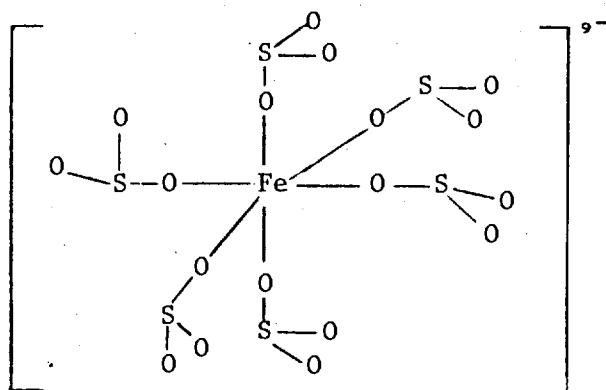
Vibrational Spectra.

No Raman studies of complexes containing the monodentate

sulphito group appear to have been reported, although spectra

have been published for the $M^{II}SO_3.nH_2O$ species (M = Zn, Mn, Co,

Mg).[88] The infrared spectra of some compounds have been documented,

allowing structures to be postulated.

A number of iridium(III)[89] and rhodium(III)[90] sulphito

complexes have been investigated by infrared spectroscopy, and

the monodentate sulphito groups appear to be coordinated via

sulphur in most cases. Exceptions were $Na_7[Ir(SO_3)_4Cl_2]$ and

$(NH_4)_5[Ir(SO_3)_2Cl_4]$,[89] for which bonding via oxygen could not be

ruled out; the latter was subsequently shown to contain trans

groups with sulphur coordination.[83] Platinum(II)[91] and palladium(II)[92]

sulphito complexes again appear likely to be sulphur-bonded.

Ruthenium and osmium sulphito complexes have been studied to a lesser

extent by infrared spectroscopy, data only being available for

$[Ru(NH_3)_4(SO_2)Cl]Cl$, $[Ru(NH_3)_4(HSO_3)_2]$ and $[Ru(NH_3)_5(SO_2)]Cl_2$.[84]

Infrared data have been reported for the oxygen-bound $[Fe(SO_3)_6]^{9-}$ ion[93] and for some sulphur-bound cobalt complexes.[94]

Figure 3.1

Possible Modes of Bonding of the Sulphito Group, SO_3^{2-}.
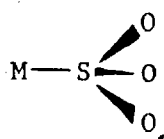
a

b

c
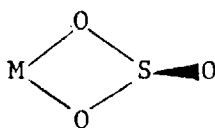
d
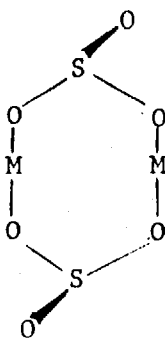
e
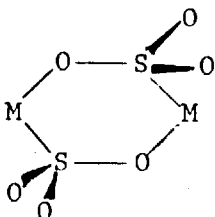
f

The free SO_3^{2-} ion is pyramidal, with C_{3v} symmetry:

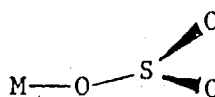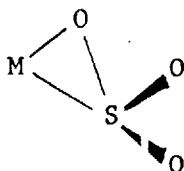$$\left[\begin{array}{c} \text{O} \\ \diagup \overset{\displaystyle S}{\underset{\text{O}}{\big\uparrow}} \diagdown \text{O} \end{array} \right]^{2-}$$
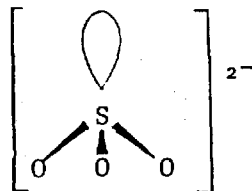
Two a_1 and two e modes are expected, ν_1 (a_1) being the symmetric stretch, ν_2 (a_1) the symmetric bend, ν_3 (e) the asymmetric stretch and ν_4 (e) a bending mode.

	ν_1	ν_2	ν_3	ν_4 (cm^{-1})
solid Na$_2$SO$_3$[95] (ir)	983	632	947	494
solid Na$_2$SO$_3$[96] (ir)	1010	633	961	496
SO_3^{2-} solution[96] (ir)	1002	632	954	–
SO_3^{2-} solution[96] (R)	967	620	933	469

The large discrepancy between the infrared and Raman solution data is ascribed to the strong intermolecular forces.[96]

Sulphur-coordinated monodentate SO_3^{2-} will retain a local symmetry of C_{3v} and four vibrational modes are again expected for the ligand. On coordination via sulphur (Figure 3.1a), a shift to higher frequencies of ν(S-O) modes is predicted following an increase in the sulphur-oxygen bond order.[97,98] Coordination via an oxygen (Figure 3.1b) will lower the local symmetry of the SO_3^{2-} group to C_s, the degeneracy of the e modes will be lifted and six bands are anticipated for the ligand. A lowering of one of the S-O stretching frequencies (that connected to the metal via the oxygen) is likely.

The overall idealised symmetry of the complex is also worthy of consideration when relating the number of observed bands to possible structures. Where more than one sulphito group is present, inter-action of vibrations results. The effect of hydrogen bonding to water of hydration, and the site symmetry for the complex may also be to increase the number of vibrational modes observed. These latter effects may be avoided by measuring the spectra of aqueous solutions.

Bidentate coordination of the sulphito group, via sulphur and oxygen (Figure 3.1c) or oxygen only (Figure 3.1d) is possible, and bridged species may also be considered (Figure 3.1e and f). Infrared studies on bidentate sulphites have not enabled the structures to be distinguished,[90] since the S-O bonds in unidentate and bidentate sulphite appear to be of comparable strength.

No M-O or M-S stretching modes have yet been assigned for sulphito complexes. In other complexes, ν(M-S) bands have been seen in the range 480-210 cm^{-1}, e.g., for the thiourea complexes [Pd(thiourea)$_4$]$C\ell_2$ at 277, 256 and 248 cm^{-1} and [Pt(thiourea)$_4$]$C\ell_2$ at 278, 268 and 258 cm^{-1}.[99] The dimethylsulphide species Pd[(CH$_3$)$_2$S]$_2$$C\ell_2$ has ν_{M-S} at 310 cm^{-1} (322 cm^{-1} in the Raman) and Pt[(CH$_3$)$_2$S]$_2$$C\ell_2$ at 311 cm^{-1} (346 cm^{-1} in the Raman).[100] Metal-oxygen stretches have been found in the range 1100-200 cm^{-1}; for the dimethylsulphoxide complexes of Fe^{II} and Co^{II}, ν_{M-O} is seen at 438 and 415 cm^{-1} (Fe^{II}) and 436 cm^{-1} (Co^{II}).[101]

Section 3-B. Vibrational Spectra of Platinum Group Metal Sulphito

Complexes.

The vibrations of the coordinated sulphito groups ($v_1 - v_4$)
are assigned by reference to earlier infrared studies.[84,89,90,91,92]
Symmetric S-O stretches appear with greater intensities than the
asymmetric modes in the Raman spectra. Where possible, assignments
of v(M-S) or v(M-O) in the Raman spectra are made. Bands due to
other ligands are assigned by reference to Nakamoto.[102] The spectra
are tabulated, with assignments, in Table 3.1, the nomenclature
$v_1 - v_4$ being used to describe SO_3^{2-} ligand modes by analogy to the
free ion.

3-B-1. Monosulphito Complexes.

The palladium complex, $[Pd(SO_3)(NH_3)_3]$ has been shown to
contain a sulphur-coordinated monodentate sulphito group, with the
three ammine ligands completing a square planar arrangement.[82] Although
the local symmetry of the sulphito group is C_{3v}, the overall symmetry
is C_s, and on this basis, splitting of the sulphite e modes is
anticipated. In the Raman spectrum, v_3 is split, while in the
infrared, v_3 is broadened and v_4 is split. The assignment of $v_1 - v_4$
is confirmed by the immobility of these bands on deuteriation.
The Raman band at 253 cm^{-1} is a good candidate for v(Pd-S). The Raman
and infrared spectra of $[Os(NH_3)_4(SO_3)C\ell]$ and $[Os_2N(NH_3)_8(SO_3)(H_2O)]C\ell_3$
show bands in regions typical of sulphur-coordinated SO_3^{2-}, with v_3
and v_4 resolved into two bands in some cases. An idealised overall
symmetry of C_s is probable. The high Raleigh scattering background
prevented investigation of the v(Os-S) region.

Table 3.1

Vibrational Spectra of Sulphito Complexes.

Complex		ν_1	ν_2	ν_3	ν_4	$\nu(M-S)$	Other Bands
				SO$_3$ Modes			
Monosulphito Complexes.							
[Pd(SO$_3$)(NH$_3$)$_3$]	IR	977s	633ms	1060vs,b	518mw,505m		NH$_3$: 3220s, 3120s, 1600ms, 1288m, 1265m 830sh, 808m, 490sh, 415mw.
(square planar) C$_s$	IR*	976m	652m, 615mw	1068vs,b	515m, 505sh		N^{2}H$_3$: 2350sh, 2280ms 1160sh, 1023mw, 1000 390w. ^{2}H$_2$O 2445s.
	R	978s	640m	1090w, 1075vw	518w	253ms	NH$_3$: 1340vw, 1280 w, 1272w,490sh, 478vs, 427mw, 279m. 301m.
[Os(NH$_3$)$_4$(SO$_3$)Cl]	IR	965mw	615ms,sp	1090s, 1055s	568w		H$_2$O: 3400ms, 1570sh. NH$_3$: 3180vs, 1605s, 1320s, 843ms, 820s, 460mw, 447m. Cl: 297ms,sp.
† C$_s$ (trans)	R	983ms	620w	1085w, 1060w	570w, 550w		NH$_3$: 880w, 495m, 475
[Os$_2$N(NH$_3$)$_8$(SO$_3$)(H$_2$O)]Cl_3	IR	957m,sp	625m	1090sh, 1045m	508w		H$_2$O: 3420s. NH$_3$: 3260vs, 3160vs, 1620 1340s, 853ms, 465mw. Os$_2$N: 1108s.Also 1218ms,1197ms, 1025m 575mw.
† C$_s$ (axial)							

Table 3.1 (cont).

Complex		SO$_3$ Modes				ν (M-S)	Other Bands
		ν_1	ν_2	ν_3	ν_4		
$[Os_2N(NH_3)_8(SO_3)(H_2O)]C\ell_3$	R	990m	646w	1135m, 1102m	505m		NH$_3$: 490m. Os$_2$N: 285s. Also 803m, 700w, 572w.
$[Ru(NH_3)_5(SO_3)].2H_2O$	IR	922s	631s	970vs,b	525w		H$_2$O: 3340ms, 1650m,b. NH$_3$: 3140s,b, 1625m,b 1300w, 1267s, 794w, 498m
$^+$ C$_s$	R	920w	633mw	1080w,b, 950w	560w,b, 510w,b	230w^a	NH$_3$: 805s, 750sh, 44? 408m, 285vs. Also 128s.
Bis-sulphito complexes (NH$_4$)$_5$[Ir(SO$_3$)$_2$Cℓ_4].H$_2$O	IR	943vs	635ms	1010vs	519mw		H$_2$O: 3440m, 1750w,b, 1623w. NH$_4$: 3170vs, 1670mw, 1400obsc. Ir-Cℓ: 328m
C$_{2h}$ (trans)	R	990m	640w	1075w, 1030w	510vw	250w	Ir-Cℓ: 325vs, 305s
K$_5$[Ir(SO$_3$)$_2$Cℓ_4].6H$_2$O	IR	975s, 945vs	650sh, 630s	1073vs, 1024vs	520ms		H$_2$O: 3580sh, 3550sh, 3520s, 3400vs, 1660sh 1635ms, 1607ms,1560mw Ir-Cℓ: 330sh, 318ms.
$^+$ C$_{2h}$ (trans)	R	982sh, 972s, 940w	655mw	1090w, 1050mw,b 1030mw	530sh	252m	Ir-Cℓ: 350m, 312vs. also 275m, 170m
Na$_3$[Ir(SO$_3$)$_2$(NH$_3$)$_2$Cℓ_2].6H$_2$O IR $^+$ C$_{2h}$ (trans)		993ms, 967vs	660s, 635s	1085s, 1050vs	520ms		H$_2$O: 3490s, 1665ms. NH$_3$: 3330vs, 3230vs 1635m, 1302m, 1282m. Ir-Cℓ: 340m.

Table 3.1 (cont).

Complex		SO$_3$ Modes				ν(M–S)	Other Bands
		ν_1	ν_2	ν_3	ν_4		
Na$_3$[Ir(SO$_3$)$_2$(NH$_3$)$_2$Cl$_2$].6H$_2$O R		1000s	670vw	1110w, 1070mw	520vw	258m	NH$_3$: 1300vw, 465vs. Ir–Cl: 318vs.Also 200mw, 175vw, 125w.
Tris-sulphito Complexes							
Na$_3$[Ir(SO$_3$)$_3$(NH$_3$)$_3$].7H$_2$O IR		975vs	660sh, 633ms	1100vs, 1050s	520m		H$_2$O: 3400s, 1630m. NH$_3$: 3300vs, 3200s, 1630m, 1302m, 830w.
†C$_{3v}$ (cis) IR*		960s	665sh, 637s, 620s	1100vs,b	530m		^{2}H$_2$O: 2590m. N^{2}H$_3$: 2320s, 2240m, 2130mw, 1260mw, 800m, 450mw.
R		995s, 980sh	620mw	1090m,b	530m	250m,b	NH$_3$: 460s. Also 350w, 320w.
(NH$_4$)$_3$[Rh(SO$_3$)$_3$(NH$_3$)$_3$].1$\frac{1}{2}$ H$_2$O IR		938vs	661m,sp, 620vs	1120s, 1028vs	532ms		H$_2$O: 3440sh,b, 1675sh. NH$_3$: 3320s, 3150s, 1620m, 1240mw, 1203w, 880sh, 772mw, 408m. NH$_4^+$: 1410obsc. Also 333mw.
† C$_{3v}$ (cis) IR*		940vs	678mw, 621s	1100vs, 1030vs	520m		^{2}H$_2$O: 2480sh, 2360s. N^{2}H$_3$: 2280s, 2210s, 2100s,1200sh. Also 330m.
R		997ms, 963w 955w	663mw,630mw	1130vw,1100vw, 1050w	528mw	247s,b	NH$_3$: 1240mw, 474w, 427s, 415sh Also 332mw

Table 3.1 (cont).

Complex		SO$_3$ Modes				ν(M-S)	Other Bands
		ν_1	ν_2	ν_3	ν_4		
$(NH_4)_3[Rh(SO_3)_3(NH_3)_3]$ (Aqueous solution)	R	982mw, 963w	66ũw, 630w	1070mw,b, 1010ms	520w	220ms,b	NH$_3$: 1240w, 430s.Also 320w
$K_4[Os(SO_3)_3(H_2O)_3]$	IR	980s	600m	1120s, 1070s, 1030m	508m		H$_2$O: 3380vs,b, 1620m, 370m.Also 890s, 780s, 480sh,330mw
† C_{3v} (cis)	R	950m	610vw	1114m, 1082s, 1056sh	500v	255m	310vw, 225w, 195m
Tetrasulphito Complexes							
$K_6[Pt(SO_3)_4].2H_2O$	IR	968vs	660m, 640ms	1085vs,1058ms	538m, 527m		H$_2$O:3310ms, 3230ms, 1685m.Also, 1305mw, 1170w,1150w, 740ms, 560m, 512m, 309m,288m
† C_{4h} (square planar)	R	977mw	690mw, 627w	1077mw, 1066m, 1027s	532mw, 515w	248vs	1124m, 608w, 502mw, 288m, 276w, 232m,223w 202s, 160m, 150mw,120
$Na_6[OsO_2(SO_3)_4].2H_2O$	IR	977vs	647ms	1115vs, 1077vs	522ms		H$_2$O: 3560sh, 3380s,b, 1638m. Os=0: 842m,sp. Also 1025w, 888mw, 780m, 377m, 332w
† C_{4h} (trans)	R	917m,sh	646w,b	1002m,b	496vs	280m,b	Os=0: 858w,b. Also 748w,b, 480sh, 210w
$K_6[OsO_2(SO_3)_4].2\frac{1}{2}H_2O$	IR	977sh, 955vs	650sh, 632s	1107vs, 1075vs	535sh, 518ms		H$_2$O: 3340vs, 1672m Os=0: 835s,sp.
† C_{4h} (trans)	R	930ms,sp	665w,630w	1020w, 990w	480vs,b		720w

Table 3.1 (cont).

| Complex | | SO$_3$ Modes | | | | ν(M-S) | Other Bands |
		ν_1	ν_2	ν_3	ν_4		
Na$_7$[Ir(SO$_3$)$_4$Cℓ_2].7H$_2$O	IR	965vs	635?, 625sh	1110ms, 1070s 1053vs, 1030s	525m		H$_2$O: 3400s, 3230vs, 1650sh, 1630m. Ir-Cℓ: 337m,sp. Also 830w, 555mw
$^+$C$_{4h}$ (trans)	R	980w	670mw, 640mw	1090m, 1028s	540w	240w	Ir-Cℓ: 308s. Also 205m
(NH$_4$)$_7$[Ir(SO$_3$)$_4$Cℓ_2].2½ H$_2$O	IR	945vs, 910s	630s	1065vs, 1020vs	531ms		H$_2$O: 3450sh,b, 1680m. NH$_4^+$: 3160vs, 1645m, 1400obsc. Ir-Cℓ: 340w Also 1262ms, 768vw, 470w.
$^+$C$_{4h}$ (trans)	R	960mw, 935vw	665w, 640w	1080mw, 1040mw 1007s	540w, 520sh	220ms	Ir-Cℓ: 313vs. Also 1260w, 820vw, 590vw, 467ms, 132mw
Other Sulphito Complexes							
(NH$_4$)$_9$[Fe(OSO$_2$)$_6$]	IR	815s	638ms	943vs	520mw	b	NH$_4^+$: 3140s,b, 1715vw, 1680w, 1405obsc. Also 2350w, 2140mw, 1910m, 1140sh, 320mw
(Oxygen-coordinated)	R	828s	638ms	991vs, 967ms	520ms	b	296m, 211m
K$_3$[Rh(SO$_3$)$_3$].2H$_2$O (bidentate sulphite)	IR	970sh, 945s	687m, 640ms	1150s, 1112ms, 1073s, 1053s	550vw, 530mw		H$_2$O: 3390s, 3250s, 1645m Also 372w, 360w 295w.

Table 3.1 (cont).

| Complex			SO$_3$ Modes				ν(M–S)	Other Bands
			ν_1	ν_2	ν_3	ν_4		
K$_3$[Rh(SO$_3$)$_3$].2H$_2$O	R		960sh, 937s	690w, 642mw	1160mw,b, 1110ms, 1090sh	560w, 525w	250ms[c]	200w
[Ru(NH$_3$)$_4$(SO$_2$)Cℓ]	IR		1090s,b		1305ms, 1282ms	557s,sp		NH$_3$: 3260s,b, 3150s,b, 1620s,b, 1247s, 815m, 782s, 476w, 460w,420s, 277m. Ru-Cℓ: 330m. Also 965m,b, 395sh, 365w.
(planar RuSO$_2$, trans Cℓ)	R		1120sh, 1102s		1320vw, 1257mw	560ms	243mw	NH$_3$: 485m, 475mw, 425vw, 280w, Ru-Cℓ: 333w. Also 362vs, 202mw, 185w
[Ru(NH$_3$)$_4$(HSO$_3$)$_2$]	IR		1000vs,b		1230ms,b, 1100s,b	570vs, 500s,sp		O-H: 3310s.NH$_3$: 3260sh 3180s,b, 1630s,b, 1302vs, 790s, 740vs, 475sh, 440w, 263m.Also 305sh, 290m
(Trans -SO$_2$OH)	R		999s	619mw	1110m	570vw	243ms	NH$_3$: 779mw, 745w, 488mw, 458m, 446vw, 417mw, 265m.Also 358vw 213mw.

All frequencies in cm^{-1}, * deuteriated sample, † idealised overall symmetry best in agreement with spectra.

a or ν(Ru-O) at 373m cm^{-1}.　　b ν(Fe-O) at 458m (IR), 461w (R) cm^{-1}.　c also ν(Rh-O) at 373mw cm^{-1}.

The $\nu(S-O)$ bands of $[Ru(NH_3)_5(SO_3)].2H_2O$ fall in rather lower

regions than most of the other sulphito complexes considered here.

For this reason, bonding via oxygen of the sulphito group may

not be excluded. The weak Raman band at 230 cm^{-1} may be $\nu(Ru-S)$,

or a band at 373 cm^{-1} could be $\nu(Ru-O)$.

3-B-2 Bis-sulphito Complexes.

A trans, sulphur coordinated structure has been found by

X-ray crystallography for $(NH_4)_5[Ir(SO_3)_2Cl_4]$.[83] Infrared and

Raman spectra of $K_5[Ir(SO_3)_2Cl_4].6H_2O$ and of $(NH_4)_5[Ir(SO_3)_2Cl_4].H_2O$

are found to be similar, although the Raman spectrum of the ammonium

salt was of poor quality. Splitting of ν_1, ν_2 and ν_3 is observed.
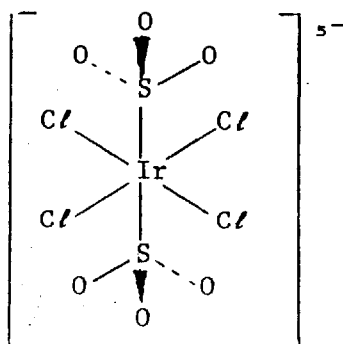

For the structure of C_{2h} idealised overall symmetry,

$\Gamma_{S-O} = 2a_g + b_g + a_u + 2b_{2u}$, and three Raman active (a_g, b_g) and

four infrared active (b_g, a_u, b_u) S-O stretching modes are expected.

The observed spectra are in broad agreement with the predictions,

the infrared of the ammonium salt lacking two bands and the Raman

of the potassium salt displaying three additional bands. Bands

assigned to ν(Ir-S) are seen at 250 cm^{-1},(NH$_4$)$_5$[Ir(SO$_3$)$_2$Cℓ_4].H$_2$O

and 252 cm^{-1}, K$_5$[Ir(SO$_3$)$_2$Cℓ_4].6H$_2$O. In C$_{2h}$ symmetry, two Raman

(a$_g$) and two infrared active (a$_u$, b$_u$) metal-chloride stretching

modes are expected. Two Raman, and two infrared active, non-

coincident bands are indeed seen for the potassium salt, between

310 and 350 cm^{-1}, while one is missing from the infrared spectrum

of the ammonium salt. These observations suggest that the <u>trans</u>

C$_{2h}$ structure is a reasonable choice.

The complex Na$_3$[Ir(SO$_3$)$_2$Cℓ_2(NH$_3$)$_2$].6H$_2$O shows three Raman

and four infrared ν(S-O) bands, suggesting a <u>trans</u> arrangement. A

band assigned to ν(Ir-S) is seen at 258 cm^{-1}. Two ν(Ir-Cℓ) modes

are seen, one infrared and one Raman active; as expected for a <u>trans</u>

structure.

<u>3-B-3 Tris-Sulphito Complexes</u>.

Two structures are possible for three sulphur-bonded sulphito

groups in an octahedral complex,
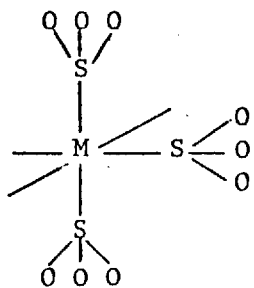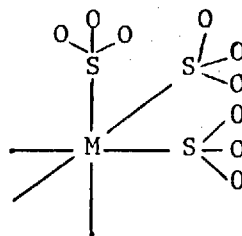
<u>mer</u> C$_s$ <u>fac</u> C$_{3v}$

A _cis_ (_fac_) structure has been suggested for $Na_3[Ir(SO_3)_3(NH_3)_3].7H_2O$.[103]

For a C_{3v} structure, $\Gamma_{S-O} = 2a_1 + a_2 + 3e$. The a_1 and e modes

are both infrared and Raman active, predicting a total of five

bands in each spectrum. The lower symmetry, C_s requires more bands.

For the three tris-sulphito complexes investigated,

$Na_3[Ir(SO_3)_3(NH_3)_3].7H_2O$, $(NH_4)_3[Rh(SO_3)_3(NH_3)_3].1\frac{1}{2} H_2O$ and

$K_4[Os(SO_3)_3(H_2O)_3]$, only three or four bands are seen in the infrared

and in the Raman spectrum. The higher symmetry structure thus seems

more likely. Bands assigned to $\nu(M-S)$ are seen at 250 cm^{-1} (Ir),

247 cm^{-1} (Rh) and 255 cm^{-1} (Os) in the Raman spectra. The species

$K_3[Rh(SO_3)_3].2H_2O$ (Section 3-B-5) which appears to contain bidentate

sulphito groups, gives more complicated spectra than these complexes

of monodentate sulphite. The infrared band at 370 cm^{-1} for

$K_4[Os(SO_3)_3(H_2O)_3]$ may be assigned to $\nu(Os-OH_2)$.

3-B-4   Tetra-Sulphito Complexes.

In an octahedral complex, with four sulphito groups, the other

two ligands may be _cis_ or _trans_.
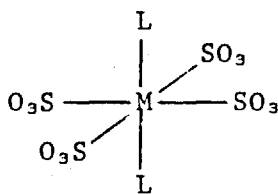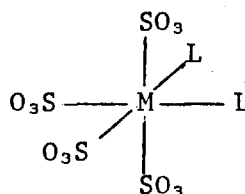
trans, C_{4h} cis, C_{2v}

The structure of the higher symmetry, <u>trans</u>, C_{4h} is likely to be found for $Na_6[OsO_2(SO_3)_4].2H_2O$ and $K_6[OsO_2(SO_3)_4].2\frac{1}{2}H_2O$, for which $\nu(Os=O)$ is seen near 840 cm^{-1}, and $K_6[Pt(SO_3)_4]$ is expected to have a square planar structure. A <u>cis</u> arrangement, however, has been suggested for $Na_7[Ir(SO_3)_4Cl_2]$.[89,104] Bonding via the sulphur seems likely on the basis of the observed spectra. In C_{4h} symmetry, $\Gamma_{S-O} = 2a_g + 2b_g + e_g + a_u + b_u + 2e_u$, give Raman active modes (a_g, b_g, e_g) and three infrared active modes (a_u, e_u) are predicted. More bands would be expected for the C_{2v} structure.

The infrared and Raman spectra of $K_6[Pt(SO_3)_4].2H_2O$, $Na_6[OsO_2(SO_3)_4].2H_2O$, $K_6[OsO_2(SO_3)_4].2\frac{1}{2}H_2O$, $Na_7[Ir(SO_3)_4Cl_2].7H_2O$ and $(NH_4)_7[Ir(SO_3)_4Cl_2].2\frac{1}{2}H_2O$ display fewer $\nu(S-O)$ bands than predicted for either structure; the <u>trans</u> C_{4h} arrangement is thus favoured. In the Raman, bands attributed to $\nu(M-S)$ are seen at 248 cm^{-1} (Pt), 180 cm^{-1} (Os), and 240 and 260 cm^{-1} (Ir). Two bands, one each in the infrared and Raman spectra, as expected for a <u>trans</u> structure, are assigned to $\nu(Ir-Cl)$ for $Na_7[Ir(SO_3)_4Cl_2].7H_2O$ and $(NH_4)_7[Ir(SO_3)_4Cl_2].2\frac{1}{2}H_2O$.

3-B-5 Other Sulphito Complexes.

The iron complex $(NH_4)_9[Fe(OSO_2)_6]$ has been shown by an X-ray study[87] to contain oxygen-coordinated monodentate sulphito groups, the iron being at the centre of an octahedron of oxygen atoms. The vibrational spectra reflect the bonding arrangement. Thus, $\nu(S-O)$ modes are seen at lower frequencies than for S-coordinated sulphito species, ν_1 dropping to near 820 cm^{-1}. The metal-oxygen stretching

mode, involving a lighter atom, and less π-bonding, is expected

at higher frequencies than ν(M-S). The bands in the infrared

and Raman near 460 cm^{-1} are candidates for assignment to ν(Fe-O).

Bidentate sulphito groups, with some bonding via oxygen, must

be present in $K_3[Rh(SO_3)_3].2H_2O$. Five sulphur-oxygen stretching

modes are seen in the Raman, and six in the infrared, in similar

regions to those seen for monodentate sulphite. The Raman band at

250 cm^{-1} may be assigned to ν(Rh-S), while the 373 cm^{-1} band

(372 cm^{-1} in the infrared) may be ν(Rh-O). A mononuclear structure:-

is possible, or a polynuclear $-O-\overset{\overset{\textstyle O}{\|}}{\underset{\underset{\textstyle O}{}}{S}}-$ bridged structure would
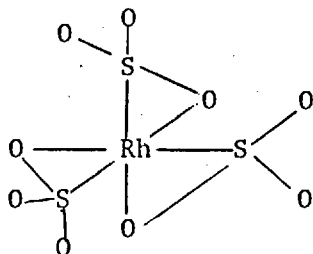
involve less strained bonding and would be in accordance with

the very low solubility of the complex, and the absence of an

X-ray powder pattern.

A planar sulphur dioxide group is found in $[Ru(NH_3)_4(SO_2)Cl]Cl$,[84]

ν(S-O) is observed at higher frequencies than for coordinated SO_3^{2-}.

The Raman band at 243 cm^{-1} may be assigned to ν(Ru-S). The bisulphito

complex, $[Ru(NH_3)_4(HSO_3)_2]$ is readily converted to the trans

$[ClRu(SO_2)NH_3)_4]^+$ ion, so a trans structure is probable. Somewhat

higher ν(S-O) values are seen than for coordinated sulphite. Sulphur

coordination is likely, to judge by the spectra, the Raman band at

243 cm^{-1} being assigned to ν(Ru-S).

Table 3.2.

Analytical Data for Sulphito Complexes.

Compound	Found %					Required %				
	H	N	S	Cℓ	K	H	N	S	Cℓ	K
Iron										
$(NH_4)_9[Fe(OSO_2)_6]$	4.9	17.1	27.3	–	–	5.2	18.1	27.5	–	–
Iridium										
$Na_7[Ir(SO_3)_4C\ell_2].7H_2O$	1.0	–	13.9	8.4	–	1.6	–	14.7	8.2	–
$(NH_4)_7[Ir(SO_3)_4C\ell_2].2\frac{1}{2}H_2O$	4.4	13.0	16.0	9.4	–	4.4	13.0	17.0	9.4	–
$K_5[Ir(SO_3)_2C\ell_4].6H_2O$	1.4	–	7.8	17.7	22.3	1.5	–	8.0	17.8	24.5
$(NH_4)_5[Ir(SO_3)_2C\ell_4].H_2O$	3.7	11.2	10.5	24.3	–	3.7	11.6	10.6	23.6	–
$Na_3[Ir(SO_3)_3(NH_3)_3].7H_2O$	2.2	6.2	13.1	–	–	3.4	6.2	14.2	–	–
$Na_3[Ir(SO_3)_2(NH_3)_2C\ell_2].6H_2O$	2.8	3.9	9.9	10.8	–	2.9	4.4	10.1	11.2	–
Osmium										
$Na_6[OsO_2(SO_3)_4].2H_2O$	0.5	–	14.0	–	–	0.5	–	17.9	–	–
$K_6[OsO_2(SO_3)_4].2\frac{1}{2}H_2O$	0.5	–	12.6	–	27.8	0.6	–	15.6	–	28.6
$K_4[Os(SO_3)_3(H_2O)_3]$	0.9	–	14.6	–	23.4	0.9	–	15.0	–	24.4

Table 3.2 (cont).

Compound	Found %					Required %				
	H	N	S	Cℓ	K	H	N	S	Cℓ	K
Osmium										
$[Os(NH_3)_4(SO_3)C\ell]$	3.4	15.1	8.6	8.0	-	3.2	15.0	8.6	9.5	-
$[Os_2N(NH_3)_8(SO_3)(H_2O)]C\ell_3$	3.5	16.6	5.0	14.0	-	3.6	17.2	4.4	14.5	-
Palladium										
$[Pd(SO_3)(NH_3)_3]$	3.9	16.4	13.4	-	-	3.8	17.7	13.5	-	-
Platinum										
$K_6[Pt(SO_3)_4].2H_2O$	0.5	-	14.7	-	29.3	0.5	-	16.3	-	29.9
Rhodium										
$K_3[Rh(SO_3)_3].2H_2O$	0.8	-	18.9	-	24.0	0.8	-	19.4	-	23.6
$(NH_4)_3[Rh(SO_3)_3(NH_3)_3].1\frac{1}{2}H_2O$	4.6	16.6	20.6	-	*	5.1	17.7	20.2	-	*

Table 3.2 (cont).

Compound	Found %					Required %				
	H	N	S	Cl	K	H	N	S	Cl	K
Ruthenium										
[Ru(NH$_3$)$_4$(HSO$_3$)$_2$]	4.2	16.7	18.4	–	–	4.3	16.9	19.3	–	–
[Ru(NH$_3$)$_4$(SO$_2$)Cl]Cl	3.4	18.8	10.9	23.2	–	4.0	18.4	10.5	23.3	–
[Ru(NH$_3$)$_5$(SO$_3$)].2H$_2$O	6.2	22.3	10.1	–	–	6.3	23.2	10.6	–	–

*   NH$_4^+$, Found 11.1%, Required 11.4%.

Section 3-C. Osmium and Ruthenium Sulphito Complexes.

Osmium Species.

Attempted preparation of a material claimed to be " $K_6H_2[Os(SO_3)_4Cl_4]$ "[105]

from $K_2[OsCl_6]$ with hot aqueous potassium bisulphite solution gave

a pale brown, diamagnetic solid analysing as $K_4[Os^{II}(SO_3)_3(H_2O)_3]$.

Infrared and Raman data (Section 3-B-3) indicate that the sulphito

groups are bonded via sulphur, with the water coordinated to the

osmium, and the cis (fac) structure being likely.

Reaction of $[Os(NH_3)_5Cl]Cl_2$ in hot aqueous HSO_3^- solution with

SO_2, using experimental conditions similar to those described for

the preparation of $[Ru(NH_3)_4(HSO_3)_2]$ from $[Ru(NH_3)_5Cl]Cl_2$,[84]

gave a pink-red product. The analytical data for this paramagnetic

species (μ_{eff} = 1.45 B.M. at 294 K), suggest a formulation as

$[Os^{III}(NH_3)_4(SO_3)Cl]$. Vibrational spectra (Section 3-B-1) are

consistent with a monodentate sulphito group, coordinated via

sulphur, probably trans to the chloro ligand. A magenta complex,

$[Os(NH_3)_5(SO_2)]Cl_2$ has recently been reported, prepared from

$[Os(NH_3)_5(H_2O)]^{3+}$ with HSO_3^- and SO_3 at 80 °C.[106]

Treatment of an aqueous solution of the binuclear species

$[Os_2N(NH_3)_8Cl_2]Cl_3$ with sulphur dioxide gives a sulphito complex, precipitated

on addition of ethanol. Analytical data suggest formulation as $[Os_2N(NH_3)_8$-

$(SO_3)(H_2O)]Cl_3$; the sulphito and aquo ligands are probably in axial

positions, exchange of the axial groups is known to occur readily. It has

been noted that replacement of chloro by aquo ligands takes place on

standing in aqueous solution for $[Os_2N(NH_3)_8Cl_2]Cl_3$.[15] Infrared and

Raman spectra (Section 3-B-1) suggest the presence of a monodentate sulphur-

coordinated sulphito group in the complex.

The ease of formation of $[Os_2N(NH_3)_8(SO_3)(H_2O)]Cl_3$ with SO_2 in aqueous solution is reminiscent of that observed for the osmium ammine complex of Gautier[35] (formulated as $[Os_3N_2(NH_3)_{14}(OH)_4(H_2O)_2]Cl_7$ in Section 2-E). Gautier's compound finds application, after treatment with SO_2 in aqueous solution, as a Feulgen-type staining reagent for aldehydic groups generated from DNA by acid hydrolysis.[35] Other osmium ammine complexes, $[Os_3N_2(NH_3)_8(H_2O)_6]Cl_6$ (osmium violet, Section 2-E) and the dimer $[Os_2N(NH_3)_8Cl_2]Cl_3$, when used in the same manner with SO_2, stain tissue to a similar degree (Section 2-G). No sulphito complexes of the trinuclear species have yet been isolated. The mode of interaction of the coordinated sulphito group with aldehydic groups is not clear. Formation of species such as

$$R-Os-\overset{\overset{\textstyle O}{\|}}{\underset{\underset{\textstyle O}{\|}}{S}}-O-\overset{\overset{\textstyle H}{|}}{\underset{\underset{\textstyle OH}{|}}{C}}-R' \quad \text{is a possibility.}$$

Ruthenium

Treatment of ruthenium red, $[Ru_3O_2(NH_3)_{14}]^{6+}$ in aqueous solution at $75\,°C$ with SO_2, with or without HSO_3^- added, leads to loss of the strong red colouration. The grey precipitate formed contains much $[Ru(NH_3)_4(HSO_3)_2]$, to judge by the infrared spectrum. Presumably, decomposition of ruthenium red under the reducing conditions leads to the formation of species such as $[Ru(NH_3)_4(H_2O)_2]^{3+}$ and subsequent uptake of HSO_3^-. Ruthenium red, after SO_2 treatment, has been used as a Feulgen-type stain for aldehydic moieties,[57] mononuclear species may well be responsible for the staining activity.

Table 3.3

X-Ray Powder Diffraction Data (XRD) for Sulphito Complexes.*

| $Na_7[Ir(SO_3)_4-Cl_2].7H_2O$	$(NH_4)_7[Ir(SO_3)_4-Cl_2]2\frac{1}{2}H_2O$	$K_5[Ir(SO_3)_2-Cl_4].6H_2O$	$(NH_4)_5[Ir(SO_3)_2-Cl_-].H_2O$	$Na_3[Ir(SO_3)_3-(NH_3)_3].7H_2O$	$Na_3[Ir(SO_3)_2(NH_3)_2-Cl_2].6H_2O$	$Na_6[OsO_2(SO_3)_4].-2H_2O$
7.8s	10.0s	9.5s	7.35s	7.75s	8.3m	8.4m
7.4s	8.5s	6.9s	6.4s	6.4mw	7.3s	6.3mw
6.0s	8.1s	5.8mw	6.15s	5.58ms	6.4s	5.9s
5.5m	7.5ms	5.5mw	5.65s	5.30m	5.8ms	4.2mw
4.24mw	6.8s	5.2m	4.70m	3.0mw	5.7m	3.75w
3.47m	6.5s	4.6mw	4.25m	2.79m	5.3m	3.40m
3.32mw	6.25ms	3.9mw	3.90m	2.57mw	4.5m	3.15m
3.13m	5.9ms	3.48mw	3.63m		4.2m	2.95m
3.10w	5.8ms	3.40m	3.58m		3.72ms	2.64ms
3.06m	5.6ms	3.12ms	3.42mw		3.61mw	2.51w
2.78w	5.5ms	2.88m	3.29m		3.32ms	2.32mw
2.75w	5.08m	2.56ms	2.84ms		3.23mw	2.23mw
2.72mw	4.99m	2.38m	2.75mw		3.03mw	2.18mw
2.62m	4.52mw	2.22mw	2.71mw		2.74mw	
2.52s	4.42mw	2.11m	2.66mw		2.64m	
2.45m	4.08mw		2.63mw		2.63m	
2.21m	3.86mw		2.58mw		2.43m	
2.15m	3.40m		2.51mw		2.40m	
2.05m	3.22m		2.43m		2.38mw	
	3.16m		2.36mw		2.15mw	
			2.27mw		2.08mw	

Table 3.3 (cont).

X-Ray Powder Diffraction Data (XRD) for Sulphito Complexes.[*]

$_6[OsO_2(SO_3)_4].$ $2\frac{1}{2} H_2O$	$K_4[Os(SO_3)_3$ $(H_2O)_3]$	$[Os(NH_3)_4$ $(SO_3)Cl]$	$[Os_2N(NH_3)_8(SO_3)$ $(H_2O)].Cl_3$	$(NH_4)_3[Rh(SO_3)_3$ $(NH_3)_3].1\frac{1}{2} H_2O$	$[Ru(NH_3)_4(HSO_3)_2]$	$[Ru(NH_3)_5(SO_3)].$ $2H_2O$
8.8s	8.0s	8.9mw	7.5s	7.6s	5.75m	6.8mw
7.65ms	7.6s	7.8m	3.82m	6.35ms	5.50s	6.7mw
7.40ms	6.9ms	5.75s	3.41m	6.20s	5.21ms	5.75s
5.80s	6.6ms	4.72m	3.03mw	5.47ms	5.00mw	5.65s
5.42ms	6.2ms	4.40m	2.72m	4.79m	4.57m	5.15m
3.68mw	5.05m	3.97ms		4.02m	4.31m	4.61mw
3.5mw	4.12m	3.75ms		3.60m	4.05mw	3.43m
3.28mw	3.95ms	3.45ms		3.38mw	3.59mw	3.09m
3.10mw	3.69m	3.39s		3.25m	3.30mw	3.05mw
3.03m	3.48m	2.93ms		3.02m	3.19m	2.84m
2.98mw	3.01ms	2.74mw		2.86ms	3.11mw	2.57ms
2.94mw	2.86mw	2.55m		2.80mw	2.84m	2.32m
2.86mw	2.81m	2.40m		2.76mw	2.64m	2.24m
2.55m	2.67m	2.33m		2.72mw	2.35m	2.23mw
2.45m	2.63mw	2.20mw		2.68mw	2.28m	2.11mw
2.36mw	2.51m	2.17mw		2.56m	2.16m	2.08mw
	2.43m			2.52mw	2.08mw	2.04mw
	2.25mw			2.46mw	2.03mw	
	2.10mw			2.29mw		
				2.23mw		
				2.16mw		

[*] Observed inter-planar spacings (in °A) are listed with estimated intensities. Many weak lines are not reported. No lines were observed for $K_3[Rh(SO_3)_3].2H_2O$

Section 3-D. E X P E R I M E N T A L.

Analytical data are presented in Table 3.2 and X-ray powder d-spacings in Table 3.3.

Iron.

$(NH_4)_9[Fe(OSO_2)_6]$.
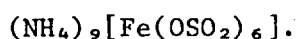
This was prepared according to the literature method.[107] Addition of ammonia solution to aqueous $FeCl_3$ produced $Fe(OH)_3$, which was filtered off and washed to remove Cl^-. Sulphur dioxide was passed into a cold ammoniacal suspension of $Fe(OH)_3$. On standing, orange microcrystals of $(NH_4)_9[Fe(OSO_2)_6]$ formed and were collected.

Iridium.

$Na_7[Ir(SO_3)_4Cl_2].7H_2O$.
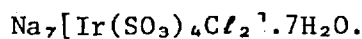
The complex was prepared as a pale yellow microcrystalline solid by warming $Na_3[IrCl_6]$ (0.5 g) with sodium bisulphite solution (6 g $NaHCO_3$ in 60 cm^3 water, saturated with SO_2) at 75 °C for two hours, following the literature method.[104]

$(NH_4)_7[Ir(SO_3)_4Cl_2].2\frac{1}{2}H_2O$.
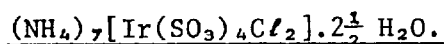
Attempted preparation of $(NH_4)_5[Ir(SO_3)_3Cl_2]$[108] by warming an aqueous solution of $(NH_4)_3[IrCl_6]$ with ammonium sulphite solution (10 g $(NH_4)_2CO_3$ in 60 cm^3 water, saturated with SO_2) gave on standing a light yellow solid, $(NH_4)_7[Ir(SO_3)_4Cl_2].2\frac{1}{2}H_2O$.

$K_5[Ir(SO_3)_2C\ell_4].6H_2O.$

Attempted preparation of $K_4[Ir(SO_3)_2C\ell_3].6H_2O$[109] by warming

a solution of $K_3[IrC\ell_6]$ (0.64 g in 9 cm^3 water) with potassium

sulphite solution (0.33 g K_2CO_3 in water, with SO_2) for two hours,

and allowing the solution to stand, gave $K_5[Ir(SO_3)_2C\ell_4].6H_2O$,

a light orange solid.

$(NH_4)_5[Ir(SO_3)_2C\ell_4].H_2O.$

Reaction of $(NH_4)_2[IrC\ell_6]$ with ammonium sulphite solution[110] gave

$(NH_4)_5[Ir(SO_3)_2C\ell_4].H_2O.$ This orange product was also obtained in

an attempted preparation of $(NH_4)_4[Ir(SO_3)_2C\ell_3].5H_2O.$[109]

$Na_3[Ir(SO_3)_3(NH_3)_3].7H_2O.$

Treatment of $Na_7[Ir(SO_3)_4C\ell_2].7H_2O$ with excess ammonia solution

produced the white ammine complex.[103] Evaporation to dryness in vacuo

of a solution in ^2H_2O yielded the deuteriated material.

$Na_3[Ir(SO_3)_2C\ell_2(NH_3)_2].6H_2O.$

To ammonium bisulphite solution (1.2 g $(NH_4)_2CO_3$ in 12 cm^3

water, saturated in SO_2) was added $(NH_4)_2[IrC\ell_6]$ (1 g) which dissolved

on warming and stirring, giving an orange solution. The product

formed on standing overnight was dissolved in warm water, and sodium

tetraphenylborate solution added to precipitate the ammonium ions.

The pale yellow $Na_3[Ir(SO_3)_2C\ell_2(NH_3)_2].6H_2O$ was precipitated from solution

with acetone.

Osmium.

$Na_6[OsO_2(SO_3)_4].2H_2O.$
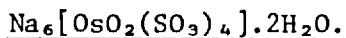
The preparation described in the literature[111] was adopted.

Sulphur dioxide was passed into a cooled solution of osmium tetra-

oxide (0.66 g) in aqueous sodium hydroxide (2.6 g in 35 cm^3 water)

until the solution reached neutrality. A saturated solution of

$Na_2S_2O_5$ was added, and the tan precipitate collected, washed with

a little cold water, ethanol and ether, and dried _in vacuo_.

$K_6[OsO_2(SO_3)_4].2\frac{1}{2} H_2O.$
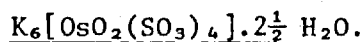
This was prepared in a similar manner to the sodium salt,

from osmium tetraoxide in potassium hydroxide solution,

$K_2[OsO_2(OH)_4]aq.$, with sulphur dioxide.[111]

$K_4[Os(SO_3)_3(H_2O)_3].$
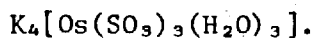
$K_2[OsC\ell_6]$ (1.65 g) was added to aqueous potassium bisulphite

(5 g $K_2S_2O_5$ in 25 cm^3 water) and the mixture warmed to 70°C for

two hours. On cooling, the light brown solid was collected. This

method corresponds to that described for the preparation of material

claimed to be $K_6H_2[Os(SO_3)_4C\ell_4].$[105]

$K_4[Os(SO_3)_3(H_2O)_3]$ is diamagnetic, mass susceptibility

$\chi = -4.95 \times 10^{-9} m^3 kg^{-1}$ at 294 K, suggesting the presence of

octahedral osmium(II) (d^6).

$[Os(NH_3)_4(SO_3)C\ell].$
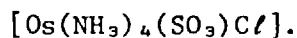
Treatment of a hot (75°C) solution of $[Os(NH_3)_5C\ell]C\ell_2$

(0.3 g, prepared via $[Os(NH_3)_5N_2]C\ell_2$ and $[Os(NH_3)_5I]I_2$,[76,77] in

15 cm^3 water) with $Na_2S_2O_5$ (0.5 g) and SO_2 for six hours gave

a red-brown solution. A small amount of a brown material was

removed by centrifugation, addition of ethanol to the red-brown

supernatant brought down a pink-red precipitate of $[Os(NH_3)_4(SO_3)Cl]$.

Mass susceptibility $\chi = 2.49 \times 10^{-8}$ m^3 kg^{-1} at 294 K,

effective magnetic moment $\mu_{eff} = 1.45$ B.M.

$[Os_2N(NH_3)_8(SO_3)(H_2O)]Cl_3$.

Sulphur dioxide was passed into a solution of $[Os_2N(NH_3)_8Cl_2]Cl_3$

(prepared as in reference 13, 0.2 g dimer in 30 cm^3 water) for

15 minutes. Addition of ethanol precipitated the yellow-brown

complex.

Palladium.

$[Pd(SO_3)(NH_3)_3]$.

The literature preparation,[112] via $[Pd(SO_3)(H_2O)_3]$, was

employed. Palladium chloride, $PdCl_2$, with silver sulphite,

Ag_2SO_3, and water generated $[Pd(SO_3)(H_2O)_3]$ as a brown solid.

Ammonia solution was added to aqueous $[Pd(SO_3)(H_2O)_3]$ (0.25 g in

10 cm^3 water), giving a white precipitate of $[Pd(SO_3)(NH_3)_3]$. The

deuteriated species, $[Pd(SO_3)(N^2H_3)_3]$ was obtained by dissolving

$[Pd(SO_3)(H_2O)_3]$ (0.1 g) in ^2H_2O (15 cm^3) with addition of 0.1 cm^3

of concentrated ammonia solution. The white solid was collected by

centrifugation, washed with acetone and ether, and dried in vacuo.

Platinum.

$K_6[Pt(SO_3)_4]$.

The literature method was followed;[113] a warm aqueous solution

of $K_2[PtCl_6]$, (1 g in 10 cm^3 water) was added to potassium bisulphite

solution (5 g K_2CO_3 in 20 cm^3 water, with SO_2) and the mixture

warmed to 80 °C for a few minutes before cooling. White crystals of

$K_6[Pt(SO_3)_4]$ were obtained.

Rhodium.

$K_3[Rh(SO_3)_3].2H_2O$.

The literature method,[114] was followed. A hot solution of

$K_2S_2O_5$ (12 g in 20 cm^3) was added to a boiling solution of $RhCl_3$

(2 g in 3 cm^2 water and 2 cm^3 concentrated hydrochloric acid, dilute

in 40 cm^3 water) and heating for an hour, produced $K_3[Rh(SO_3)_3].2H_2O$

as a yellow powder.

$(NH_4)_3[Rh(SO_3)_3(NH_3)_3].1\frac{1}{2} H_2O$.

A hot solution of $RhCl_3$ (1 g in 1.5 cm^3 water and 1 cm^3

concentrated hydrochloric acid) was added to ammonium bisulphite

solution (10 cm^3 of 50% w/v in SO_2). After warming until the mixture

was colourless, the solution was allowed to cool and evaporate down.

The first crop of crystals was $(NH_4)_2SO_3$, which was discarded. The

white solid obtained next was recrystallised from water-acetone as

white crystals, $(NH_4)_3[Rh(SO_3)_3(NH_3)_3].1\frac{1}{2} H_2O$. A deuteriated sample

was prepared by evaporation to dryness _in vacuo_ of a solution in ^2H_2O.

Ruthenium.

$[Ru(NH_3)_4(HSO_3)_2]$.

To a solution of $[Ru(NH_3)_5Cl]Cl_2$, (1 g, prepared via

$[Ru(NH_3)_6]Cl_3$ [75]) in water (40 cm³) at 80 °C was added $Na_2S_2O_5$

(1.5 g) and sulphur dioxide passed into the solution for an hour .

The off-white product, formed on cooling under an atmosphere of

SO_2, was $[Ru(NH_3)_4(HSO_2)_2]$. [84,115]

$[Ru(NH_3)_4(SO_2)Cl]Cl$.

$[Ru(NH_3)_4(HSO_3)_2]$, (0.6 g) was boiled with 1:1 hydrochloric

acid (70 cm³) for 15 minutes. Tan needle crystals of

$[Ru(NH_3)_4(SO_2)Cl]Cl$ [84,116] formed on cooling.

$[Ru(NH_3)_5(SO_3)].2H_2O$.

Treatment of a solution of $[Ru(NH_3)_4(SO_2)Cl]Cl$ (0.05 g in

1 cm³ water) with aqueous ammonia (0.880, 2 cm³) decolourised the

solution. [116] A white precipitate of $[Ru(NH_3)_5(SO_3)].2H_2O$ is obtained

on addition of ethanol (5 cm³). The white solid loses weight (approx.

14% on heating for 24 hours), turning a deep blue-black on standing

or heating.

Mass susceptibility of $[Ru(NH_3)_5(SO_3)].2H_2O$, $\chi = -5.61 \times 10^{-9}$ m³ kg^{-1}

at 294 K, effective magnetic moment μ_{eff} = 0.2 B.M.,implying a diamagnetic

octahedral ruthenium(II), (d^6) species.

The blue-black decomposition product has a mass susceptibility

$\chi = 7.03 \times 10^{-9}$ m³ kg^{-1} at 294 K, effective magnetic moment μ_{eff} = 0.8 B.M.

Chapter Four

Interaction of Lead, Uranyl and Tungstophosphoric Acid Solutions with Amino Acids and Nucleotides.

ABSTRACT
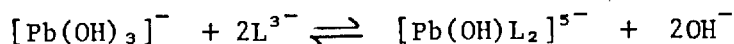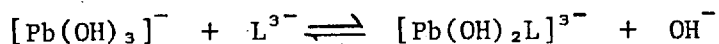
Lead(II) and dioxouranium(VI) solutions, widely used as counter-stains in studies of electron microscopy, have been investigated. Sulphur-containing amino acids are found to bind lead, and nucleotides also to uranium species. The rôle of hydroxo-bridged polynuclear species in the staining solutions is considered. The anionic stain, tungstophosphoric acid, $H_3PW_{12}O_{40}$, is also discussed.

Section 4-A. Introduction.

Lead(II) or dioxouranium(VI) acetate (hereafter called uranyl)

solutions, or both in succession, are frequently applied to thin

sections of fixed cell tissues to improve selectively   the contrast

of cell constituents.[117,118] This post-staining or counterstaining

technique enhances the effect of stains applied at an earlier stage

in the preparation of the cell tissues for study. The cell tissues

by this stage, will have been treated by fixatives such as aldehydes

or osmium tetraoxide, so the functional groups available for binding

the counterstain may differ from those in vivo.[117] Tungstophosphoric

acid, $H_3PW_{12}O_{40}$, known as PTA, is used as an anionic stain before

or after sectioning.[118]

(a) Lead(II)

Solutions containing lead(II) species are widely used in electron

microscopy studies of biological tissues. The contrast of sections

is much improved by treatment with lead solutions after glutaraldehyde

or osmium tetraoxide fixation. Membranes are stained under some

conditions; nucleoproteins, particularly those containing RNA, and

glycogen are well stained and contrasted. It was found that alkaline

lead(II) solutions are more effective[119]; acetate[120] or citrate[121]

salts are often used, adjusted to pH 11-12 with sodium hydroxide.

It seems probable that at these higher alkalinities, phosphate, thiol

and carboxyl groups of biopolymers are more likely to be ionised,

and so be able to interact with cationic lead species.[120] The

plumbite ion, $[Pb(OH)_3]^-$ will probably be present in this pH range.

In the presence of citrate ion, L^{3-} ($^-OOCCH_2.C(OH)COO^-.CH_2COO^-$), in

alkaline solution, the following equilibria are important:[122]

$$[Pb(OH)_3]^- + L^{3-} \rightleftharpoons [Pb(OH)_2L]^{3-} + OH^-$$

$$[Pb(OH)_3]^- + 2L^{3-} \rightleftharpoons [Pb(OH)L_2]^{5-} + 2OH^-$$

$$2[Pb(OH)_3]^- + L^{3-} \rightleftharpoons [Pb_2(OH)_3L]^{2-} + 3OH^-$$

There is a possibility that polynuclear hydroxo-bridged species are present in the staining solution, such as $[Pb(OH)_2Pb]^{2+}_{aq}$. In perchlorate solutions, the species $[Pb_4(OH)_4]^{4+}$,[123] and $[Pb_6O(OH)_6]^{4+}$ [124] have been identified by Raman spectroscopy, and a solid-state X-ray structure for the latter reported.[125] A Raman study of the $[Pb(OH)_3]^-$ ion has recently been made.[141] The $[Pb_4(OH)_4]^{4+}$ ion has also been found in a lead nitrate species.[126]

(b) Underline Uranium

Uranyl solutions, or more correctly, dioxouranium(VI) species, $[UO_2(L)_n]^{m+}$, are widely used to increase the electron contrast of tissue sections, although poorer results are obtained with material that has been fixed by osmium tetraoxide.[118] Binding of cationic uranium species to nucleic acids and phosphate groups is found, DNA being well contrasted.[127,128] Proteins and membranes also bind some uranium.

The commonest solution employed is that of uranyl acetate, $[UO_2(CH_3COO)_2(H_2O)_2]$ in water. Owing to hydrolysis, a saturated solution is near pH 3.5. It has been proposed that solid uranyl acetate contains the structure:[129]
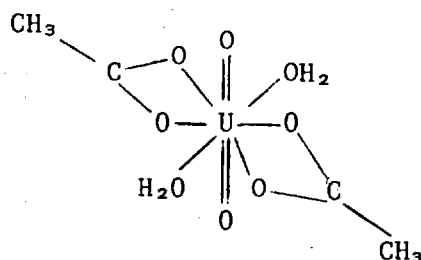
with six coplanar coordination sites. The symmetric and asymmetric

U-O stretching modes are seen at 867 and 970 cm^{-1} respectively

in the infrared.[129] In solution, extinction and potentiometric

data suggest that $[UO_2(CH_3COO)aq.]^+$, $[UO_2(CH_3COO)_2.aq]$ and

$[UO_2(CH_3COO)_3]^-$ are present.[130]

A structure postulated for the product of the interaction between

the uranyl ion and ATP (adenosine triphosphate) is:[131]
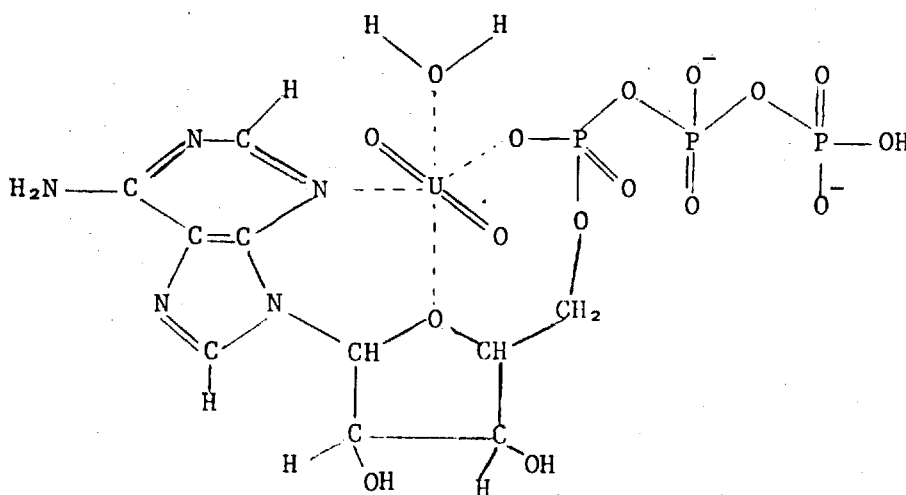
By following the hydrolysis in aqueous solution of uranyl

complexes, a range of hydroxo species have been shown to form,

and polymerisation may then occur. Amongst others, the ions

$[UO_2(OH)]^+_{aq}$, $[(UO_2)_2(OH)_2]^{2+}_{aq}$ and $[(UO_2)_3(OH)_5]^+_{aq}$ have been identified

as present in solution.[132] The solid state structures of several

hydrolysis products have been obtained. An example is

$[(UO_2)_3O(OH)_3(H_2O)_6]NO_3.4H_2O;$[133]

(protons omitted)
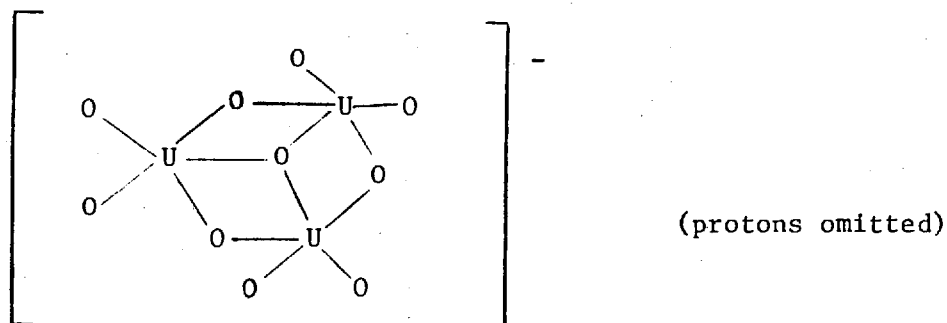
the O=U=O axes being perpendicular to the page and omitted for clarity.

(c) Tungstophosphoric acid.

The heteropoly acid, $H_3PW_{12}O_{40}.nH_2O$, 12-tungstophosphoric acid

or dodecatungstophosphoric acid, abbreviated to PTA (phosphotungstic

acid) is used in electron microscopy studies as an anionic stain for

positively charged moieties. Aqueous solutions are acidic, near

pH 1.5. When used at this pH, binding to polysaccharides[134] and

basic proteins[135,136] is found, staining decreasing as the pH is

raised. Membranes are generally not stained. Staining with PTA

of cell tissue blocks is normally carried out before sectioning.

In the low pH regions, protonation of hydroxyl groups on polysaccharides allows binding of the $[PW_{12}O_{40}]^{3-}$ anion. Likewise, protonation of amido $-NH_2$ groups of proteins will allow binding of PTA. At pH > 1.5, the $[PW_{12}O_{40}]^{3-}$ unit is less stable towards loss of W, initially forming $[PW_{11}O_{39}]^{2-}$, and under alkaline conditions, $[WO_4]^{2-}$,[134,137] giving rise to anomalous staining observations. Infrared[138] and Raman[139] spectra of $H_3PW_{12}O_{40}$ have been reported; there is a recent review of heteropolymolybdates and heteropoly-tungstates.[140]

Section 4-B. Interactions of Lead, Uranium and Tungsten Species with Amino Acids and Nucleotides.

4-B-1 Lead(II) Solutions.

Identification of Species Present in Alkaline Lead(II) Solutions.

Although the presence of sodium hydroxide in the solution rendered collection of data difficult by being responsible for much Raleigh scattering and some fluorescence, the Raman spectrum of a saturated aqueous solution of PbO in 1 M NaOH was measured. The polarised band near 420 cm^{-1} (410 cm^{-1} in a solution in ^2H_2O) is assigned to ν^s(Pb-OH) of the $[Pb(OH)_3]^-$ ion. A similar assignment has recently been reported.[141] No bands corresponding to those of the clusters $[Pb_4(OH)_4]^{4+}$ [123] or $[Pb_6O(OH)_6]^{4+}$ [124] were observed in this lead hydroxide solution, used by Karnovsky[142] as a stain for electron microscopy work. The Raman spectrum of an alkaline lead(II) citrate solution, prepared according to Reynolds,[121] also showed a band near 420 cm^{-1}, indicating the presence of $[Pb(OH)_3]^-$ in this staining reagent.

Table 4.1

Interaction of Lead, Uranium and Tungstophosphoric Acid Containing Solutions with Molecules of Biological Interest.

		5% Lead Nitrate	Alkaline 3% Lead Citrate	8% Uranyl Acetate	10% PTA
R [a]	Amino Acids				
$-CONH_2$	Asparagine	-	-	-	-
$-COOH$	Aspartic Acid	-	+	++	-
$-SH$	Cysteine	++	++	+	-
$-SH$	N-acetyl Cysteine		++		
-imidazole	Histidine	-	-	++	+
$-(CH_2)_3NH_2$	Lysine	-	-	-	++
$-CH_2SCH_3$	Methionine	-	-	-	-
$-SH$	Penicillamine		++		
$-OH$	Serine	-	-	-	-
[b]	Bases Adenine	-	-	-	++
[c]	Cytosine	-	-	-	++
[c]	1(3)Methyl Cytosine	-	-	+	++

[a] $R-CH_2-CH(NH_2)COOH$.　[b] Purine base.　[c] Pyrimidine base.　[d] Ethanol solution.

- No observed interaction.　+ Turbidity.　++ Precipitation.

Table 4.1 (cont).

		5% Lead Nitrate	Alkaline 3% Lead Citrate	8% Uranyl Acetate	10% PTA
	Nucleosides				
b	Adenosine	−	−	−	++
b	Deoxyadenosine	−	−	−	++
c	Cytidine	−	−	−	+
b	Guanosine	−	−	−	+
	Nucleotides				
b	AMP	++	−	++	++
b	dAMP	++	−	++	+
c	CMP	++	−	++	−
b	GMP	++	−	++	$\pm$
b	dGMP	++	−	++	+
c	TMP	++	−	++	−
	Others				
d	Dipalmitoyl Phosphatidyl Choline	++		++	+
	Ethanolamine Phosphoric Acid	+	−	+	−
	D-ribose-5-phosphate			++	

Interactions of lead nitrate solutions (5% in water, pH 3.8)

and alkaline lead citrate solutions (3% in Pb, pH 12) with

amino acids, components of nucleic acids, and other molecules of

biological interest are listed in Table 4.1. No precipitation of any

of these materials was observed with lead hydroxide solution (saturated

PbO in 1 M NaOH), the concentration of lead presumably being too

low to effect precipitation. The main classes of molecule precipitated

by lead(II) species are nucleotides, such as adenosine 5' monophosphate,

AMP; and amino acids such as cysteine, which contain the -SH group.

Analyses of the products obtained are listed in Table 4.2.

Amino Acids.

The amino acid-containing lead salts analyse in the ratio

1 Pb : 1 amino acid, suggesting that the amino acid is present as

a 2^- anion following deprotonation of the thiol group.

$$^-S-CH_2-CH-COO^- \qquad\qquad (cysteine)^{2-}$$
$$\underset{NH_2}{|}$$

The infrared spectra of the products from the lead nitrate solution

and the alkaline lead citrate solution with cysteine are identical.

A study of the infrared spectra of metal-cysteine complexes has

been reported, coordination via $-S^-$ and $-NH_2$ groups for the lead

complex was proposed;[143] the spectrum listed for the lead-cysteine

complex is the same as that found in the present work. The band at

2540 cm^{-1} in free cysteine, assigned to $\nu(S-H)$ is absent in the complex.

Penicillamine, $(CH_3)_2C(SH)CH(NH_2)COOH$, and N-acetyl cysteine also

have bands in this region, missing on complexation, coordination by

-S⁻ is suggested. The infrared spectra of cysteine, N-acetyl

cysteine and penicillamine, with their lead(II) complexes, are

given in Table 4.3. The infrared bands of the cysteine and

penicillamine complexes are generally sharp, suggesting that

little hydrogen bonding is present. The 3275 and 3095 cm^{-1}

bands in the cysteine complex and 3220 and 3125 cm^{-1} in the

penicillamine complex are assigned to ν(N-H) modes of a coordinated

-NH₂ group. The 1577 cm^{-1} band of the cysteine complex, and the

1598 cm^{-1} band of the penicillamine complex fall within the range

expected for a free carboxylate ion $-CO_2^-$, with the NH₂ deformation

vibration also falling in this region.

N-acetyl cysteine shows a band at 3367 cm^{-1} due to ν(N-H) of

the amido linkage. In the lead complex, this appears at 3170 cm^{-1},

a shift to lower frequencies would be expected on coordination.

The ν(C=O) of the amido linkage, at 1710 cm^{-1} in the free amino

acid, drops on complexing to 1675 cm^{-1}. The 1633 cm^{-1} band of

the complex may be assigned to $\nu_{as}(CO_2^-)$ of a coordinated carboxylate

group. Thus, coordination to lead of thiol -S⁻, amido C=O and

N-H, and carboxylate of N-acetyl cysteine is suggested on the basis

of the infrared spectrum, although some inter-molecular hydrogen

bonding may not be excluded in this complex. Cysteine and penicillamine

coordinate via thiol and amino groups.

Nucleotides.

While alkaline lead citrate solution gives no precipitation with

nucleotides, lead nitrate solution does. The product with AMP

(adenosine monophosphate, a constituent nucleotide of RNA) corresponds

to 1 Pb^{2+} - 1 AMP^{2-} on the basis of analytical data (Table 4.2).

AMP^{2-}
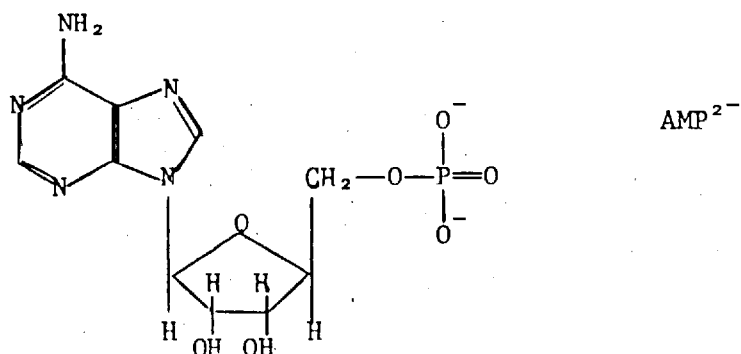
Binding of lead to the phosphate group is likely.

Phospholipid.

Interaction of Pb^{2+} with the phosphate group of the lecithin-type phospholipid, dipalmitoyl phosphatidyl choline,

$$CH_2—O—CO—R$$
$$CH—O—CO—R$$
$$CH_2—O—\overset{O}{\underset{O^-}{\overset{\|}{P}}}—O—CH_2CH_2—\overset{CH_3}{\underset{CH_3}{\overset{+}{N}}}CH_3$$
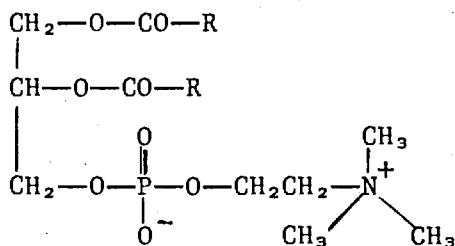
$(R = CH_3(CH_2)_{14}-)$

seems likely; the odd ratio 5 Pb^{2+} : 4(phospholipid) : 10 NO_3^- is found.

4-B-2 Uranyl Acetate Solution.

Hydrolysis product.

On standing an 8% aqueous solution of uranyl acetate (pH 3.6) for a period of days, a yellow crystalline product was obtained,

Table 4.2

Analytical Data for Lead, Uranium and Tungstophosphoric Acid Products.

|	% Found					% Required				
	C	H	N	P ·	S	C	H	N	P	S
Alkaline Lead Citrate										
Cysteine $Pb[SCH_2CH(NH_2)COO]$	11.2	1.5	4.2		6.5	11.0	1.5	4.3		9.8
Penicillamine $Pb[SC(CH_3)_2CH(NH_2)COO]$	17.2	2.5	3.9		7.0	16.9	2.6	4.0		9.1
N-Acetyl Cysteine $Pb[SCH_2CH(COO)NHOCOCH_3]$	15.9	1.7	3.2		4.6	15.6	1.8	3.7		8.3
Lead Nitrate										
AMP $Pb(C_{10}H_{12}N_5O_7P).H_2O$	19.5	2.3	11.3	6.7		21.0	2.5	12.2	5.4	
Phospholipid $Pb_5(C_{40}H_{80}NO_8P)_4(NO_3)_{10}$	41.8	7.1	4.4	2.9		41.8	7.0	4.3	2.7	
Uranyl Acetate										
Aspartic acid $(UO_2)_3(C_4H_5NO_4)(OH)_4$	5.0	1.1	1.3			4.8	0.9	1.4		
Histidine $(UO_2)_4(C_6H_8N_3O_2)(CH_3COO)(OH)_6(H_2O)_2$	6.6	1.4	3.0			6.7	1.4	2.9		
$(UO_2)_2(C_6H_8N_3O_2)(CH_3COO)(OH)_2$	12.5	1.8	5.8			12.2	1.7	5.3		
AMP $(UO_2)(C_{10}H_{12}N_5O_7P)(H_2O)_2$	17.8	2.3	10.1	2.1		18.4	2.5	10.8	4.8	
dAMP $(UO_2)(C_{10}H_{12}N_5O_6P)(H_2O)_2$	18.0	2.2	9.8	4.3		18.9	2.5	11.0	4.9	
CMP $(UO_2)(C_9H_{12}N_3O_8P)(H_2O)_4$	16.4	2.3	6.1	4.2		16.3	3.0	6.3	4.7	

Table 4.2 (cont).

	% Found					% Required				
	C	H	N	P	S	C	H	N	P	S
GMP $(UO_2)_4(C_{10}H_{12}N_5O_8P)_3(OH)_2(H_2O)_6$	15.9	2.2	8.9	4.0		15.6	2.2	9.1	4.0	
dGMP $(UO_2)_4(C_{10}H_{12}N_5O_7P)_3(OH)_2(H_2O)_4$	17.4	2.3	9.7	3.9		16.2	2.1	9.5	4.2	
TMP $(UO_2)_2(C_{10}H_{13}N_2O_8P)(OH)_2$	13.9	1.8	2.9	3.4		13.4	1.7	3.1	3.5	
Ribose Phosphate $(UO_2)_3(C_5H_9O_7P)(OH)_4(H_2O)_2$	5.3	1.5		2.3		5.3	1.5		2.8	
Phospholipid $(UO_2)_4(C_{40}H_{80}NO_8P)_3(CH_3COO)_8$	43.4	7.1	1.2	1.5		43.5	7.1	1.1	2.5	
Tungstophosphoric Acid										
Adenine $(PW_{12}O_{40})(C_5H_6N_5)_3.4\frac{1}{2}\ H_2O$	4.8	0.7	5.3			5.3	0.8	6.2		
Cytosine $(PW_{12}O_{40})(C_4H_6N_3O)_3$	4.8	0.7	4.1			4.5	0.6	3.9		
Adenosine $(PW_{12}O_{40})(C_{10}H_{14}O_4N_5)_3$	10.3	1.3	5.9			9.8	1.2	5.7		
AMP $(PW_{12}O_{40})(Na_2C_{10}H_{13}N_5O_7P)_3.6H_2O$	8.8	1.2	5.3			8.6	1.2	5.0		

which differed from $[UO_2(CH_3COO)_2(H_2O)_2]$. This hydrolysis product

analyses as $[(UO_2)(CH_3COO)(OH)(H_2O)_2]$. The sharp infrared band

at 3560 cm^{-1} is assigned to ν(O-H) of a terminal hydroxo group.

Since the complex is not soluble in water, a polynuclear species

is suggested, one possible structure being
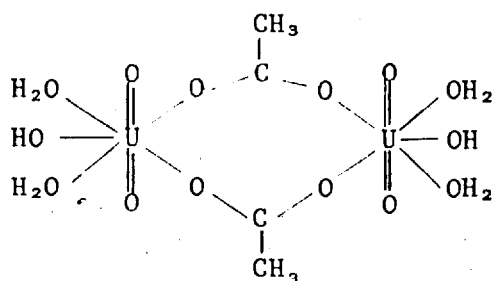
Some reactions of 8% aqueous uranyl acetate with molecules of

biological interest are listed in Table 4.1, with analyses of

some products in Table 4.2. Amino acids with acidic (aspartic acid)

or imidazole (histidine) groups precipitate with uranyl solutions,

as do nucleotides found in RNA and DNA.

Amino Acids.

The product with aspartic acid, ($^-$OOCCH$_2$CH(NH)$_2$COO$^-$) analyses

as $3(UO_2)^{2+}$: $1(asp)^{2-}$: $4(OH)^-$, while two different products,

empirically $4(UO_2)^{2+}$: $1(his)^-$: $1(CH_3COO)^-$: $6(OH)^-$: $2H_2O$ and $2(UO_2)^{2+}$:

$1(his)^-$: $1(CH_3COO)^-$: $2(OH)^-$ are found in separate reactions with histidine.

(histidine)$^-$
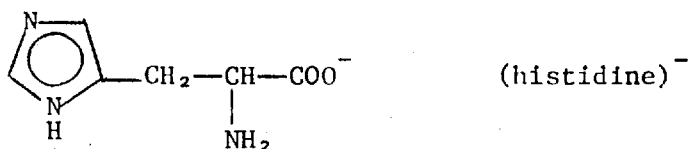
These odd ratios suggest that uranyl-containing clusters are present, if not in the staining solution, then in the amino acid complexes. At this stage it is not possible to put forward structures for these species.

A product is obtained with imidazole, the heterocyclic base of histidine, which conforms to the empirical formula $(UO_2)_2^{2+}(C_3H_3N_2)^-(CH_3COO)_2^-(OH)^-(H_2O)_4$. Reaction of uranyl acetate with imidazole in ethyl acetate solution is reported to yield a product, $[UO_2(C_3H_3N_2)(CH_3COO)H_2O]$, for which a polymeric imidazole-bridged structure has been postulated.[144]

Nucleotides

Uranyl acetate solution is found to give 1:1 products with adenosine 5' monophosphate (AMP), deoxyadenosine 5' monophosphate (dAMP) and cytidine 5' monophosphate (CMP). With guanosine 5'-monophosphate (GMP), deoxyguanosine 5' monophosphate (dGMP) and thymidine 5' monophosphate (TMP), the products analyse as $4(UO_2)^{2+} : 3(GMP \text{ or } dGMP) : 2(OH)^-$ and $2(UO_2)^{2+} : 1(TMP) : 2(OH)^-$. Hydroxo-bridged uranyl species may be present. AMP, CMP and GMP are found in ribonucleic acids, RNA; dAMP, dGMP and TMP in deoxyribonucleic acids, DNA. Cytidine and thymidine contain the pyrimidine bases, cytosine and thymine, adenosine and guanosine the purine bases, adenine and guanine. The sugar-phosphate moiety common to all the nucleotides, D-ribose-5-phosphate, gives a product $[(UO_2)_3(C_5H_9O_7P)(OH)_4-(H_2O)_2]$; binding to the phosphate group is probable.

The lecithin-type phospholipid, dipalmitoyl phosphatidyl choline forms a product analysing as $[UO_2(CH_3COO)_2]_4$ (phospholipid)$_3$.

Section 4-B-3. Tungstophosphoric Acid.

A 10% aqueous solution of tungstophosphoric acid $H_3PW_{12}O_{40} \cdot nH_2O$,

which has a pH of 1.5, was added to aqueous solutions of molecules

of biological interest. Results are given in Table 4.1. While

amino acids were in general not precipitated, pyrimidine and purine

bases, and nucleosides (sugar-base moieties) were brought out of

solution. Analyses of some products may be found in Table 4.2;

ratios of 1 PTA^{3-} : 3(protonated base)$^+$ are found. Under the

acid conditions, NH_2 groups of adenine and cytosine may be protonated

and precipitate out with the PTA^{3-} anion.

Section 4-C. E X P E R I M E N T A L.

Aqueous lead(II) (5% lead nitrate, pH 3.8; or 3% lead citrate

in 1 M NaOH, pH 12.1), uranyl (8% uranyl acetate, pH 3.6) and

tungstophosphoric acid (10% $H_3PW_{12}O_{40} \cdot nH_2O$) solutions were added

in approximately equimolar quantities to saturated solutions of

a range of amino acids, pyrimidine and purine bases, nucleosides,

nucleotides (as the disodium salts) and two phosphate-containing

molecules. The interactions are listed in Table 4.1. To ethanolic

solutions of the phospholipid, dipalmitoyl phosphatidyl choline, was

added ethanolic or aqueous-ethanolic solutions of lead nitrate,

uranyl acetate, or tungstophosphoric acid. In certain cases, where

precipitates were formed, these were collected by centrifugation, washed

with water followed by ethanol and ether, and dried in vacuo. The

uranyl species were yellow, the lead and PTA species white. Analytical

data are given in Table 4.2.

Table 4.3

Infrared Spectra of Sulphur-Containing Amino Acids and Their Lead Complexes.

Assignment	Cysteine	Pb-cys	Penicillamine	Pb-pen	N-Acetyl Cysteine	Pb-Nac.cys
		3320m				3430ms,b
ν(N-H)	3160s	3275mw	3150s	3220s	3367s	
		3200m				
ν(N-H)		3095s		3125s		3170s
ν(S-H)	2540m		2550m		2540ms	
		1595sh		1638sh		
			1612vs	1618vs		
Amido C=O					1710s	1675w
(CO_2^-)	1580s	1577vs	1570s	1598vs	1570s	1633vs
	1525m	1560s	1523ms		1525s	1560m
	1420mw	1540sh			1412m	1512s
Other Bands	1340mw	1308m	1340m	1348ms	1297m	1304mw
	1290m	1300m	1275m	1305m	1273m	1260mw
	1270mw	1243mw	1205w	1292m	1253m	1228mw
	1190m	1173mw	1190mw	1212ms	1224m	1145m
	1132m	1151mw	1153m	1187m	1195m	1076m
	1100mw	1060ms	1085m	1157w	1125m	983ms

Table 4.3 (cont).

Assignment	Cysteine	Pb-cys	Penicillamine	Pb-pen	N-Acetyl Cysteine	Pb-Nac.cys
Other Bands	1053m	1042m	1047m	1115mw	1037m	928m
	1000w	1016ms	1008w	1060ms	1003m	888m
	936ms	950w	955w	1010m	987ms	830ms
	839ms	908mw	905w	970w	939mw	780w
	818m	850s	893w	940w	900mw	740w
	803m	797m	860mw	899ms	790s	670m
	767mw	692w	757m	761s	767m	593ms
	750m	657mw	668w	702m	695w	516s
	687ms	636mw	575ms	642m	672m	473ms
	628s	565ms	545s	597m	649m	375ms
	532s	442m	475ms	554m	568vs	332ms
	440ms	390m	408ms	440m	542ms	
	353ms	332m	330m	417ms	494ms	
	280m	265w		392m	387vs	
				364m	355s	
				328m	290ms	
				280mw		

Lead Hydroxide Solution.

The literature method[142] was employed, an excess of freshly prepared lead(II) oxide (0.675 g) was added to sodium hydroxide solution (2 g NaOH in 50 cm^3 water); most of the PbO dissolved after boiling for five minutes. The material formed on cooling was centrifuged off, leaving the clear staining reagent.

The deuteriated species $[Pb(O^2H)_3]^-$ was obtained by dissolution of PbO in $NaO^2H/^2H_2O$ solution. The NaO^2H was prepared from sodium metal and ^2H_2O.

Alkaline Lead Citrate Solution.[121]

Lead(II) citrate (1.5 g) was stirred with water (50 cm^3) at 40-50 °C; on addition of sodium hydroxide solution (10 M, 1 cm^3) the solution cleared. On cooling to room temperature, the solution was at pH 12.1.

Uranyl Acetate Hydrolysis Product, $[(UO_2)(CH_3COO)(OH)(H_2O)_2]_2$.

On setting aside a saturated (8%) aqueous uranyl acetate solution, yellow crystals formed, insoluble in water or ethanol.

Found: C, 6.4 ; H, 1.8%. $C_4H_{14}O_{14}U_2$ requires: C, 6.3 ; H, 1.9%. Infrared: 3560s,sp, 3400sh, 3320s,b, 3190s,b, 1640s, 1525vs, 1040ms, 1012m, 960sh, 935vs, 888ms, 678ms, 638m, 518ms, 450ms, 400sh, 370s, 350 ms, 260m (cm^{-1}).

Uranyl Acetate-Imidazole, $[(UO_2)_2(C_3H_3N_2)(CH_3COO)_2(OH)(H_2O)_4]$.

To a saturated aqueous solution of imidazole, was added dropwise saturated uranyl acetate solution until a cream-yellow precipitate formed. On standing overnight, a yellow crystalline solid formed and was collected.

Found: C, 10.2 ; H, 2.1 ; N, 3.3%. $C_7H_{18}N_2O_{13}U_2$ requires

C, 10.3 ; H, 2.1 ; N, 3.5%.

Infrared: 3570sh, 3390vs,b, 3150s, 3100m, 1620m, 1590m, 1535vs,

1200w, 1120w, 1100w, 1077mw, 1047m, 1013m, 980ms, 944m, 895vs, 860m,

810m, 767mw, 684m, 660w, 645w, 632m, 523ms, 475m, 455m, 375ms, 335mw,

250ms (cm^{-1}).

Physical Measurements

Microanalyses were performed by the Microanalytical Laboratory, Imperial College, and F. Pascher (Bonn). Ammonium, potassium and caesium were estimated gravimetrically as their tetraphenylborate salts. Osmium was determined spectrophotometrically as the thiourea complex after fusion with sodium peroxide.[145] Infrared spectra of mulls in liquid paraffin, between caesium iodide plates, or of samples in potassium bromide discs were measured (4000-200 cm^{-1}) on Perkin-Elmer 457 and 597 instruments. Solution electronic absorption spectra, 250-850 nm range, 1 cm cells, were recorded on a Perkin-Elmer 402 instrument.

Raman spectra were measured on a Spex Ramalog 5 (14018) double monochromator instrument, with a DPC-2 detector, using exciting radiation from a Coherent Radiation model 52 Kr^+ laser. Colourless solids were run in capillaries, lightly coloured and slightly photosensitive samples 1:1 with potassium bromide in a spinning KBr disc, using excitation wavelengths remote from electronic absorption bands. Resonance Raman spectra were obtained for dilute aqueous solutions (10^{-4} - 10^{-5} M) in a spinning solution cell, or at the dilution of 0.1% sample in spinning potassium bromide discs, using excitation near the electronic absorption bands. Local heating and photodecomposition were minimised by spinning the samples.

Conductivity measurements on solutions in deionised water were made using a Wayne-Kerr a.c. bridge and a glass cell, capacity 10 cm^3, held at 25 $°C$. The conductivity was measured for a range of concentrations, where solubility allowed, and extrapolation from a plot of the molar conductance Λ_M against $C^{\frac{1}{2}}$ (C = concentration) lead to a value for the limiting conductance $\Lambda°$. Comparison of $\Lambda°$ values, for cations of similar charge and shape, and with identical counter-ions,[146] was used to estimate the ion type in solution. Polarographic measurements were made on degassed aqueous solutions, using Beckmann and Princeton Applied Research instruments with a dropping mercury electrode, or a hanging drop electrode for cyclic voltammetry.

Magnetic susceptibilities of powdered samples were measured using the Gouy-Rankine method, diamagnetic corrections were applied.[147] The calibration was checked using $[Ni(en)_3](S_2O_3)$.

X-ray powder diffraction patterns were recorded photographically by Dr. R.S. Osborn of the University of London Intercollegiate X-ray Service, using a Guinier Nonius Mark II camera with Cu(Kα) radiation. X-ray photoelectron spectra were recorded by the Electron Optics Unit, Johnson, Matthey Research Centre, using a Vacuum Generators ESCA 3 instrument and Aℓ(Kα), Mg(Kα) sources.

R E F E R E N C E S

1. W.P. Griffith, Coord. Chem. Revs., 1970, 5, 459.

2. W.P. Griffith, Coord. Chem. Revs., 1972, 8, 369.

3. B. Jezowska-Trzebiatowska and W. Wojciechowski, Transition Metal Chem., 1970, 6, 1.

4. J-P. Deloume, R. Faure and G. Thomas-David, Acta Cryst., 1979, B35, 558.

5. M. Ciechanowicz and A.C. Skapski, J. Chem. Soc. (A), 1971, 1792.

6. J.D. Dunitz and L.E. Orgel, J. Chem. Soc., 1953, 2594.

7. P.M. Smith, T. Fealey, J.E. Earley and J.V. Silverton, Inorg. Chem., 1971, 10, 1943.

8. C.K. Jørgensen and L.E. Orgel, Mol. Phys., 1961, 4, 215.

9. W.P. Griffith and D. Pawson, J.C.S. (Dalton), 1973, 1315.

10. A.R. Middleton, G. Wilkinson, A.P. West, M.A.A.F. de C.T. Carrondo and A.C. Skapski, submitted to Inorg. Chim. Acta.

11. M. Ciechanowicz, W.P. Griffith, D. Pawson and A.C. Skapski, J.C.S. (Chem. Comm.), 1971, 876.

12. W.P. Griffith, J. Chem. Soc. (A), 1969, 211.

13. M.J. Cleare and W.P. Griffith, J. Chem. Soc. (A), 1970, 1117.

14. D.J. Hewkin and W.P. Griffith, J. Chem. Soc. (A), 1966, 472.

15. M.J. Cleare, Ph.D. Thesis, University of London, 1970.

16. W.P. Griffith, J. Chem. Soc. (A), 1969, 2270.

17. L. Mangin, Compte Rendus acad. Sci., 1892, 116, 653.

18. D.E. Hanke and D.H. Northcote, Biopolymers, 1975, 14, 1.

19. J.H. Luft, Anat. Rec., 1971, 171, 347.

20. P.R. Blanquet, Histochemistry, 1976, 47, 63.

21. M.A. Hayat, Positive Staining for Electron Microscopy, 1975, Van Nostrand Reinhold, New York.

22. A. Joly, Compte Rendus acad. Sci., 1892, 114, 291.

23. G.T. Morgan and F.H. Burstall, J. Chem. Soc., 1936, 41.

24. K. Gleu and W. Breuel, Z. Anorg. Chem., 1938, 237, 350.

25. J.M. Fletcher, B.F. Greenfield, C.J. Hardy, D. Scargill and
    J.L. Woodhead, J. Chem. Soc., 1961, 2001.

26. C. Sterling, Amer. J. Bot., 1970, 57, 172.

27. M. Jaber, F. Bertin and G. Thomas-David, C.R. Acad. Sci. Paris, C,
    1977, 285, 317.

28. J.E. Earley and T. Fealey, Inorg. Chem., 1973, 12, 323.

29. G.W. Watt and W.C. McMordie, J. Inorg. Nucl. Chem., 1965, 27, 262.

30. J. Berzelius, Pogg. Ann. Phys. u. Chem., 1829, 15, 213.

31. C. Claus, J. prakt. Chem., 1863, 90, 97.

32. D. Pawson, Ph.D. Thesis, University of London, 1973.

33. G.W. Watt and E.M. Potrafke, J. Inorg. Nucl. Chem., 1961, 17, 248.

34. G.W. Watt and W.C. McMordie, Jr., J. Inorg. Nucl. Chem., 1965, 27, 2013.

35. R. Cogliat. and A. Gautier, C.R. Acad. Sci. Paris, D, 1973, 276, 3041.

36. M. Schröder, Ph.D. Thesis, University of London, 1978.

37. T.G. Spiro and P. Stein, Ann. Rev. Phys. Chem., 1977, 28, 501.

38. J. Behringer, Chem. Soc. Spec. Per. Rep., Molecular Spectroscopy,
    1975, 3, 163.

39. R.J.H. Clark in Advances in Infrared and Raman Spectroscopy, ed.
    R.J.H. Clark and R.E. Hester, Heyden, London, 1975, 1, 143.

40. R.J.H. Clark and B. Stewart, Structure and Bonding, 1979, 36, 1.

41. M.A.A.F. de C.T. Carrondo, Ph.D. Thesis, University of London, 1978.

42. M.A.A.F. de C.T. Carrondo, W.P. Griffith, J.P.Hall and A.C. Skapski,
    (Biochim. Biophys. Acta, in press).

43. R.J.H. Clark, M.L. Franks and P.C. Turtle, *J. Amer. Chem. Soc.*, 1977, 99, 2473.

44. J. San Filippo, Jr., R.L. Grayson and H.J. Sniadoch, *Inorg. Chem.*, 1976, 15, 269.

45. J. San Filippo, Jr., P.J. Fagan and F.J. Di Salvo, *Inorg. Chem.*, 1977, 16, 1016.

46. J.M. Friedman, D.L. Rousseau, G. Navon, S. Rosenfeld, P. Glynn, and K.B. Lyons, *Arch. Biochem. Biophys.*, 1979, 193, 14.

47. J.R. Campbell, R.J.H. Clark, W.P. Griffith and J.P. Hall, submitted to *J.C.S. (Dalton)*.

48. W.P. Griffith, *J. Chem. Soc.(A)*, 1966, 899.

49. M.W. Bee, S.F.A. Kettle and D.B. Powell, *Spectrochim. Acta*, 1975, 31A, 89.

50. M.W. Bee, S.F.A. Kettle and D.B. Powell, *Spectrochim. Acta*, 1975, 30A, 139.

51. R.J.H. Clark and C. Sourisseau, *Nouveau J. Chim.*, (Submitted).

52. J.R. Campbell, R.J.H. Clark, and J. Dilworth, to be published.

53. R.W. Stoddart, I.P.C. Spires and K.F. Tipton, *Biochem. J.*, 1969, 114, 863.

54. N.B. Fouzder, unpublished work.

55. F. Herbelin, J.D. Herbelin, J.P. Mathieu and H. Poulet, *Spectrochim. Acta* 1966, 22, 1515.

56. R.J.H. Clark and C.S. Williams, *Inorg. Chem.*, 1965, 4, 350.

57. A. Gautier and M. Schreyer, *Microscopie Electronique*, 1970, 1, 559.

58. F.K. Patterson and R. Ward, *Inorg. Chem.*, 1966, 5, 1312.

59. P. Burroughs, A. Hamnett and A.F. Orchard, *J.C.S. (Dalton)*, 1974, 565.

60. P.H. Citrin, *J. Amer. Chem. Soc.*, 1973, 95, 6472.

61. C.A. Clausen, R.A. Prados and M.L. Good, *Inorg. Nucl. Chem. Letts.*, 1971, 7, 485.

62. D.L. White, S.B. Andrews, J.W. Faller and R.J. Barrnett, Biochim. Biophys. Acta, 1976, 436, 577.

63. C.K. Jørgensen, Theoretica Chimica Acta, 1972, 24, 241.

64. L.R. Subbaraman, J. Subbaraman and E.J. Behrman, Inorg. Chem., 1972, 11, 2621.

65. G.W. Watt and L. Vaska, J. Inorg. Nucl. Chem., 1958, 5, 308.

66. M.A. Hepworth, P.L. Robinson and G.J. Westland, J. Chem. Soc., 1954, 4269.

67. R. Colton and R.H. Farthing, Aust. J. Chem., 1968, 21, 589.

68. R.V. Casciani and E.J. Behrman, Inorg. Chim. Acta, 1978, 28, 69.

69. V.S. Syrokomskii, Dokl. Akad. Nauk. SSSR, 1945, 46, 307; English translation, 1945, 46, 280.

70. C.L. Moore, Biochem. Biophys. Res. Comm., 1971, 42, 298.

71. F.D. Vasington, P. Gazzotti, R. Tiozzo and E. Carafoli, Biochim. Biophys. Acta, 1972, 256, 43.

72. K.C. Reed and F.L. Bygrave, Biochem. J., 1974, 140, 143.

73. C. Sargent and J.L. Grey, Physiological Plant Pathology, 1977, 11, 195.

74. C. Sargent, unpublished work.

75. J.E. Fergusson and J.L. Love, Inorg. Synths., 1972, 13, 210.

76. A.D. Allen and J.R. Stevens, Can. J. Chem., 1972, 50, 3093.

77. A.D. Allen and J.R. Stevens, Can. J. Chem., 1973, 51, 92.

78. L.W. Winkler, Z. Angew. Chem., 1914, 27, 630.

79. R.F. Wilson and L.J. Baye, J. Amer. Chem. Soc., 1958, 80, 2652.

80. R.F. Wilson and L.J. Baye, J. Inorg. Nucl. Chem., 1959, 9, 140.

81. W.P. Griffith, The Chemistry of the Rarer Platinum Group Metals, Os, Ru, Ir, Rh, Interscience, London, 1967.

82. M.A. Spinnler and L.N. Becka, J. Chem. Soc.(A), 1967, 1194.

83. M.A. Porai-Koshits, S.P. Ionov and Z.M. Novozhenyuk, Zh. Strukt. Khim., 1965, 6, 173; J. Struct. Chem., (USSR), 1965, 6, 161.

84. L.H. Vogt, J.L. Katz and S.E. Wiberley, Inorg. Chem., 1965, 4, 1157.

85. C.L. Raston, A.H. White and J.K. Yandell, Aust. J. Chem., 1978, 31, 999.

86. E.N. Maslen, C.L. Raston, A.H. White and J.K. Yandell, J.C.S. (Dalton), 1975, 327.

87. L.O. Larsson and L. Niinistö, Acta Chem. Scand., 1973, 27, 859.

88. H.D. Lutz, S.M. El-Suradi, B. Engelan, Z. Naturforsch., B:Anorg. Chem., Org. Chem., 1977, 32B, 1230.

89. A.V. Babaeva, Yu. Ya. Kharitonov and Z.M. Novozhenyuk, Russ. J. Inorg. Chem., 1961, 6(10), 1151.

90. A.V. Babaeva, Yu. Ya. Kharitonov and E.V. Shenderetskaya, Russ. J. Inorg. Chem., 1962, 7(7), 790.

91. A.V. Babaeva, Yu. Ya. Kharitonov and Z.M. Novozhenyuk, Zh. Neorg. Khim., 1961, 6, 2263; Russ. J. Inorg. Chem., 1961, 6, 1159.

92. G. Newman and D.B. Powell, Spectrochim. Acta, 1963, 19, 213.

93. O. Erämetsä and J. Valkonen, Suom. Kemistilehti B, 1972, 45, 91; Chem. Abstr., 76, 132703 [k].

94. A.V. Babaeva, Yu. Ya. Kharitonov and I.B. Baranovskii, Zh. Neorg. Khim., 1962, 7, 1247; Russ. J. Inorg. Chem., 1962, 7, 643.

95. A. Simon and K. Waldmann, Z. Phys. Chem. (Leipzig), 1955, 204, 235.

96. J.C. Evans and H.J. Bernstein, Can. J. Chem., 1955, 33, 1270.

97. B. Nyberg and R. Larsson, Acta Chem. Scand., 1973, 27, 63.

98. F.A. Cotton and R. Francis, J. Amer. Chem. Soc., 1960, 82, 2986.

99. D.M. Adams and J.B. Cornell, J. Chem. Soc. (A), 1967, 884.

100. J.R. Allkins and P.J. Hendra, J. Chem. Soc. (A), 1967, 1325.

101. C.V. Berney and J.H. Weber, Inorg. Chem., 1968, 7, 283.

102. K. Nakamoto, Infrared Spectra of Inorganic and Coordination Compounds, Wiley, New York, 1963.

103. V.V. Lebedinskii and M.M. Gurin, C.R. Acad. Sci. URSS, 1941, 33, 241.

104. V.V. Lebedinskii and M.M. Gurin, C.R. Acad. Sci. URSS, 1943, 38, 128.

105. A. Rosenheim, Z. Anorg. Chem., 1900, 24, 422.

106. J. Sen and H. Taube, Acta Chem. Scand., 1979, A33, 125.

107. O. Erämetsä, Ann. Acad. Sci. Fenn., 1943, A59, 5; Chem. Abstr., 1946, 40, 6359[8].

108. M.M. Gurin, C.R. acad. Sci. URSS, 1944, 44, 100.

109. V.V. Lebedinskii and M.M. Gurin, C.R. acad. Sci. URSS, 1943, 40, 322.

110. V.V. Lebedinskii and Z.M. Novozhenyuk, Zh. Neorg. Khim., 1957, 2, 2490; Russ. J. Inorg. Chem., 1957, 2, 335.

111. A. Rosenheim and E.A. Sasserath, Z. anorg. Chem., 1899, 21, 122.

112. G.A. Earwicker, J. Chem. Soc., 1960, 2620.

113. J. Lang, J. Prakt. Chem., 1861, 83, 417.

114. V.V. Lebedinskii and F.V. Shenderetskaya, Zh. Neorg. Khim., 1957, 2, 1768; Russ. J. Inorg. Chem. 1957, 2(8), 89.

115. K. Gleu, W. Breuel and K. Rehm, Z. anorg. Chem., 1937, 235, 201.

116. K. Gleu and W. Breuel, Z. anorg. Chem., 1937, 235, 211.

117. C.R. Zobel ard M. Beer, Int. Rev. Cytol., 1965, 18, 363.

118. M.A. Hayat, Principles and Techniques of Electron Microscopy, Biological Applications, Vol. 1, Van Nostrand Reinhold, New York, 1970.

119. M.L. Watson, J. Biophys. Biochem. Cytol., 1958, 4, 727.

120. A.J. Dalton and R.F. Zeigel, J. Biophys. Biochem. Cytol., 1960, 7, 409.

121. E.S. Reynolds, J. Cell. Biol., 1963, 17, 208.

122. E. Bottari and M. Vicedomini, J. Inorg. Nucl. Chem., 1973, 35, 2447.

123. V.A. Maroni and T.G. Spiro, J. Amer. Chem. Soc., 1967, 89, 45.

124. T.G. Spiro, V.A. Maroni and C.O. Quicksall, Inorg. Chem., 1969, 8, 2524.

125. T.G. Spiro, D.H. Templeton and A. Zalkin, Inorg. Chem., 1969, 8, 856.

126. A.G. Cram and M.B. Davies, J. Inorg. Nucl.Chem., 1976, 38, 1111.

127. C.R. Zobel and M. Beer, J. Biophys. Biochem. Cytol., 1961, 10, 333.

128. M. Beer and C.R. Zobel, J. Mol. Biol., 1961, 3, 717.

129. B. Mentzen and G. Giorgio, J. Inorg. Nucl. Chem., 1970, 32, 1509.

130. S. Ahrland, Acta Chem. Scand., 1951, 5, 199.

131. I. Feldman, J. Jones and R. Cross, J. Amer. Chem. Soc., 1967, 89, 49.

132. R.N. Sylva and M.R. Davidson, J.C.S. (Dalton), 1979, 465.

133. M. Åberg, Acta Chem. Scand., 1978, A32, 101.

134. J.E. Scott, J. Histochem. Cytochem., 1971, 19, 689.

135. L. Silverman and D. Glick, J. Cell. Biol., 1969, 40, 761.

136. G. Quintarelli, M. Bellocci and R. Geremia, J. Histochem. Cytochem., 1973, 21, 155.

137. M.T. Pope and G.M. Varga, Inorg. Chem., 1966, 5, 1249.

138. P. Rabette and D. Olivier, Rev. Chim. Min., 1970, 7, 181.

139. C. Rocchiccioli-Deltcheff, R. Thouvenot and R. Franch, C.R. acad. Sci. Paris (C), 1975, 280, 751.

140. T.J.R. Weakley, Structure and Bonding, 1974, 18, 131.

141. K. Sone and M. Hagiwara, Nat. Sci. Rep. Ochanomizu Univ., 1977, 28(2), 67; Chem. Abstr., 88, 112851b.

142. M.J. Karnovsky, J. Biophys. Biochem. Cytol., 1961, 11, 729.

143. M. Ikram and D.B. Powell, Pakistan J. Sci. Res., 1973, 25, 53.

144. A. Marzotto, M. Nicolini, F. Braga and G. Pinto, Inorg. Chim. Acta, 1979, 34, L295.

145. F.P. Dwyer and N.A. Gibson, Analyst, 1951, 76, 104.

146. R.D. Feltham and R.G. Hayter, J. Chem. Soc., 1964, 4587.

147. P.W. Selwood, Magnetochemistry, Interscience, New York, 1956.